Helioseismic and Magnetic Imager
for
Solar Dynamics Observatory

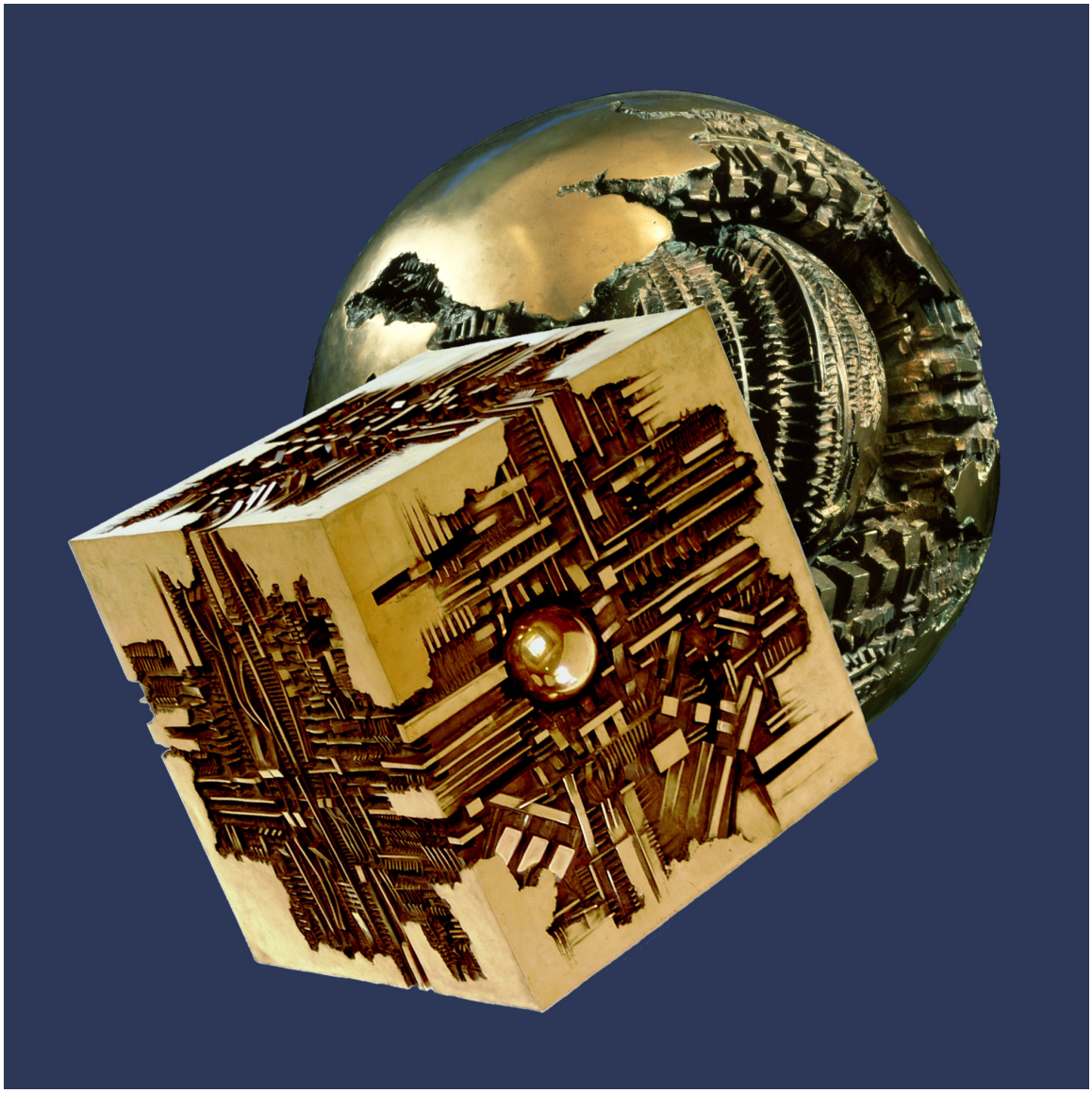

Stanford University Hansen Experimental Physics Laboratory
and
Lockheed-Martin Solar and Astrophysics Laboratory

The cover of the NASA 1984 report "Probing the Depth of a Star: The Study of Solar Oscillations from Space" featured Hirschhorn's the Pomodoro Sphere. That report led to the helioseismic study of the global Sun. Pomodoro's Cube at Stanford symbolizes HMI data cubes for investigation of localized regions in the Sun.

B. TABLE OF CONTENTS

C. THE HELIOSEISMIC AND MAGNETIC IMAGER INVESTIGATION

The primary goal of the Helioseismic and Magnetic Imager (HMI) investigation is to study the origin of solar variability and to characterize and understand the Sun's interior and the various components of magnetic activity. The HMI investigation is based on measurements obtained with the HMI instrument as part of the Solar Dynamics Observatory (SDO) mission. HMI makes measurements of the motion of the solar photosphere to study solar oscillations and measurements of the polarization in a spectral line to study all three components of the photospheric magnetic field. HMI produces data to determine the interior sources and mechanisms of solar variability and how the physical processes inside the Sun are related to surface magnetic field and activity. It also produces data to enable estimates of the coronal magnetic field for studies of variability in the extended solar atmosphere. HMI observations are crucial for establishing the relationships between the internal dynamics and magnetic activity in order to understand solar variability and its effects, leading to reliable predictive capability, one of the key elements of the Living With a Star (LWS) program. The HMI investigation directly addresses and assists the highest priority science goals of SDO.

The HMI investigation includes the following required seven elements:

1) The HMI instrument provides the observing capabilities required to complete the combined 'HMI' and 'HVMI' objectives as described in the SDO Announcement of Opportunity (AO). HMI is a "suite" as defined by the AO. The instrument has significant heritage from the Solar and Heliospheric Observatory (SOHO) Michelson Doppler Imager (MDI) with enhancements to achieve higher resolution, higher cadence, and the addition of a second channel to provide full Stokes polarization measurements. HMI

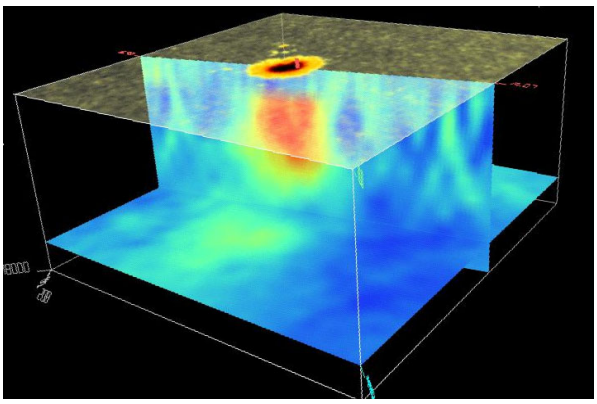

Figure C.1. Sound-speed beneath a sunspot (red –positive and blue negative perturbations) from SOHO/MDI high-resolution data (June 18, 1998).

provides stabilized 1"-resolution full-disk Doppler velocity and line-of-sight magnetic flux images every 45 seconds, and vector-magnetic field maps every 90 seconds. The basic characteristics of the HMI observables and performance of the HMI instrument are summarized in Foldout 1.K. The HMI instrument will be provided by Lockheed-Martin Solar and Astrophysics Laboratory (LMSAL) as part of the Stanford Lockheed Institute for Space Research collaboration.

2) The large data stream from HMI must be analyzed and interpreted with advanced tools that permit interactive investigation of complex solar phenomena. It will be essential to have convenient access to all data products - Dopplergrams, full vector magnetograms, subsurface flow fields and sound-speed maps deduced from helioseismic inversion, as well as coronal field estimates - for any region or event selected for analysis. This investigation will provide a data system for archiving HMI data and derived data products with convenient access to the data by all interested investigators. Sufficient computing capability will be provided to allow the complete investigation of the key HMI science objectives. The principal HMI data products are shown in Foldout 1.L.

3) The HMI investigation includes support of integration of HMI onto SDO, mission plan-

ning, HMI operations and receipt and verification of HMI data.

4) Some of the higher level HMI data products are likely to be of great value for monitoring and predicting the state of solar activity. Such products will be identified in Phase-A and produced on a regular basis at a cadence appropriate for each product.

5) HMI will obtain filtergrams in a set of polarizations and spectral line positions at a regular cadence for the duration of the mission. Several processed levels of data products will be produced from the filtergrams. The basic science observables are full-disk Doppler velocity, brightness, line-of-sight magnetic flux, and vector magnetic field. These will be available on request at full resolution and cadence. Of more interest are sampled and averaged products at various resolutions and cadence and sub-image samples tracked with solar rotation. A selection of these will be made available on a regular basis, and other data products will be made available on request. Also of great potential value are derived products such as sub-surface flow maps, far-side activity maps, and coronal and solar wind models that require longer sequences of observations. A selection of these will also be produced in the processing pipeline in near real time. A number of the HMI Co-Investigators (Co-Is) have specific tasks to provide software to enable production of these higher level products.

6) This proposal identifies a broad range of science objectives that can be addressed with HMI observations. HMI provides a unique set of data required for scientific understanding, detailed characterization and advanced warning of the effects of solar disturbances on global changes, space weather, human space exploration and development, and technological systems. HMI also provides important input data required for accomplishing objectives of the other SDO instruments. The HMI investigation will carry out the highest priority studies through to publication of the results and presentation to the scientific community.

7) SDO investigations, and HMI in particular, have aspects which will be of great interest to the public at large and offer excellent opportunities for developing interesting and timely educational material. A highly leveraged collaborative Education and Public Outreach (E/PO) program is a key part of this investigation.

The Science Objectives presented in Section C.1 and illustrated in Foldout 1 include long-standing problems in solar physics as well as questions that have developed in response to recent progress. The investigation builds on current knowledge of the solar interior, photosphere, and atmosphere, recent space- and ground-based programs, and advances in numerical modeling and theoretical understanding.

The helioseismic and line-of-sight magnetic flux measurements provide data required for the core HMI science program to characterize and understand the Sun's interior and various components of magnetic activity. The capability to measure the vector magnetic field strengthens the LWS program tremendously, in particular, for studying magnetic stresses and current systems associated with impulsive events and evolving magnetic structures.

The HMI science program has evolved from the highly successful programs of MDI, Global Oscillation Network Group (GONG) and Advanced Stokes Polarimeter (ASP). The Co-Investigators include leading experts in helioseismic and magnetic field measurements, experienced instrument developers, observers, mission planners, theorists, and specialists in numerical simulations, data processing and analyses. The HMI investigation benefits from and contributes to other space and ground based programs.

C.1 Scientific Goals and Objectives

C. 1.1 Science Overview

The Sun is a magnetic star. The high-speed solar wind and the sector structure of the heliosphere, coronal holes and mass ejections, flares and their energetic particles, and variable components of irradiance are all linked to the variability of magnetic fields which originate in the solar interior and pervade the atmosphere. Many of these phenomena can have profound impacts on our technological society, so understanding them is a key objective for LWS.

The central question is the origin of solar magnetic fields. Most striking is that the Sun exhibits 22-year cycles of global magnetic activity involving magnetic active region eruptions with very well defined polarity rules[1] resulting in global scale magnetic patterns. Coexisting with these large-scale ordered magnetic structures and concentrated active regions are ephemeral active regions and other compact and intense flux structures that emerge randomly over much of the solar surface forming a 'magnetic carpet'[2, 3]. The extension of these changing fields at all scales into the solar atmosphere creates coronal activity, which in turn is the source of space weather variability.

The HMI science investigation addresses the fundamental problems of solar variability with studies in all interlinked time and space domains, including global scale, active regions, small scale, and coronal connections. One of the prime objectives of the LWS program is to understand how well predictions of evolving space weather can be made. The HMI investigation will examine these questions in parallel with the fundamental science questions of how the Sun varies and how that variability drives global change and space weather.

Helioseismology, which uses solar oscillations to probe flows and structures in the Sun's interior, provides remarkable new perspectives on the complex interactions between highly turbulent convection, rotation and magnetism. It has revealed a region of intense rotational shear[4-6] at the base of the convection zone, called the tachocline[7, 8], which is the likely seat of the global dynamo[9-11]. Convective flows also have a crucial role in advecting and shearing the magnetic fields, twisting the emerging flux tubes and displacing the photospheric footpoints of magnetic structures present in the corona. Flows on all spatial scales influence the evolution of magnetic fields, including how fields generated near the base of the convection zone rise and emerge at the solar surface, and how the magnetic fields already present at the surface are advected and redistributed. Both of these mechanisms contribute to the establishment of magnetic field configurations that may become unstable and lead to eruptions that affect the near-Earth environment.

Methods of local-area helioseismology have begun to reveal the great complexity of rapidly evolving 3-D magnetic structures and flows in the sub-surface shear layer in which the sunspots and active regions are embedded. Most of these techniques were developed by members of the HMI team during analysis of MDI observations. As useful as they are, the limitations of MDI telemetry and the limited field of view at high resolution have prevented the full exploitation of these methods to answer important questions about the origins of solar variability. By using these techniques on continuous, full-disk, high-resolution observations, HMI will enable detailed probing of dynamics and magnetism within the near-surface shear layer, and provide sensitive measures of variations in the tachocline.

Just as existing helioseismology experiments have shown that new techniques can lead to new understanding, methods to measure the full vector magnetic field have been developed and have shown the potential for significantly enhanced understanding of magnetic evolution and connections. What existing and planned ground based programs cannot do, and what Solar-B cannot do, is to observe the full-disk vector field continuously at a ca-

dence sufficient to follow activity development. HMI vector magnetic field measurement capability, in combination with the other SDO instruments and other programs (*e.g.* STEREO, Solar-B, and SOLIS), will provide data crucial to connect variability in the solar interior to variability in the solar atmosphere, and to the propagation of disturbances in the heliosphere.

HMI brightness observations will provide important information about the area of magnetic and convective contributions to irradiance, and also about variations of the solar radius and shape.

C.1.2 Scientific Objectives

The broad goals described above will be addressed in a coordinated investigation in a number of parallel studies. These segments of the HMI investigation are to observe and understand these interlinked processes:

- **Convection-zone dynamics and the solar dynamo;**
- **Origin and evolution of sunspots, active regions and complexes of activity;**
- **Sources and drivers of solar activity and disturbances;**
- **Links between the internal processes and dynamics of the corona and heliosphere;**
- **Precursors of solar disturbances for space-weather forecasts.**

These goals address long-standing problems that can be studied by a number of immediate tasks. The description of these tasks reflects our current level of understanding and will obviously evolve in the course of the investigation. Some of these tasks are described below.

C.1.2.1 Convection-zone dynamics and the solar dynamo

Fluid motions inside the Sun generate the solar magnetic field. Complex interactions between turbulent convection, rotation, large-scale flows and magnetic field produce regular patterns of solar activity changing quasi-periodically with the solar cycle. How are variations in the solar cycle related to the internal flows and surface magnetic field? How is the differential rotation produced? What is the structure of the meridional flow and how does it vary? What roles do the torsional oscillation pattern and the variations of the rotation rate in the tachocline play in the solar dynamo?

These issues are usually studied only in zonal averages by global helioseismology[12, 13] but the Sun is longitudinally structured. Local helioseismology has revealed the presence of large-scale flows within the near-surface layers of the solar convection zone.[14-23] These flows possess intricate patterns that change from one day to the next, accompanied by more gradually evolving patterns such as banded zonal flows[24-27] and meridional circulation cells[28-33] (Foldout 1.B,C). These flow structures have been described as Solar Subsurface Weather (SSW).[34] Successive maps of these weather-like flow structures (Foldout 1.F) suggest that solar magnetism strongly modulates flow speeds and directions. Active regions tend to emerge in latitudes with stronger shear.[35] The connections between SSW and active region development are presently unknown.

Structure and dynamics of the tachocline. Observation of the deep roots of solar activity in the tachocline is of primary importance for understanding the long-term variability of the Sun. HMI will use global and local helioseismic techniques to observe and investigate the large-scale character of the convection zone and tachocline. Topics include solar differential rotation, relations between variations of rotation and magnetic fields, longitudinal structure of zonal flows ('torsional oscillations'), relations between the torsional pattern and active regions, subsurface shear and its variations with solar activity, and the origin of the 'extended' solar cycle.

Variations in differential rotation. Differential rotation (Figure C.2) is a crucial component of the solar cycle and is believed to generate the global scale toroidal magnetic field in active regions. Results from MDI and GONG have revealed intriguing 1.3-year quasi-periodic variations of the rotation rate in the tachocline,[37] which may be a key to understanding the solar dynamo.[38] HMI will extend this key series with better near-surface resolution.

Evolution of meridional circulation. Precise knowledge of the meridional circulation in the convection zone is crucial for understanding the long-term variability of the Sun.[39, 40] Helioseismology has found evidence for variation of the internal poleward flow during the solar cycle.[34, 41, 42] To understand the global dynamics we must follow the evolution of the flow. HMI will generate continuous data for detailed, 3-D maps of the evolving patterns of meridional circulation providing information about how flows transport and interact with magnetic fields throughout the solar cycle.

Dynamics in the near surface shear layer. Helioseismology has revealed that significant changes in solar structure over the solar cycle occur in the near-surface shear layer.[32, 33, 43, 44] However, the physics of these variations and their role in irradiance variations are still unknown. HMI will characterize the properties of this shear layer, the interaction between surface magnetism and evolving flow patterns, and the changes in structure and dynamics as the solar cycle advances. It will assess the statistical properties of convective turbulence over the solar cycle, including the kinetic helicity and its relation to magnetic helicity – two intrinsic characteristics of dynamo action.

C.1.2.2 Origin and evolution of sunspots, active regions and complexes of activity

Observations show that magnetic flux on the Sun does not appear randomly. Once an active region emerges, there is a high probability that additional eruptions of flux will occur nearby (activity nests, active longitudes).[36, 45-49] How

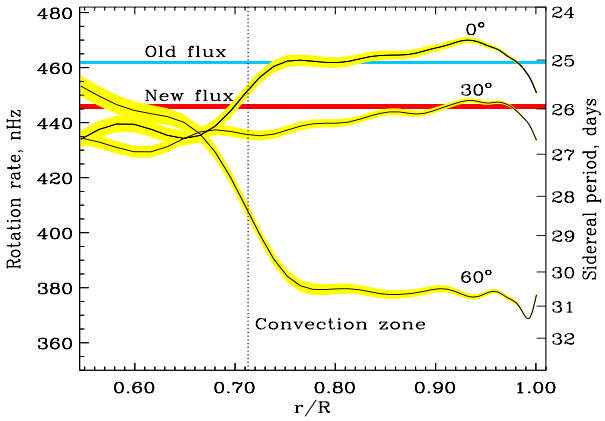

Figure C.2. Solar rotation rate vs. radius at the equator, 30, and 60 degrees latitude in 1997. The blue (red) line shows the surface rotation rate of old cycle (new cycle) emerging magnetic flux in the 1-5 (30) degree latitude range.[36]

is magnetic flux created, concentrated, and transported to the solar surface where it emerges in the form of evolving active regions? To what extent are the appearances of active regions predictable? What roles do local flows play in their evolution?

HMI will address these questions by providing tracked sub-surface sound-speed and flow maps for individual active regions and complexes under the visible surface of the Sun combined with surface magnetograms. Current thinking suggests that flux emerging in active regions originates in the tachocline. Flux is somehow ejected from the depths in the form of loops that rise through the convection zone and emerge through the surface. Phenomenological flux transport models[50-53] show that the observed photospheric distribution of the flux does not require a long-term connection to flux below the surface. Rather, field motions are described by the observed poleward flows, differential rotation, and surface diffusion acting on emerged flux of active regions. Does the active region magnetic flux really disconnect from the deeper flux ropes after emergence?

Formation and deep structure of magnetic complexes of activity. HMI will explore the nature of long-lived complexes of solar activ-

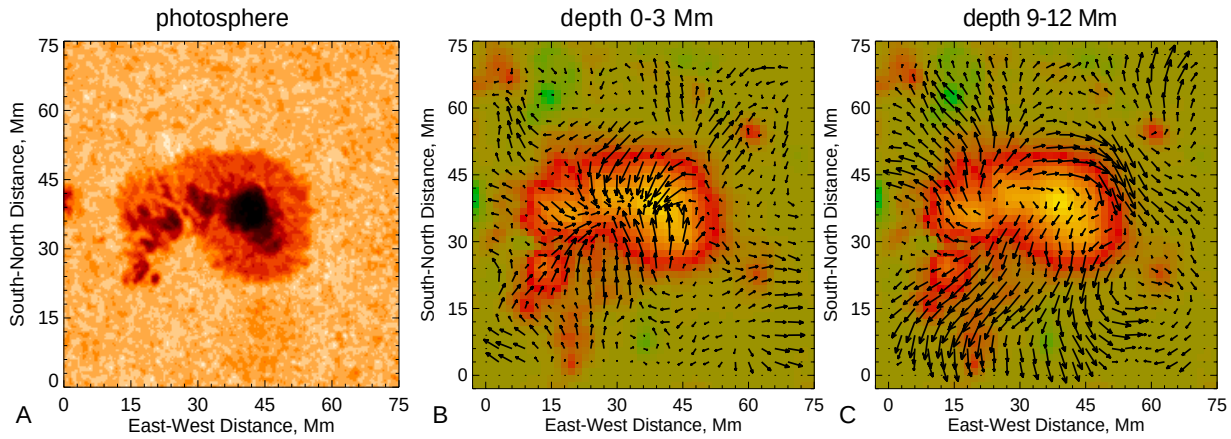

Figure C.3. Vortex flows beneath a twisting sunspot on August 8, 2000. The background color map is the corresponding MDI magnetogram.[60]

ity ('active or preferred longitudes'), the principal sources of solar disturbances. 'Active longitudes' have been a puzzle of solar activity for many decades.[54, 55] They may continue from one cycle to the next, and may be related to variations of solar activity on the scale of 1-2 years and short-term 'impulses' of activity.[56-59] HMI will probe beneath these features to 0.7R, the bottom of the convection zone, to search for correlated flow or thermal structures.

Active region source and evolution. By using acoustic tomography we can image sound speed perturbations that accompany magnetic flux emergence and disconnection that may occur. Vector magnetograms can give evidence on whether flux leaves the surface predominantly as 'bubbles', or whether it is principally the outcome of local annihilation of fields of opposing polarity. With a combination of helioseismic probing and vector field measurements HMI will provide new insight into active region flux emergence and removal.

Magnetic flux concentration in sunspots. Formation of sunspots is one of the long-standing questions of solar physics.[61-63] Recent observations from MDI have revealed complicated flow patterns beneath sunspots (Figure C.3) and indicated that the highly concentrated magnetic flux in spots is accompanied by converging mass flows in the upper 3-4 Mm beneath the surface (Foldout 1.J). The evolution of these flows is not presently known. Detailed maps of subsurface flows in deeper layers, below 4 Mm, combined with surface fields and brightness for up to 9 days during disk passage will allow investigation of the relations between flow dynamics and flux concentration in spots.

Sources and mechanisms of solar irradiance variations. Magnetic features - sunspots, active regions, and network - that alter the temperature and composition of the solar atmosphere are primary sources of irradiance variability.[64] How exactly do these features cause the irradiance variations? HMI together with the SDO Atmospheric Imaging Assembly (AIA) and Spectrometer for Irradiance (SIE), will study physical processes that govern these variations. The relation between interior processes, properties of magnetic field regions and irradiance variations, particularly the UV and EUV components that have a direct and significant effect on Earth's atmosphere will be studied for the first time.

C.1.2.3 Sources and drivers of solar activity and disturbances

It is commonly believed that the principal driver of solar disturbances is stressed magnetic field. The stresses are released in the solar corona producing flares and coronal mass ejections (CME). The source of these

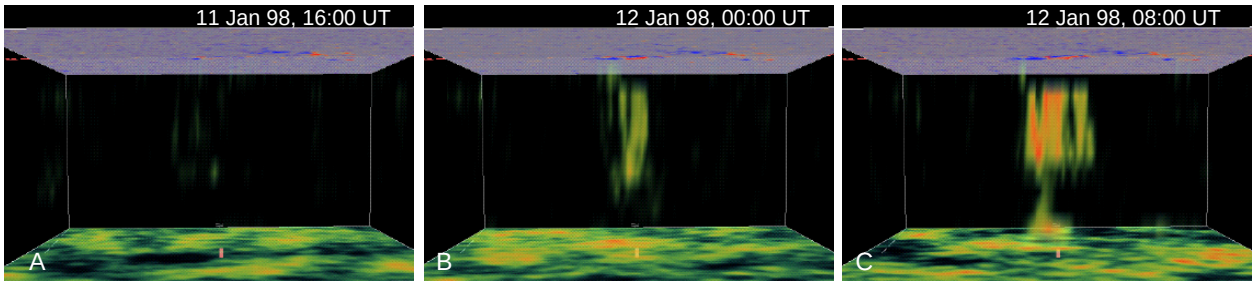

Figure C.4. MDI Images of sound-speed perturbations in an emerging active region obtained by the time-distance method with 8-hour resolution.[76] The horizontal size of the box is 460 Mm, the vertical size is 18 Mm. Magnetograms are shown on the underside of the solar surface.

stresses is believed to be in the solar interior.[65, 66] Flares usually occur in areas where the magnetic configuration is complex, with strong shears, high gradients, long and curved neutral lines, etc.[67] This implies that the trigger mechanisms of flares are controlled by critical properties of magnetic field that lead eventually to MHD instabilities. But what kinds of instability actually govern, and under what conditions they are triggered are unknown.[68] With only some theoretical ideas and models, there is no certainty of how magnetic field is stressed or twisted inside the Sun or just what the triggering process is.

Origin and dynamics of magnetic sheared structures and δ-type sunspots. The spots in Figure C.5 contain two umbrae of opposite magnetic polarity within a common penumbra and were the source of powerful flares and CMEs.[69] Such δ-type sunspot regions are thought to inject magnetic flux into the solar atmosphere in a highly twisted state.[70-72] It is important to determine what processes beneath the surface lead to development of these spots and allow them to become flare and CME productive. This investigation will be carried out by analysis of evolving internal mass flows and magnetic field topology of such spots.

Magnetic configuration and mechanisms of solar flares. Vector magnetic field measurements can be used to infer field topology and vertical electric current, both of which are essential to understand the flare process.[73] Observations are required that can continuously track changes in magnetic field and electric current with sufficient spatial resolution to reveal changes of field strength and topology before and after flares.[74, 75] HMI will provide these unique measurements of the vector magnetic field over the whole solar disk with reasonable accuracy and at high cadence.

Emergence of magnetic flux and solar transient events. Emergence of magnetic flux is closely related to solar transient events.[77-79] MDI, GONG, and BBSO data show that there can be impulsive yet long-lived changes to the fields associated with eruptive events. Emergence of magnetic flux within active regions is often associated with flares. Emerging magnetic flux regions near filaments lead to eruption of filaments.[80] CMEs are also found to accompany emerging flux regions. Further, emergence of isolated active regions can proceed without any eruptive events. This suggests that magnetic flux emerging into the atmosphere interacts with pre-existing fields leading to loss of magnetic field stability. Observations of electric current and magnetic topology differences between newly emerging and pre-existing fields will likely lead to the understanding of why emerging flux causes solar transient events.[81] Vector polarimetry provided by HMI will enable these quantitative studies.

Evolution of small-scale structures and magnetic carpet. The quiet Sun is covered with

small regions of mixed polarity, termed 'magnetic carpet' (Foldout 1.G), contributing to solar activity on short timescales.[2] As these elements emerge through the photosphere they interact with each other and with larger magnetic structures. They may provide triggers for eruptive events,[82] and their constant interactions may be a source of coronal heating.[83-85] They may also contribute to irradiance variations in the form of enhanced network emission. While HMI will certainly not see all of this flux, it will allow global scale observations of the small-scale element distribution, their interactions, and the resulting transformation of the large-scale field.

C.1.2.4 Links between the internal processes and dynamics of the corona and heliosphere

The highly structured solar atmosphere is predominately governed by magnetic field emerged from in the solar interior. Magnetic fields and the consequent coronal structures occur on many spatial and temporal scales. Intrinsic connectivity between multi-scale patterns increases coronal structure complexity leading to variability. For example, CMEs apparently interact with to the global-scale magnetic field,[86] but many CMEs, especially fast CMEs, are associated with flares, which are believed to be local phenomena. Model-based reconstruction of 3-D magnetic structure is one way to estimate the field from observations.[87-89] Models using vector field data in active regions provide the best match to the observations. More realistic MHD coronal models[90] based on HMI high-cadence vector-field maps as boundary conditions will greatly enhance our understanding of how the corona responds to evolving, non-potential active regions.

Complexity and energetics of the solar corona. Observations from SOHO and TRACE have shown a variety of complex structures and eruptive events in the solar corona. However, categorizing complex structures has not

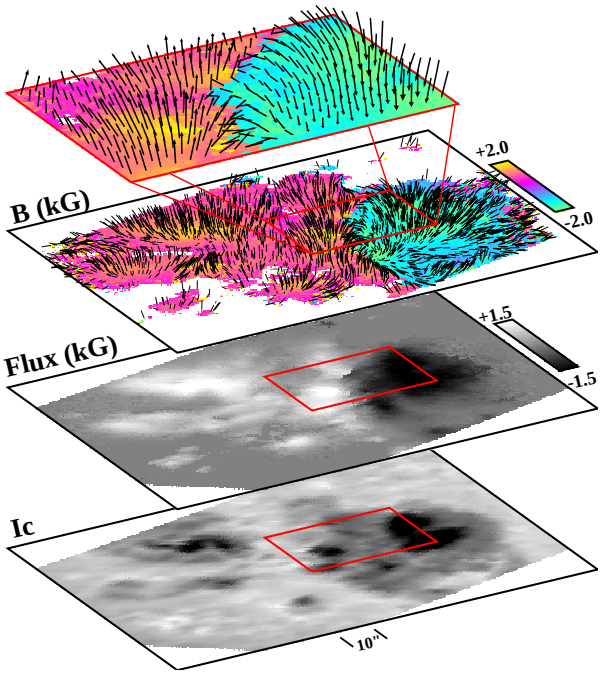

Figure C.5. Vector magnetic fields in the HMI Ni I 6768 Å line, observed with ASP, 2002 March 10, 18:58 UT, NOAA 9866: S9 W65.

revealed the underlying physics of the corona and coronal events.[91] Two mechanisms have been proposed to generate stressed magnetic fields: photospheric shear motions and emerging magnetic flux; and both may, in fact, be at work on the Sun.[92] But which plays the dominant role and how the energy injection is related to eruptive events is unknown. Magnetic helicity is an important characteristic of magnetic complexity and its conservation intrinsically links the generation, evolution, and reconnections of the magnetic field.[93-97] HMI will provide data to allow estimations of injections of energy and helicity into active regions[98, 99]: the vector magnetic field and the velocity field (from helioseismology and correlation tracking). Observations from SDO AIA and White-light Coronagraphic Imager (WCI) will show the subsequent response and propagation of complexity into the corona and heliosphere, relating the build-up of helicity and energy with energetic coronal events such as CME's.

Large-scale coronal field estimates. Models computed from line-of-sight photospheric

magnetic maps have been used to reproduce coronal forms that show multi-scale closed field structures as well as the source of open field that starts from coronal holes but spreads to fill interplanetary space.[100] Modeled coronal field demonstrates two types of closed field regions: helmet streamers that form the heliospheric current sheet and a region sandwiched between the like-polarity open field regions. There is evidence that most CMEs are associated with helmet streamers and with newly opened flux.[101, 102] HMI will provide uniform magnetic coverage at a high cadence, and together with simultaneous AIA, WCI and STEREO coronal images will enable the development of coronal field models and study of the relationship between pre-existing patterns, newly opening fields, long distance connectivity, and CMEs.

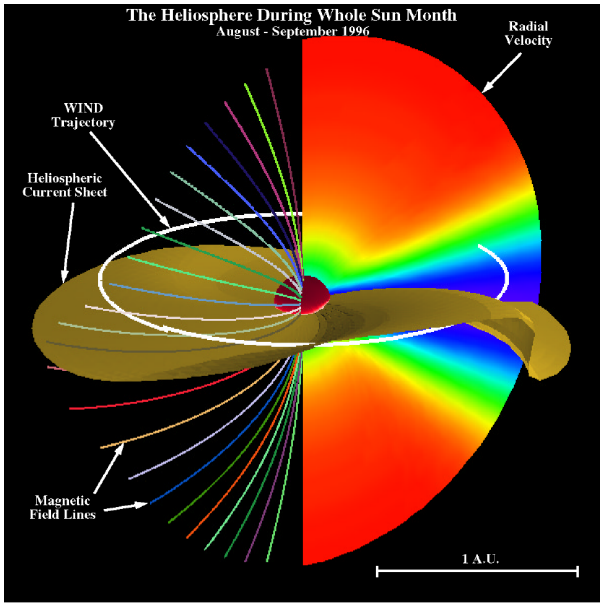

Figure C.6. MHD model of the solar corona and heliosphere driven by the observed line-of-sight photospheric magnetic field[103].

Coronal magnetic structure and solar wind. MHD simulation and current-free coronal field modeling based on magnetograms are two ways to study solar wind properties and their relations with coronal magnetic field structure[103-106] (Figure C.6). These methods have proven effective and promising, showing potential in applications of real-time space weather forecasting. It has been demonstrated that modeling of the solar wind can be significantly improved with increased cadence of the input magnetic data.[107] By providing full-disk vector field data at high cadence, HMI will enable these models to describe the distribution of the solar wind, coronal holes and open field regions, and how magnetic fields in active regions connect with interplanetary magnetic field lines.

C.1.2.5 Precursors of solar disturbances for space-weather forecasts

Variations in the solar spectral irradiance and total irradiance may have profound effects on life through their potential but poorly understood role in climate changes. The variation from cycle to cycle of the number, strength, and timing of the strongest eruptive events is unpredictable at present. We are far from answering simple questions like ‘will the next cycle be larger than the current one?' 'When will the next large eruption occur?' Or even 'when will there be several successive quiet days?' As we learn more about the fundamental processes through studies of internal motions, magnetic flux transport and evolution, relations between active regions, UV irradiance, and solar shape variations we will be vigilant for opportunities to develop prediction tools. Nevertheless, there are several near term practical possibilities to improve the situation with HMI observations.

Far-side imaging and activity index. A procedure for solar far-side imaging was developed using data from MDI[108] (Figure C.7), and has led to the routine mapping of the Sun’s far-side[109]. Acoustic travel-time perturbations are correlated with strong magnetic fields, providing a view of active regions well before they become visible as rotate onto the disk at the east limb. Synoptic images, which are now able to cover the entire far hemisphere of the Sun[110], will provide the ability to forecast the appearance of large active regions up to 2

weeks in advance and allow the detection of regions which emerge just a few days before rotating into view. HMI's full coverage to the limb will allow lower-noise farside estimates.

Predicting emergence of active regions by helioseismic imaging. Rising magnetic flux tubes in the solar convection zone may produce detectable seismic signatures[76] (Fig. C.4), which would provide warning of their impending emergence. Helioseismic images of the base of the convection zone will employ a similar range of p-modes as those used to construct images of the far side. A goal is to detect and monitor seismic signatures of persistent or recurring solar activity near the tachocline. Success here could lead to long-term forecasts of solar activity.

Determination of magnetic cloud Bs events. Potentially valuable information for geomagnetic forecasts - predictions of magnetic cloud Bs (southward field) events - can be obtained from the vector field measurements. Long intervals of large southward interplanetary magnetic field, Bs events, and high solar wind speed are believed to be the primary cause of intense geomagnetic disturbances with the Bs component the more important quantity[111]. It has been shown that orientation in 'clouds' remains basically unchanged while propagating from the solar surface to Earth's orbit[112]. This provides a plausible chain of related phenomena that should allow prediction to be made from solar observations of the geoeffectiveness of CMEs directed toward Earth. Estimates of embedded Bs will be significantly improved by incorporating frequently updated vector field maps into coronal field projections with the potential addition of coronagraphic observations from AIA, WCI, and STEREO.

C.1.3 Scientific Approach

The investigation described above is a comprehensive broad-based investigation into the sources and mechanisms of solar variability and its impact on the space environment. An

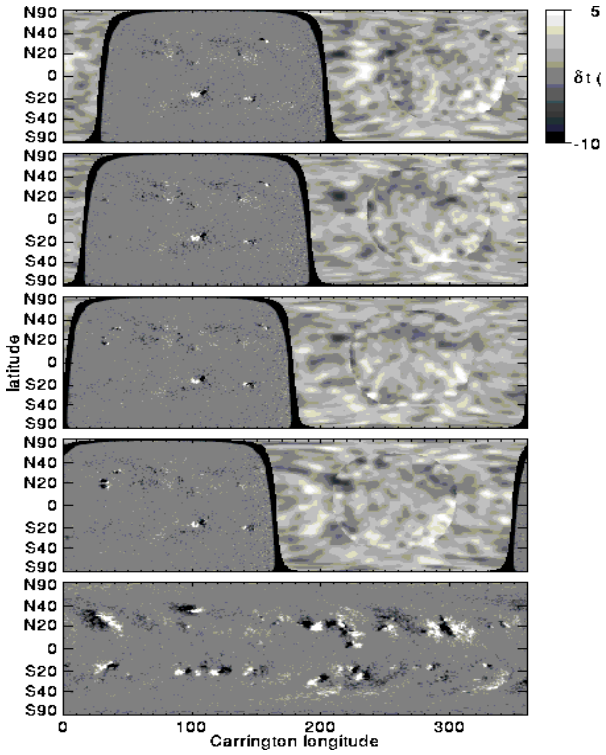

Figure C.7. Composite images of the near-side magnetic flux density (left) and far-side acoustic travel-time perturbations (right) for 1999 April 22-25.[110] The bottom panel shows a synoptic magnetogram for the subsequent Carrington rotation.

investigation with this scope requires dedicated efforts of a diverse team of researchers. HMI investigators are experts in the required disciplines including instrument design and development, data handling and access, instrument calibration, data analysis, theory, modeling, and presentation of results to the broader science community and the public at large. But the opportunity and challenges of LWS, SDO and HMI require a larger effort. The real limit to the scientific return is likely to be the support of people to pursue data analysis and theory development. We will maximize the scientific return by providing convenient access to high-level data products to Guest Investigators (GIs) and other scientists. The members of our research team will also actively participate in the coordinated SDO GI and LWS Theory and Modeling Programs.

HMI data and results will be crucial for the success of the SDO mission by providing necessary key data for the coronal and irradiance instruments, in particular, magnetic field measurements, energetic characteristics of active regions, and flow maps associated with developing active processes. The goal is, in cooperation with the coronal instruments, particularly, with AIA, SIE and WCI, to develop knowledge and understanding of the solar and heliospheric aspects of the Sun-Earth system that directly affect life and society.

Important cooperation will be developed with other space missions and ground-based observatories. In particular, to support STEREO data interpretation, HMI magnetic data will provide the basis for modeling the corona and solar wind around CMEs, as well as indications of the causes of these transients. HMI will also provide global context for Solar-B vector measurements that are focused on specific active regions, and also information on coronal holes and solar wind stream structure used in the interpretation of L1 solar wind monitor data from spacecraft such as ACE. In the area of helioseismology cooperation with the GONG+ project will provide some cross-checks of helioseismic inferences.

C.1.4 Theoretical Support and Modeling

Exploiting the full scientific potential of HMI requires access to advanced theoretical 3-D simulations of global-scale turbulent convection interacting with rotation and magnetic fields; local-domain near-surface magneto-convection simulations of granulation, meso-granulation and supergranulation including realistic equations of state, opacities and radiative transfer; local and global dynamo processes variously within the tachocline and the near-surface shear layer; wave excitation and propagation in magnetized plasmas; and upper atmosphere and coronal magnetic field configurations and their evolution, including the response to footpoint displacements and flux emergence. Given rapid developments in massively-parallel supercomputing, major advances are feasible in these theoretical areas in the next five years as HMI is implemented. HMI Co-Is are playing pivotal roles in such theoretical efforts, but will require suitable organized investments from many programs, including the LWS Theory and Modeling program. Theoretical models for inversion of helioseismic and magnetic data are also extremely important for HMI data analyses. This range of the theoretical efforts needed to exploit fully HMI opportunities exceeds the scope of this investigation. However we must directly support integration of analytical methods and models developed elsewhere into the suite of tools available to the broad HMI team.

C.1.5 Scientific Operation Modes and Requirements

The scientific operation modes and data products can be divided into four main areas: global helioseismology, local-area helioseismology, line-of-sight and vector magnetography and continuum intensity studies. The principal data flows and products are summarized in Foldout 1.L. These four primary scientific analyses cover all main HMI objectives, and have the following characteristics:

- *Global Helioseismology: Diagnostics of global changes inside the Sun.* The normal-mode method will be used to obtain large-scale axisymmetrical distributions of sound speed, density and flow velocities throughout the solar interior from the energy-generating core to the near-surface convective boundary layer. These diagnostics will be based on frequencies and frequency splittings of modes of angular degree (l) up to 1000, obtained for intervals of several days each month and up to l=300 for each 2-month interval. These will be used to produce a regular sequence of internal rotation and sound-speed inversions to allow observation of the tachocline and the near-surface shear layer.

• *Local Helioseismology: 3D imaging of the solar interior.* The time-distance technique, ring-diagram analysis and acoustic holography represent powerful tools for investigating physical processes inside the Sun. These methods are based on measuring local properties of acoustic and surface gravity waves, such as travel times, frequency and phase shifts. The targeted high-level regular data products include:

- synoptic maps of mass flows and sound-speed perturbations in the upper convection zone for each Carrington rotation with a 2-degree resolution, from averages of full disk time-distance maps;
- synoptic maps of horizontal flows in the upper convection zone for each Carrington rotation with a 5-degree resolution from ring-diagram analyses;
- higher-resolution maps zoomed on particular active regions, sunspots and other targets, obtained with 4-8-hour resolution for up to 10-day transits;
- deep-focus maps covering the whole convection zone depth, 0-200 Mm, with 10-15 degree resolution;
- farside images of travel-time perturbations associated with large active regions every 12 hours.

These observations require uninterrupted series of Dopplergrams of lengths 8 to 24 hours with the following characteristics: 50-second (or higher) cadence, spatial sampling of 2 Mm for distances up to 75 degrees from the disk center, and the noise level better than 20 m/s.

• *Magnetography. Complete coverage of magnetic processes in the photosphere.* The traditional line-of-sight component of the magnetic flux is produced as a co-product with the Doppler velocity. Several products will be computed with various cadence (up to 10 minutes) and resolution for use as input to coronal field and solar wind models and correlative studies. To accurately model the global fields the zero point accuracy should be better than 0.1G.

•*The vector magnetic field.* This is one of the most important physical observables of the active solar atmosphere. HMI will produce several standard data series of vector fields. A simple 'magnetograph mode' analysis will be computed continuously in real time for large scale coronal modeling and other space weather applications. With help of inversion techniques[113], HMI will also provide tracked and full-disk vector magnetic field, filling factor, and thermodynamic parameters of photospheric plasma within reasonable errors. The data will be used to measure free energy, stresses and helicity of the magnetic field, providing important input to many prime science objectives and tasks of HMI and other SDO investigations. These polarimetric observations require a few minutes temporal cadence, a spatial sampling of 0.5", and a 0.3% polarization precision to yield 5% accuracy of the magnetic field strength, a few tens of degrees in inclination and azimuth in strong fields.

• *Continuum Intensity: Identification of irradiance sources.* The observations of the intensity in the continuum near the HMI spectral line will give a very useful measure of spot, faculae area and other sources of irradiance. This will be important for studying the relationship between the MHD processes in the interior and lower atmosphere and irradiance variations. The continuum data will be also used for limb shape analysis, and for public information and education purposes. These measurements require calibration of system pixel-pixel gain variations to a level 0.1%, as demonstrated with MDI.

C.2 HMI Science Implementation

The HMI instrument design and observing strategy are based on the highly successful MDI instrument [1] (**Foldout 2.D**), with several important improvements. Like MDI, HMI will observe the full solar disk in the Ni I absorption line at 6768 Å, but with a higher resolution of 1 arc-second. HMI consists of a refracting telescope, a polarization selector, an image stabilization system, a narrow band tunable filter and two 4096² pixel CCD cameras with mechanical shutters. The polarization selector, a pair of rotating waveplates, enables measurement of Stokes I, Q, U and V with high polarimetric efficiency. The tunable filter, a Lyot filter with one tunable element and two tunable Michelson interferometers, has a tuning range of 750 mÅ and a FWHM filter profile of 84 mÅ. Examples of the filter profiles are shown in **Figure C.8**.

C.2.1 HMI Measurement Technique

The basic HMI observables are filtergrams taken at a number of wavelengths and polarizations, all of which are transmitted to the ground. The primary observables, Dopplergrams, longitudinal and vector magnetograms, and continuum intensity images, are constructed from the raw filtergrams by a combination of simple MDI-like algorithms and more complex inversion algorithms. Performing these calculations on the ground is a significant improvement over MDI, because more comprehensive instrumental corrections can be made and sophisticated algorithms can be used in determining the physical solar parameters.

C.2.1.1 Line Choice and Filter Profile

The Ni I absorption line at 6768 Å has been chosen on the basis of our experience with MDI. This line is well characterized and provides continuity with the MDI and GONG helioseismology and magnetic field observations. It has a clean continuum although there are some molecular blends in sunspot umbra. The absence of terrestrial blends allows easy ground calibration and comparison with ground-based data. It has a low-level excitation potential[2] of 1.826 eV with little variation in the depth of formation, so its observables apply to approximately the same height in the atmosphere.

The choice of spectral line for magnetic field measurement is driven by conflicting scientific requirements. For magnetic field measurements, a high effective Landé g factor increases the signal, but it also increases the required dynamic range requirements, from ±6.5 km/s (solar rotation, oscillations, convection, and the SDO orbit) to ±12 km/s (g = 3 and a 2 kG field). The Ni line provides a compromise with an effective[2] g = 1.426, sufficient to reliably measure magnetic fields. ASP observations of an active region in the Ni line (**Figure C.5)** show that this line performs well for vector field determinations.

The inherent dynamic range of the instrument, ±15 km/s, is set by the spectral range of the filter elements. The effective dynamic range is set by the number and wavelengths of the tuning positions. With five positions spaced by 75 mÅ, the dynamic range is ±6 km/s and each additional tuning position adds ±1.5

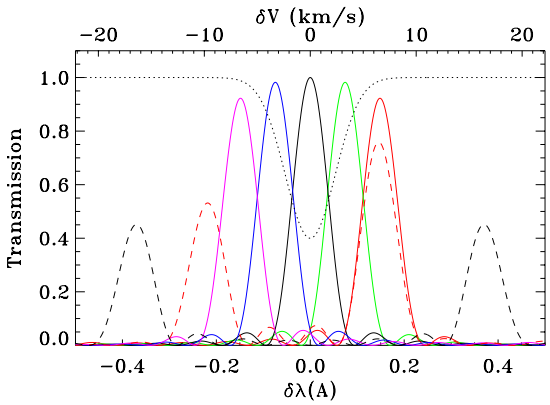

Figure C.8: The solid lines show the HMI filter transmission profiles at 75 mÅ spacing. The black dashed line is the profile used for the continuum filtergram. The red dashed line shows one of the corresponding profiles for MDI. The dotted line shows the Ni I line profile.

km/s. Increasing the spacing much beyond 75 mÅ undersamples the line profile. The dynamic range requirement can be reduced by ±1.7 km/s by changing the tuning positions twice per day to follow the orbital Doppler shift. This may introduce discontinuities and increase the calibration accuracy required. Increasing the number of tuning positions reduces the cadence without improving the accuracy per measurement, increasing the noise per unit time.

C.2.1.2 Observing Sequence

The observing sequence design requires careful consideration of cadence, dynamic range, noise level, required polarizations, solar feature temporal evolution, and instrumental effects. Experience with MDI observations shows that deviation from a uniform sequence, such as for synoptic magnetograms or intermittent campaign sequences, causes noise and false peaks in the velocity spectrum. Therefore, it is essential to use a single continuously running sequence for all HMI observations. The continuity requirement for helioseismology is to recover more than 95% of the Dopplergrams.

Observing requirements for simultaneous measurement of the Doppler velocity and line-of-sight and vector magnetic field impose significant constraints on the sequence. Scanning in wavelength is required for velocity determinations, while making multiple polarization measurements quickly is a priority for the magnetic field. An optimal sequence would provide four polarization measurements at five wavelengths in less than 50 seconds. The available detector technology, however, cannot accomplish this with a single camera. State-of-the-art space-qualified CCD cameras require about 2.4 seconds to readout a 4096² pixel detector. Based on the HMI design, an exposure of 250 msec is required to fill the CCD full well to 80% of capacity (125,000 electrons/pixel). A 20 image sequence results in a cadence well over 50 seconds not including margin.

In order to provide adequate margin in the instrument performance, a two camera design has been adopted. To ensure optimal Doppler performance, one camera is used for the Doppler and line-of-sight magnetic field measurements, the other for the vector field measurements, each with a specific polarization sequence. Based on the above requirements, a baseline observing sequence is detailed in **Figure C.9**. The same sequence of wavelength tunings is used for both the vector and line-of-sight measurements. This limits the wear on the tuning motors and ensures that changes in the tuning sequence do not cause artifacts in the line-of-sight measurements.

To measure the full polarization vector at a given wavelength, at least four filtergrams are required. The four polarization measurements are spread out over twice the time required for the line-of-sight measurements. The choice of polarizations and the order in which they are taken drive the observing sequence design for the vector measurements. The sequence shown in **Figure C.9** determines Q in the first half and U in the second half of the sequence. A ¼ waveplate followed by a ½ waveplate

Time (sec)	0		8		16		24		32		40	45		53		61		69		77		85
λ Tuning	I1		I2		I3		I4		I5		IC	I1		I2		I3		I4		I5		IC
Doppler Seq	L	R	R	L	L	R	R	L	L	R	C	L	R	R	L	L	R	R	L	L	R	C
Vector Seq	1	2	2	1	1	2	2	1	1	2	C	3	4	4	3	3	4	4	3	3	4	C
Polarization	L = I + V = LCP				R = I - V = RCP				1 = I + aQ + bV			2 = I – aQ + bV				3 = I + aU – bV				4 = I – aU - bV		

Figure C.9: Details of the HMI observing sequence: *Time* indicates the beginning of the exposures at a given wavelength. The *wavelength Tuning* positions I1 through I5 are spaced evenly 75 mÅ apart, with I3 centered on the line (see Figure C.8). *Doppler Seq* and *Vector Seq* indicate the order and polarizations settings for the two cameras, with the states L, R, 1, 2, 3, 4 identified by *Polarization*. For $a^2=2/3$ and $b^2=1/3$, Q, U and V have identical noise equal to 0.22% in the continuum. IC is a continuum filtergram taken in linear polarization.

provides the required polarization states while minimizing wear in the mechanisms.

A 45 second cadence is achieved for the Doppler and longitudinal magnetic field and a 90 second cadence is achieved for the vector magnetic field. Including a continuum tuned image in the sequence results in an image cadence of 4.1 seconds for each camera. The exposures and readouts are interleaved. The images from the two cameras will not be combined during normal analysis.

Image data will be compressed using a look-up table followed by the lossless Rice-type compression scheme similar to that used for MDI. This algorithm can be implemented very easily in hardware to run at the required rate, and its performance is well understood. The technique has been simulated using very high resolution images from La Palma, blurring them to make diffraction-limited HMI images, adding appropriate noise and quantization, compressing and decompressing. The compression process adds noise which is statistically well-behaved and is a small fraction of the photon shot noise in magnitude at all intensity levels. A worst case continuum image of a large sunspot required 6.2 bits/pixel, and quiet Sun areas require only 5.5 bits/pixel, Adding a 10% margin to account for potential differences between the La Palma and HMI images gives a baseline compression efficiency of 6.1 bits/pixel, and bandwidth of 50 Mbps to downlink 4096² pixel images with a cadence of 2.05 seconds.

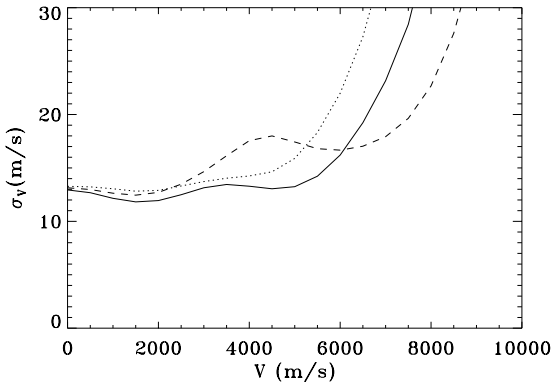

Figure C.10: Doppler velocity noise for the different algorithms. Solid line is for the full maximum likelihood algorithm at B=0 kG, dashed line is for B=2 kG and dotted is for the simple algorithm at B=0 kG.

C.2.1.3 Doppler and Line-of-Sight Flux Measurement Technique

Since the computations of the physical observables are performed on the ground, more sophisticated algorithms than those used for MDI can be applied. The optimal algorithm for deriving Doppler velocity and line-of-sight flux from the filtergrams is a maximum likelihood fit. The performance of this algorithm for Doppler velocity (**Figure C.10**) is very good out to ±6 km/s, with noise of 13 m/s rms at moderate velocities and field strengths. The 0.5 arc-second pixels result in a spatial sampling of 0.37 Mm at disk center and 1.4 Mm at 75º, sufficient for helioseismic studies.

For a line-of-sight field and 100% filling factor, this corresponds to approximately 10 G rms noise in flux density. This corresponds to 4 G for a five minute average, which is consistent with the AO requirements. Fields up to 4 kG can be measured with less than 50% increase in the noise. In order to keep the mean field noise induced by the shutter below 0.1 G, the variations in the actual exposure time must be known to an accuracy of 5 μsec.

A simpler and faster algorithm constructs a Doppler velocity signal from each polarization (LCP and RCP). The Doppler velocity measurement is the average of these signals, and the line-of-sight flux density is proportional to the difference. The individual velocities are derived with a simple explicit algorithm, avoiding the computationally expensive maximum likelihood fit. The performance of this algorithm (**Figure C.10**) is essentially as good as the performance of more complex algorithms for moderate field strength, and will be used where fast processing is required, such as for real time magnetograms.

C.2.1.4 Vector field measurement

A sample strong transverse field signal has been observed with MDI using a sequence similar to the proposed HMI observing sequence. **Figure C.11** shows a clear Q/I polarization signal. MDI is unable to observe U. In the averaged image, linear polarization is visible in the plage, showing that useful signals can be obtained outside of sunspots with a modest amount of temporal averaging.

HMI vector field parameters will be derived with at least two different algorithms. A fast, but not very accurate, algorithm will be applied to the filtergrams as they arrive. A more complex and accurate algorithm will be applied to selected images and to derotated time averages taken over several minutes. The fast algorithm is based on weak-field approximations[3-5]and calibration curves[6, 7], and provides flux density as well as inclination and azimuth of the magnetic field, but not the filling factor or the intrinsic field strength.

The more accurate algorithm fits modeled Stokes I, Q, U, and V signals to the observations using a least-squares minimization method[8] and provides the full magnetic field vector as well as its filling factor. The model profiles are generated with the DIAGONAL algorithm.[9] The minimization uses a singular value decomposition to limit the parameter search to reasonable values and to weight the I, Q, U, and V signals to improve accuracy. This routine is initialized with the results from the simple algorithm supplemented by initial guesses for the filling factor.

The performance of the latter algorithm has been tested by applying it to simulated data generated using a Milne-Eddington (ME) model, based upon realistic solar values of field strengths, filling factors, and ME thermodynamic parameters. Instrumental details such as the actual filter profiles, photon noise and spacecraft velocity are included in these tests. The differences between the inversion result and the input parameters are taken as a measure of the performance of the proposed instrument. The results are summarized in **Figure C.12** and **Foldout 1.K**. More sophisticated algorithms may be used for the inversions, however the ME results are likely to be representative.

As can be seen from **Figure C.12,** the derived precisions meet the requirements of the active region and sunspot science objectives as well as those for eruptive events at a faster cadence than required. The polarization precision is 0.22% versus 0.3% required; the field precision is 0.8% versus 5% required and the azimuth and inclination errors 0.6º and 1.4º, well within the few degrees required by the AO. Observing network fields is more challenging. The total flux density, for example, has a relative error of 32%. However, for most purposes it is possible to average spatially or temporally. Averaging over 7 observations (10.5

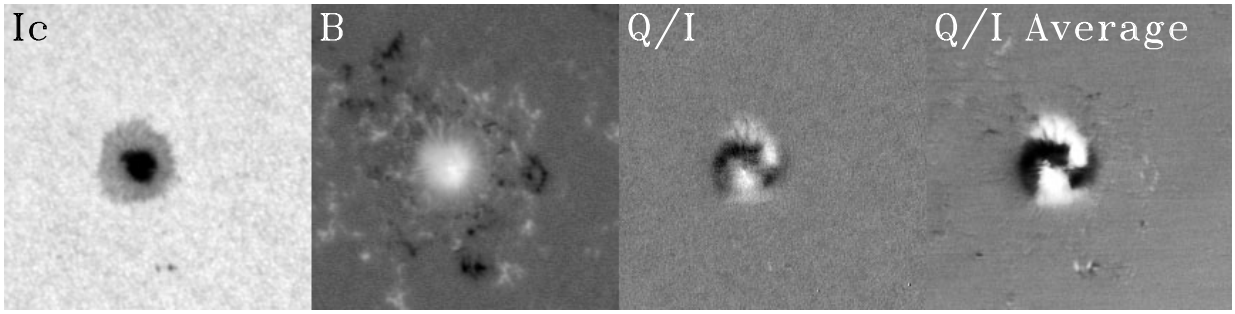

Figure C.11: MDI observations of AR 9516 on 27 June 2001. From left to right: Ic - continuum intensity, B - line-of-sight magnetic field, Q/I - from a single line scan and Q/I Average - a derotated average over 43 observations. The grayscales are not linear in order to accommodate the large dynamic range. The field of view is square of 90Mm on a side with disk center outside the image towards the lower right. The MDI results were taken at a slower cadence than proposed here and without the third tunable element, making them noisier than the expected HMI results.

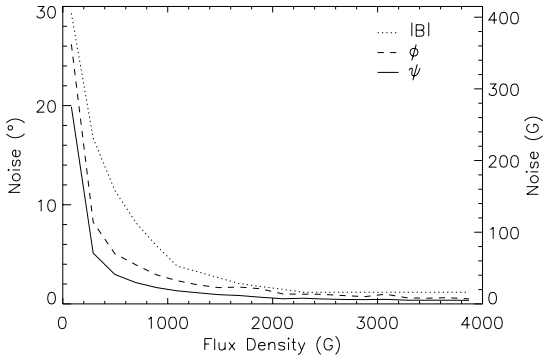

Figure C.12: Azimuth, inclination and field strength at 68% confidence intervals derived from the inversion algorithm. Precisions are for single unaveraged pixels.

minutes) gives a polarization precision of 0.085%. This translates to a sunspot field precision of 6.5 G or 0.3% in |B|, 0.2º in field inclination, 10 G or 0.9% in the transverse field component, and 0.5º in the transverse field direction. For quiet Sun fields, the precision is 6.1 G or 12% in longitudinal flux density, 17 G or 32% in transverse flux density, 13 G or 12% in total flux density, 6.7º in inclination, and 8.9º in azimuth. Comparable improvements can be obtained by spatial averaging.

C.2.1.5 Other Observables

In addition to Doppler shift and field measurements, continuum intensity images will be produced from the continuum filtergram with a small correction for the line contribution. **Figure C.8** shows that the addition of the third tunable element greatly reduces sidelobes which cause crosstalk of velocity and magnetic field into the continuum images. Line depth (modulation) images and various calibration measurements will be produced as needed.

C.2.1.6 Observable Calibration

Several corrections and calibrations will be applied to the raw filtergrams in order to generate observables with required accuracy and precision. The high radiation levels in geosynchronous orbit generate corrupted pixels in the images. These artifacts are easily identified by statistical means and corrected by interpolating adjacent pixels or marked as missing. The filtergrams will be corrected for the bias and actual exposure time and flat fielded. This allows the filtergrams to be interpolated to compensate for relative offsets introduced by the polarization and wavelength selectors and by solar rotation.

The ±3.5 km/s variation in the line of sight velocity due to the SDO orbit provides a means of velocity calibration over a large fraction of the tuning range.

Wavelength and polarization selection are accomplished by rotating elements that may cause small image displacements. In order to allow for spatially interpolating the data, the offsets should ideally be less than 0.1 pixel. Since the optical PSF is sampled without aliasing, larger offsets can be compensated, especially if they are highly repeatable. This also means that one should avoid combining images from the two cameras. Similar problems are introduced by the different alignment of the cameras and any differences in the PSF or flat field.

Since the images are taken at slightly different times, some of the filtergrams, such as the pairs used for measuring polarization, will be interpolated in time to compensate for the change in the line Doppler shift. Simulations show that the needed interpolations can be made without adding significantly to the photon noise.

The measured Stokes parameters are derived from linear combinations of the observations taken in the four polarization states. These need to be corrected for the instrumental effects of the telescope and polarizers to obtain the true (input) Stokes vector. This is performed by multiplication of the observed vector by an instrument response matrix obtained by measuring the response of the instrument to known polarization states.

C.2.2 HMI Instrument Description

The HMI instrument is shown in **Foldout 2.A**. Sunlight travels through the instrument from right to lower middle in the schematic. The front window is a multilayer metal-dielectric filter with a 50 Å bandpass centered at 6768 Å that reflects most of the incident sunlight. The window is followed by the 14 cm diameter refracting telescope.

Two focus/calibration mechanisms, two polarization selection mechanisms and the image stabilization system tip-tilt mirror are located between the telescope and the polarizing beamsplitter feeding the tunable filter. The filter section consists of the following elements, which are contained in a precisely temperature-controlled enclosure:

- A telecentric lens
- An 8 Å bandpass dielectric blocking filter
- A Lyot filter with a single tunable element
- Two tunable wide-field polarizing Michelson interferometers
- Reimaging optics

Following the oven is a beam splitter, which feeds two identical shutters and CCD camera assemblies. There are two mechanisms external to the optics package: a front door, which protects the front window during launch, and an alignment mechanism that adjusts the optics package pointing.

C.2.2.1 Optics

The primary imaging optics are a refracting telescope similar to the MDI design except that the primary lens has a 14 cm aperture compared with 12.5 cm on MDI. This gives a critically sampled diffraction limited image with 1.0 arc-second resolution. The primary and secondary lenses are connected with a low coefficient of expansion metering tube to maintain focus.

The total optical path length is 225 cm with an effective focal length of 485 cm and a focal ratio at the final image of 34.6. The raytrace (**Foldout 2.C)** shows the imaging mode paths in black and the calibration mode paths in red.

The HMI calibration configuration and focus adjustment method is identical to the MDI instrument. Two calibration/focus wheels each contain optical flats of varying thickness in four positions to provide focus adjustment in 16 steps. Besides allowing best focus to be set on orbit, this capability also provides a highly repeatable means for measuring the instrument focus and assessing image quality through phase diversity analysis.

In calibration mode, a lens in the fifth position of each wheel images the entrance pupil onto the focal plane to provide uniformly integrated sunlight. This provides an excellent velocity calibration source for the instrument. Calibration mode images are used to provide Doppler calibrations, monitor the instrument transmission and assess variations in the detector flat-field.

The polarization selectors rotate optical retarders to convert the desired incoming polarization into vertically polarized (s-component) light. The light is folded by the ISS mirror and then split by a polarizing beamsplitter to send the s-component light to the filters while passing the orthogonal light onto the limb sensor. The limb sensors receive the full 50 Å bandwidth, while light for the rest of the instrument continues through the 8 Å bandpass blocking filter located just inside the oven.

A telecentric lens at the entrance of the filter oven produces a collimated beam for the subsequent filters. This ensures that the angular distribution of light passing through the filters is identical for each image point, resulting in a uniform wavelength selection over the detector.

At the exit of the oven, a pair of lenses reimages the primary focus onto the detectors. A beamsplitter evenly divides the light between the two camera paths with a pair of folding mirrors used to provide convenient placement

of the vector magnetic field camera. The shutters are placed near the pupil image.

The glass-vacuum interfaces are anti-reflection coated for high efficiency at 6768 Å. The polarization selection and tuning waveplates will be manufactured to tight wedge and distortion tolerances in order to minimize displacements due to their rotation. The MDI Michelson tuning waveplates met these stringent conditions.

C.2.2.2 Filters

The heart of the HMI instrument is the filter system consisting of the front window, a fixed blocker filter, a Lyot filter with a single tunable element, and two tunable Michelson interferometers. Doppler shift measurements of solar oscillations require a filter system with a very stable and reproducible passband. Both the Lyot filter and the Michelson have temperature compensating designs, and all the filters, except the front window, are mounted in an oven stable to ±0.1 ºC. The filter system enables narrow-band filtergrams to be made across the Ni I 6768 Å line by co-tuning one Lyot tunable element and the Michelson interferometers. The combined filter bandpass is 84 mÅ with a tunable range of 750 mÅ.

The front window is a 50 Å bandpass filter. It is similar to the MDI design that consists of bonded glass optical flats with a multilayer dielectric coating sandwiched in between. The design will be reviewed to ensure that appropriate radiation hardened materials and processes are used in fabrication.

The blocking filter is a three-period all-dielectric interference filter with a bandpass of 8 Å. The MDI blocker transmission profile has a ripple of about 1%, which averages out to less than 0.1% over the beam. The temperature sensitivity of the MDI blocker is 0.2 Å/ºC, and current ion-assisted coating technology will provide an order of magnitude lower temperature sensitivity.

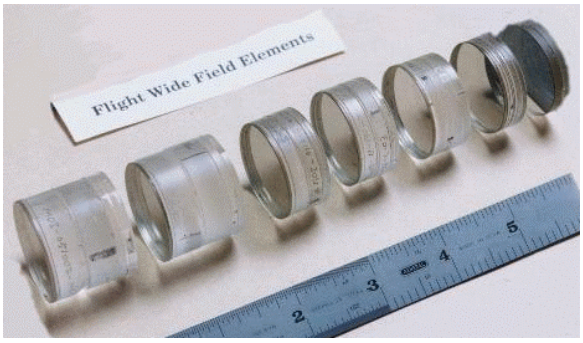

Figure C.13: The MDI Lyot elements and blocking filter.

The wide-field, temperature-compensated Lyot filter (**Figure C.13**) will use the same basic design as the MDI filter with the addition of a fifth tuned element. By pairing KDP or ADP elements with the calcite elements, the temperature sensitivity in the calcite is compensated by an opposite change in the KDP/ADP. The MDI Lyot has a measured temperature sensitivity of less than 8 mÅ/ºC. The five-element Lyot filter has a 1:2:4:8:16 design, and a bandwidth of 380 mÅ. The Lyot components are held in optical contact by optical grease, and are keyed to hold the elements in proper relative alignment.

Figure C.14: The MDI flight Michelsons are shown with the 'Stonehenge' copper spacers to reduce stress. Kapton tape maintains cleanliness prior to installation.

The final filters are a pair of wide-field, tunable solid Michelson interferometers (**Figure C.14**) with a clear aperture of 45 mm and free spectral ranges of 190 mÅ and 380 mÅ (95 mÅ and 190 mÅ bandpasses respectively). The design is identical to that used in MDI and incorporates a polarizing beamsplitter with a vacuum leg and a solid glass leg. The

vacuum leg is maintained with temperature compensating copper standoffs. Tuning is accomplished by rotating half-wave retarders mounted between the interferometers.

The MDI Michelsons have gradients in central wavelength of tens of mÅ across their faces; after calibration these gradients have not significantly affected MDI measurements. For HMI, we expect lower gradients as a result of our experience in fabricating the MDI and GONG Michelsons.

C.2.2.3 HMI Mechanisms

The HMI instrument contains 11 mechanisms of 5 different types, each of which has extensive heritage on the MDI, TRACE, SXI-N, and Solar-B/FPP programs. On-orbit performance with MDI gives us confidence that we will achieve the high performance required of the two most frequently used mechanism types – the camera shutters and the hollow-core motors used for polarization selection and filter tuning. **Figure C.15** shows the positions of each of these mechanisms in the HMI optics package.

The shutters are identical to those on MDI and SXI, and provide relative exposure measurement with an digitization of 4 µsec. Because every HMI image will be downlinked, variations more than an order of magnitude larger than those seen on MDI after 60 million operations will cause no detrimental effects.

The hollow-core motors are copies of the units being used in the SECCHI coronagraphs, which are improved versions of those that have made more than 60 million moves on MDI. The repeatability required of these units has been demonstrated on MDI. The HMI

Mechanism (# required)	Performance		Illustration
Shutter (2) MDI and SXI heritage stepper motor with 94 mm blade.	Maximum Beam Diameter: Exposure Range: Repeatability / Knowledge Required Life:	15.2 mm 40 msec to 90 sec 100 µs / 4 µs 80 M operations	
Polarization Selector (2) and Filter Tuning (3) Motors MDI and SECCHI heritage, 50 mm clear-aperture hollow core motor with 2.5° step size.	Maximum Beam Diameter: Single Operation Time: Repeatability /Accuracy: Required Life:	39.5 mm < 800 msec / 60° 30 arcsec / 2 arcmin 160 M operations	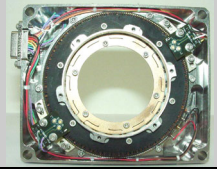
Calibration-Focus Wheel (2) MDI and SXI heritage, 90 mm brushless DC motor with five 30 mm apertures.	Maximum Beam Diameter: Single Operation Time: Required Life:	26.0 mm < 800 msec (1 filter step) 20,000 operations	
Image Stabilization System MDI and Trace heritage ISS design.	Stability: Range: Frequency Range: Required Life:	0.1 arcsec / 30 sec ± 10 arcsecs X & Y 0-200 Hz 10 years	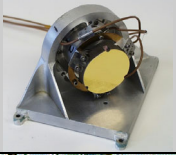
Aperture Door MDI heritage design. Includes redundant drive motors.	Aperture Diameter: Required Life:	160 mm 1000 Operations	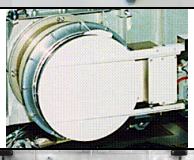
Alignment Mechanism MDI heritage two-leg adjustment system.	Range / Resolution: Required Life:	±720 arcsec / ±5 arcsec 1000 operations	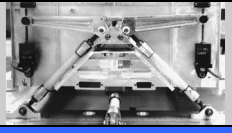

Table C.1 - HMI Mechanisms

focus/calibration wheels are functional copies of SXI-N units with five rather than six elements. They will primarily be used for calibration a few times per day.

The aperture door and pointing alignment mechanisms are based on MDI designs. The HMI alignment mechanism can adjust the optics package pointing over approximately 13 arc-minutes, and will be used to center the solar image on the CCD. The duty cycle will be similar to MDI, where the front door has been operated only three times on orbit and the alignment mechanism is typically used once every eight weeks.

Table C1 details the design and heritage of each of the HMI mechanisms. The shutter, focus/calibration wheel, and wavelength selector mechanisms use brushless DC motors that have high torque margins and robust bearing designs. The mechanisms are constructed for an operational lifetime at the image capture cadence of four seconds for 10 years. Preliminary analysis indicates that angular momentum compensation is not required.

Because of their frequent use, life testing is planned for the hollow core motors and shutters. The lifetests will be performed in a vacuum chamber with the mechanisms at their nominal operating temperatures (20 ºC for the polarization selector and shutters and 35 ºC for the Michelson tuning motors), after having been subjected to vibration testing. The lifetest goal is to achieve the equivalent of 10 years of mechanism moves. The basic design, performance, and life test methodology is similar to the MDI mechanism lifetest.[10]

C.2.2.4 Image Stabilization System

The HMI Image Stabilization System (ISS) is a closed loop system with a tip-tilt mirror to remove jitter measured at a primary image within HMI. This system is based on the MDI ISS limb sensor, mirror and servo loop.

Jitter of photospheric features results in intensity fluctuations that translate into velocity and magnetic field errors. Even though image co-alignment can be performed on the ground, interpolation of images over more than a few tenths of a pixel causes loss of information. The HMI stabilization requirement is set at 0.10 arc-second (3-σ) in each axis.

The ISS uses the image of the solar limb projected onto four orthogonal detectors at the guiding image focal plane. Each detector consists of a redundant photodiode pair. The electronic limb sensor photodiode preamplifier has two gains, test mode and Sun mode, and selectable prime or redundant photodiodes. This is identical to the MDI design, with only an obsolete op-amp being replaced for HMI.

The mirror uses a 3-point piezoelectric transducer (PZT) actuator to remove errors in the observed limb position. The tip-tilt mirror uses the same low voltage PZT's and drive circuitry as MDI. This mirror design has a first resonance (>500 Hz) much higher than the structural mode of the HMI optics package, enabling a simple analog control system.

The range of the tilt mirror is approximately ±12 by ±18 arc-second. This can be increased significantly by using longer PZT's of the same type, if judged necessary during Phase A evaluation of the spacecraft pointing.

The servo gains and other parameters are fully adjustable by ground commands. In particular, offsets can be added to the X and Y axis error signals to change the nominal pointing while maintaining lock. Individual PZT actuator offsets can be specified to fix the nominal position of the mirror anywhere in its range during open loop operation or during special calibrations.

The error and mirror signals are continually sampled, and down-linked to monitor jitter and drift. For special calibrations, these signals can be sampled at a higher rate.

C.2.2.5 CCD and Camera Design

The HMI instrument contains two identical CCD detectors, with a 4096×4096 pixel format. These CCDs are a Marconi Applied Technologies (formerly EEV) design that is an extension of the 2048×4096 pixel devices being used on the Solar-B/FPP. The CCDs are front-illuminated with 12-μm pixels and operated non-inverted to ensure a full well capacity of 150k to 200k electrons with an anticipated readout noise of less than 12 electrons. They will be cooled to below –65 ºC resulting in a 1 nA/cm² dark current (0.2 e^-/pixel-sec). They feature low-voltage clocking of the serial output register to minimize power dissipation in the clock driver electronics. Marconi has a long history of manufacturing excellent CCD devices for space flight applications, including the sensors for Solar-B/FPP and the SECCHI instruments.

In order to achieve readout in less than 3 seconds, they have a readout rate of 2 Mpixels/s through each of four quadrant readout ports. Multiple ASIC and surface-mount electronics packaging technologies minimize the size, mass, and power requirements of the cameras.

A single HMI camera electronics unit controls both CCDs. The HMI camera electronics unit is comprised of:

1. Two CCD Driver Cards, one dedicated to each CCD detector.
2. A camera Housekeeping and Telemetry card with master crystal oscillator clock supply for the CCD Driver Cards.
3. A DC-DC Power Converter mounted on the base of the electronics box.
4. A backplane interface for inter-connection of the daughter PCBs.

Each CCD is clocked from its own dedicated sequencer and clock drivers, and is read out through four correlated double samplers and 14-bit analog to digital converters operating in parallel. The electronics exploits the same basic waveform generator and clock driver circuit topologies used for the SECCHI cameras. This design is implemented in an ASIC similar to the radiation tolerant chip developed for the SECCHI program at Rutherford Appleton Laboratory (RAL), but re-optimized for the 2 Mpixels/s readout rate and signal gain of the HMI CCD. The video output gain and DC offset level are programmable.

Each CCD Driver Card communicates with the instrument computer via an IEEE 1355-SpaceWire link, enabling camera programming, camera command, gathering of housekeeping data, and the transmission of digitized data at up to 200 Mbps. Exposure timing is controlled directly from the HMI instrument computer.

The camera controller contains a DC-DC power converter driven from the 28V spacecraft primary power, while the decontamination heater power for the CCD heads is routed from the HMI power distribution system. The controller's internal temperature and power supply voltages are monitored by the camera electronics while the CCD temperatures are monitored by the HMI computer.

C.2.2.6 Structure

The HMI Optics Package (**Foldout 2.B**) structure is a bonded honeycomb design similar to that used for the much larger Solar-B FPP, the structural model of which recently completed qualification vibration tests. The HMI structure is a six-sided box with a removable cover made up of panels consisting of vented aluminum honeycomb core with aluminum face sheets (**Figure C.15**). The base panel is 25 mm thick with 0.5 mm face sheets, and functions as an optical bench for mounting the optical components except the CCD detector assemblies. All other panels are 6 mm thick with 0.25 mm face sheets.

Construction techniques are the same as those used on the FPP. Panels are joined by bonded L-section sheet connectors and machined sections where necessary. All panel penetrations

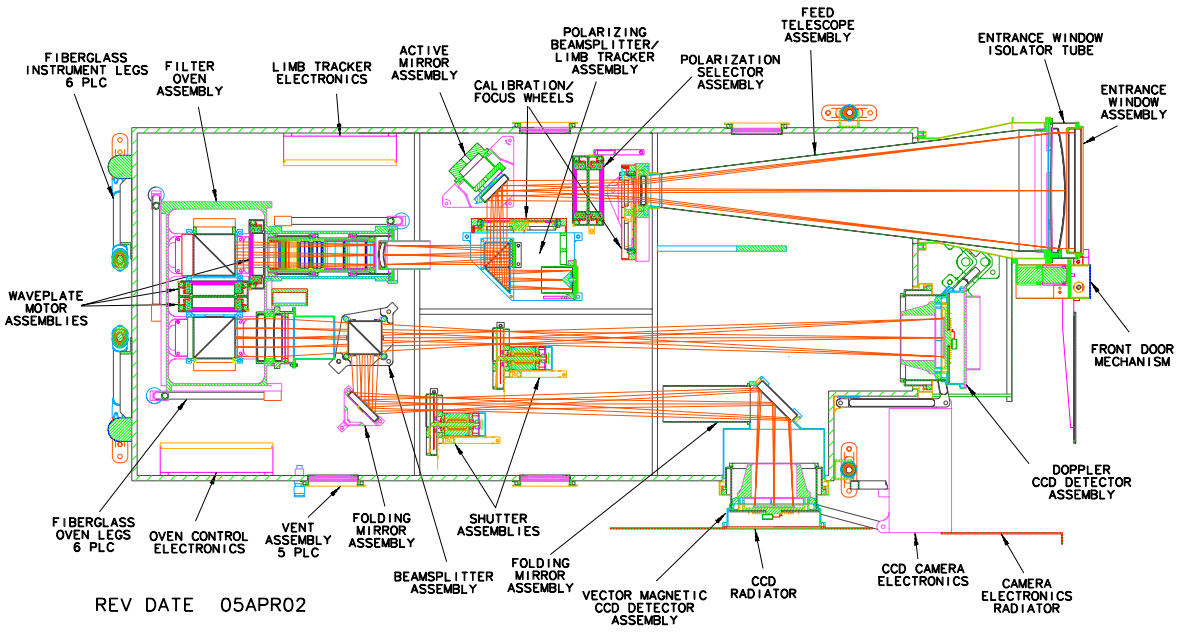

Figure C.15: HMI Optics Package Layout

are sealed with machined closeouts, and have vent paths to the exterior for cleanliness. Component subassemblies are mounted to machined brackets bonded to the optical bench; flanged through-panel inserts capture the brackets to avoid tensile loads on the bonds and crush loads on the core.

The Optics Package mounts to the spacecraft with a 6-link kinematic mounting system incorporating a pointing mechanism similar to MDI. The pointing legs and two forward/side vertical legs are located similar to MDI; the other two are reoriented to share the thrust load between them instead of the single thrust leg design used on MDI. The leg construction is identical to MDI: fiberglass tubes for thermal isolation, with bonded end fittings and rod ends to accommodate pointing motion. An alignment cube will be provided.

A finite element model has not yet been performed, but will be used to maximize the resonance frequency. Based on experience with MDI and FPP, no difficulty is anticipated in achieving adequate stiffness and strength. Both the MDI and FPP optics packages have first mode resonant frequencies of about 85 Hz. A reduce structural mass model will be provide. Mass properties and envelope dimensions are summarized in **Table C4**. The mass estimates are based on measured MDI flight hardware, the detailed HMI solid model, and on similar FPP components.

C.2.2.7 Thermal Control

Evaluation of the thermal performance of the MDI instrument and its effects on the scientific measurements provides the key to achieving the demanding thermal requirements of HMI. The MDI design experience and performance data, hardware experience on the SXI-N, Solar-B and SECCHI programs and expertise in integrated analytical tools are valuable asset to the HMI thermal engineering team.

The HMI instrument is thermally isolated from the spacecraft. Thermal stability is achieved using passive radiator surfaces and controlled heaters. The optics package is mounted on fiberglass legs to thermally isolate it from the spacecraft, and a zone heater maintains the optics package to ±0.5 ºC. The CCD

Thermal Design	Performance
Aperture Door MDI design: Coatings tailored to maintain door near ambient temperature whether open or closed.	Operating / Survival Temps: 0 to 40 °C / -20 to 65 °C Door Open Angle: 180º
Front Window Improved MDI design: Heaters around perimeter minimize recovery time after eclipse.	Operating / Survival Temps: 0 to 50 °C / -20 to 65 °C Max Oper Radial Gradient: 2 °C center to edge Max Recovery After Eclipse: 1 Hour
Filter Oven MDI design: Closed loop thermal control of isolated oven maintains temperature of critical components.	Operating Temperature: 35 ± 0.1°C Max Temperature Drift: 0.01 °C/hour
Optics Package Thermal Control System SXI design. Software-controlled zone heater to minimize gradients and transients.	Operating / Survival Temps: 15 to 25 °C / 0° to 45 °C Setpoint Control: ± 0.5 °C Max Gradient: 4 °C
CCD Detectors FPP design. CCDs thermally decoupled from housing & passively cooled via dedicated radiators.	Oper / Survival Temps: -100 to –30 °C / -120 to 45 °C Decontamination Temp: 20 to 40 °C

Table C.2 - HMI Thermal Requirements

detectors are maintained at less than –65 ºC by passive radiators.

The camera electronics box is partially decoupled thermally from the optics package and passively cooled via its own dedicated radiator. The main (remote) electronics box is passively cooled via a dedicated radiator.

A precisely controlled oven houses all of the narrow band filters. A closed loop heater similar to the MDI design maintains the oven to ±0.1 ºC of a set point with a maximum drift of 0.01 ºC/hr. The oven is mounted on a set of fiberglass legs thermally isolating it from the optics package. The operating temperature of the oven is selectable.

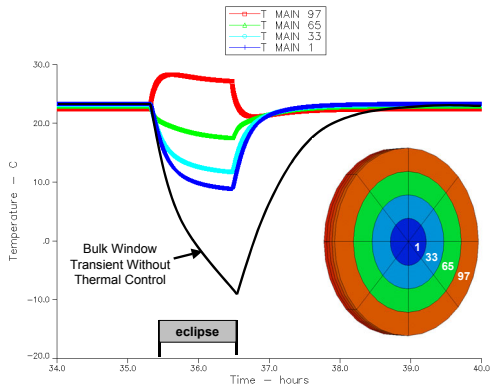

Figure C.16: Front window temperature response to a 1-hour eclipse. The black curve is with no additional thermal control. The colored curves show the temperature response from edge (red) to center (blue) with 9W heat input at the window perimeter during the eclipse.

The front window is thermally isolated from the rest of the optics package, and the absorptivity/emissivity ratio is tailored to operate near 20 ºC. Special attention must be paid to the front window thermal control during eclipses because radial gradients in the window change the instrument focus and birefringence. **Figure C.16** shows the response of the front window to a one-hour eclipse. The first case has no thermal control and indicates a recovery time of three hours. The second case has 9 W of heat applied at the edge of the window during the eclipse. Although the radial temperature gradients increase due to the heat input, the recovery time is less than an hour. Additional thermal modeling will be developed during Phase A and refined in Phase B to achieve an optimal design.

Detailed board-level and box-level thermal analysis is performed to verify that adequate heat sinking is provided. Heaters will either be Kapton film, non-inductive types or power resistors where concentrated heat is required.

C.2.2.8 Electronics

The HMI electronics are shown in the functional block diagram in **Foldout 2.E**, and can be divided into 6 subsystems: control computer; camera electronics; camera interface/buffer; ISS; mechanism control electron-

ics; and power electronics. The camera electronics (C.2.2.5) and ISS (C.2.2.4) were previously discussed.

The control computer subsystem consists of the RAD750 control computer, spacecraft interface, housekeeping data acquisition system, and a PCI bridge that uses a standard compact PCI bus. The BAe RAD750 processor is being used on the SECCHI program, and is the next generation from the RAD 6000 processor with which LMSAL has extensive experience on the SXI-N and Solar-B/FPP programs. The RAD750 control computer runs on a single 3.3-V power source and is packaged on a 3U format card with 128 MB of SDRAM, 256KB of Start-Up ROM (SUROM), and EEPROM loaded with the flight software. The HMI power-on initiates the control computer boot loader that transfers the flight software from EEPROM and starts the control software. The EEPROM data can be modified by ground command if necessary after launch.

A Summit type remote terminal controller connects to the spacecraft redundant Mil 1553 control and low rate data bus. A LVDS bus interface is provided for the 55 Mbps science data stream. The temperature, voltage, current, and other data needed to monitor the HMI instrument are acquired by the housekeeping data system and transferred to the control computer where they are formatted into CCSDS housekeeping packets. The PCI bridge provides a control interface from the PCI bus to the camera interface and buffer, mechanism control electronics, and image stabilization system.

The camera interface and buffer subsystem acquires science data from the two HMI camera systems, optionally compresses the data, and prepares it for transfer to the spacecraft LVDS interface. Two fully independent camera interface and buffer subsystems can simultaneously acquire data from their associated cameras. Each has buffer memory for two images, so that an image can be passed to the data compressor while another image is being acquired from the camera.

The single data compressor acquires data sequentially from the two camera interfaces as directed by the control computer. The data are then formatted into standard CCSDS packets and passed on to the spacecraft interface.

The mechanism control electronics are minor modifications of the control electronics developed for the Solar-B/FPP and SECCHI programs. There will be three mechanism controller boards, which also provide control for the operational heaters.

The main power subsystem, located in the electronics package, provides conditioned power for the digital electronics, mechanisms and the filter oven heater. The HMI power converters contain the inrush current limiting and EMI filters needed to meet the spacecraft EMI/EMC specifications. The power systems have heritage from the TRACE, SXI-N, and Solar-B/FPP programs and are designed around radiation hardened modules such as those from Interpoint or Lambda.

C.2.2.9 Software

The flight software uses the VxWorks operating system and will be written in C and C++ using the Tornado development environment. Extensive experience exists within LMSAL using the VxWorks operating system on programs including HIRDLS, SXI-N, and Solar-B/FPP. The flight software will interface with the spacecraft over a 1553 bus for commands and housekeeping.

Images are produced under control of stored observing sequences selected by ground command. Exposure timing is locked to an internal reference updated by the spacecraft clock signals. The flight software controls the shutters, polarization selectors, tuning motors, and calibration-focus wheels as part of observing sequences. CCD camera data are moved through the data system independent of the

processor bus. Software only controls the transfer of the images, and does not perform any on-board image processing.

The ISS and filter oven heater are closed loop systems that run independently of the flight software with control parameters updated by ground command. Other heaters are controlled by the flight software to maintain temperatures set by ground command A limited amount of on-board fault management is provided to gracefully accommodate certain malfunctions or failures.

The specified control functions will use less than 50% of the CPU capability. Memory will be sized such that less than 50% is used at launch. Capability to upload a new code image and/or to patch the flight code exists in the SUROM. An incremental code development approach will provide additional capabilities to support hardware elements as they are available for test and integration.

C.2.2.10 Radiation Protection

The RAD750 system is latchup immune, rated at 2 Mrad total dose, and has an error rate of 10^{-10} error/bit-day SEU. The other electronics are similar technologies to those used on previous missions. They include rad-hard analog components, digital electronics, FPGAs and ASICs. The power distribution system will be implemented with rad-hard converters (100K rad, no latchup or SEU, no opto-couplers). All power switching components are rad-hard MOSFETs as screened and used on previous programs.

Radiation analysis is performed on each component and, where appropriate, radiation testing of the actual component type is performed to ensure adequate radiation performance and/or shielding requirements. The electronics are designed to provide adequate margins after accounting for radiation degradation and the enclosures provide a minimum of 5 mm of Al for radiation shielding. The HMI CCDs are designed to operate in the geosynchronous orbital radiation environment, and are maintained at a temperature below –65 ºC to minimize radiation damage. The CCD mounting design has 10 mm of Al shielding.

C.2.2.11 Resources and Accommodations

The required spacecraft resources for the HMI instrument are shown in **Table C.3**. A 20% reserve has been allocated both the mass and power. The science telemetry is 50 Mbps with a 10% reserve of 5 Mpbs. The housekeeping telemetry is 10 kbps. Commanding is expected to be one to two uploads per week except during the initial commissioning activities. When in operation, HMI will not have significant power variations. Increased heater power is required during eclipses. A preliminary power profile is shown in **Table C.4**.

The optics package is mounted onto a panel of the instrument module via the support legs. The

Table C.3 HMI Resource Requirements	Optics Package	Camera Electronics	Electronics Package	Cable Harness	Reserves	Total
Mass (kg)	25	3	15	3	9	55
Length (cm)	118	19	32	200	-	-
Width (cm)	53	15	28	-	-	-
Height (cm)	24	7.5	21	-	-	-
Electronics Power (W)	-	15	40	-	11	66
Operational Heater Power (W)	5	0	0	-	1	6
Temperatures (ºC)						
Maximum Survival	45	50	50	-	-	-
Maximum Operational	25	30	30	-	-	-
Minimum Operational	15	0	0	-	-	-
Minimum Survival	0	-20	-20	-	-	-

The camera electronics volume is included in the Optics Package envelope dimensions

Mode	Time	Nominal Power (W)	Reserve (W)	Max Power (W)
Power Off		0	0	0
Survival Heat On	~12 hrs	45	9	54
Instrument On	Normal	60	12	72
Eclipse	< 70 min	69	14	83
Decontam. On	~4 hrs	70	14	84

Table C.4 - HMI Power Profile

HMI electronics box is mounted to the spacecraft separately from the optics package. Locating the HMI electronics box inside the spacecraft could save some mass required for radiation shielding. The optimal location and mounting scheme for the optics and electronics packages will be developed with the spacecraft builder during Phase A.

The HMI instrument has no special environmental requirements beyond GEVS. The spacecraft must meet cleanliness requirements much less stringent than those of EUV instruments and coronographs. HMI will require nearly continuous purging with dry nitrogen until shortly before launch.

C.2.2.12 Calibration

The success of the HMI investigation depends on an excellent calibration of the system. The HMI calibration requirements are summarized in **Table C.5** and are based on our MDI experience. HMI will be thoroughly calibrated before delivery, using techniques developed and proven during the MDI and Solar-B/FPP programs. The LMSAL Sun lab has facilities to calibrate components, subsystems and the complete instrument, using tunable laser, continuum lamp and sunlight sources, in vacuum when necessary. Most of the calibrations will also be performed on-orbit throughout the mission using the built-in capabilities for tuning, focusing, offset pointing and imaging.

For Doppler measurements, the key measurements are the central wavelengths of the Michelson and Lyot filter profiles. All GONG and MDI Michelsons have gradients in central wavelength across the face of the filter, and all have drifted slowly in wavelength over time. The gradients can be measured accurately both on the ground and in orbit, and drifts can be calibrated accurately in orbit using integrated sunlight in calibration mode as a refer-

Parameter	Accuracy	Purpose	Method
Michelsons Central Wavelength	±1 mA for narrow, ±2 mA for wide Michelson.	Accurate zero-point for velocity across the FOV, system transmission profile	Tunable laser (G), integrated sunlight in calibration mode (G, O).
Lyot Tunable Element Central Wavelength	±4 mA at each point in the FOV	Accurate zero-point for velocity across the FOV, system transmission profile	Tunable laser (G), integrated sunlight in calibration mode (G, O).
Michelson & Lyot Transmission Profile	±2% of peak transmission	Calibration of velocity & magnetic field algorithms	Tunable laser, integrated sunlight with spectrometer (G); computation using measured central wavelengths (O).
Blocking Filter Transmission Profile	transmission	Velocity zero-point , removal of "velocity fringes"	Spectrophotometer measurements (G)
Image Scale	0.01%, or 0.25 pixel limb location	Accurate mode frequencies, especially from ridge fitting; limb figure.	Targets (G, lower accuracy), solar diameter measurement (O).
Distortion of imaging system	0.2 pixel goal, with respect to uniform grid	Accurate mode frequencies; limb figure; correlation tracking.	Grid images (G, lower accuracy), S/C offset pointing, eclipses (O).
Distortion due to waveplate rotation	0.05 pixel with respect to reference position	Alignment for velocity & magnetic measurements; correlation tracking.	Local coalignment of continuum images (G & O)
Optical Point Spread Function	5% of peak	Accurate mode frequencies, especially from ridge fitting; limb figure.	Phase diversity inversion using images at various focus positions (G & O)
CCD Point Spread Function	5% of peak	Accurate mode frequencies, especially from ridge fitting; limb figure.	Direct measurement of ensemble of line spread functions (G)
CCD Flat Field	0.1%	Image correction for velocity, magnetic & continuum, limb figure.	Offsets by PZT's, legs, and occasional S/C offset pointing (G & O)
CCD Dark Images, Gain & System Noise	0.1% for darks, 5% for gain & noise	Image correction, noise estimates for observables.	Dark images & light transfer curve measurements (G & O)
Overall Optical Efficiency	0.5%	Long-term instrument monitoring.	Synoptic calibration mode images in continuum (O)
Polarization, Mueller Matrix	~ 1%	Accuracy of longitudinal & vector magnetic measurements	Measurements with accurately varied polarization using Solar-B GCU (G).
Polarization Response Changes	1%	Monitor changes from Mueller matrix measured on ground.	Consistency between ground calibration & observations (O).

G – Ground Calibration; O – On-Orbit Calibration

Table C.5 – HMI Calibration Plan

ence. For normal observing, the two Michelsons and tunable Lyot element are tuned together in wavelength. However, by tuning them independently in a "detune" calibration sequence, the central wavelength of each filter can be measured separately with respect to integrated sunlight, at each pixel on the Sun. These data will be used to calibrate the velocity and magnetic measurements with an accurate spectral response for each pixel.

The imaging system calibrations are simple in principle but are pushed to very high levels of accuracy by the requirements of helioseismology. These are based on analysis of MDI data, and some have already been achieved by MDI such as the flat field, waveplate distortion, PSF measurements, and CCD calibrations.

The observations needed to calibrate the various observables will be taken at different intervals depending on the time scale of the variations. The list of calibration measurements include solar and objective image (detuned) filtergrams used to determine Michelson gradients and flat fields, spatially offset images[11] to determine flat fields, dark exposures, sequences to calibrate the instrumental gain, sequences to determine the offsets introduced by the polarization and tuning mechanisms and sequences to determine the instrumental polarization. Most of these calibrations have been developed for MDI or will be similar to those for other vector magnetographs.

Following the strategy employed for the spectropolarimeter on the Solar-B FPP, a polarization calibration unit will not be included in HMI. The response matrix will be determined through pre-flight calibration using the Ground Calibration Unit (GCU) developed at HAO for the Solar-B spectropolarimeter. The GCU introduces beams whose polarization is varied in precisely known ways into the instrument. Analysis of the HMI data yields the polarimeter response matrix (essentially the Mueller matrix). Redundancy in the procedure allows determination of all relevant parameters of the input beam, GCU and HMI simultaneously. Experience has indicated that the instrument response matrix is very stable with time, and will be monitored in flight by comparing HMI observations with those obtained from well calibrated ground-based instruments such as ASP.

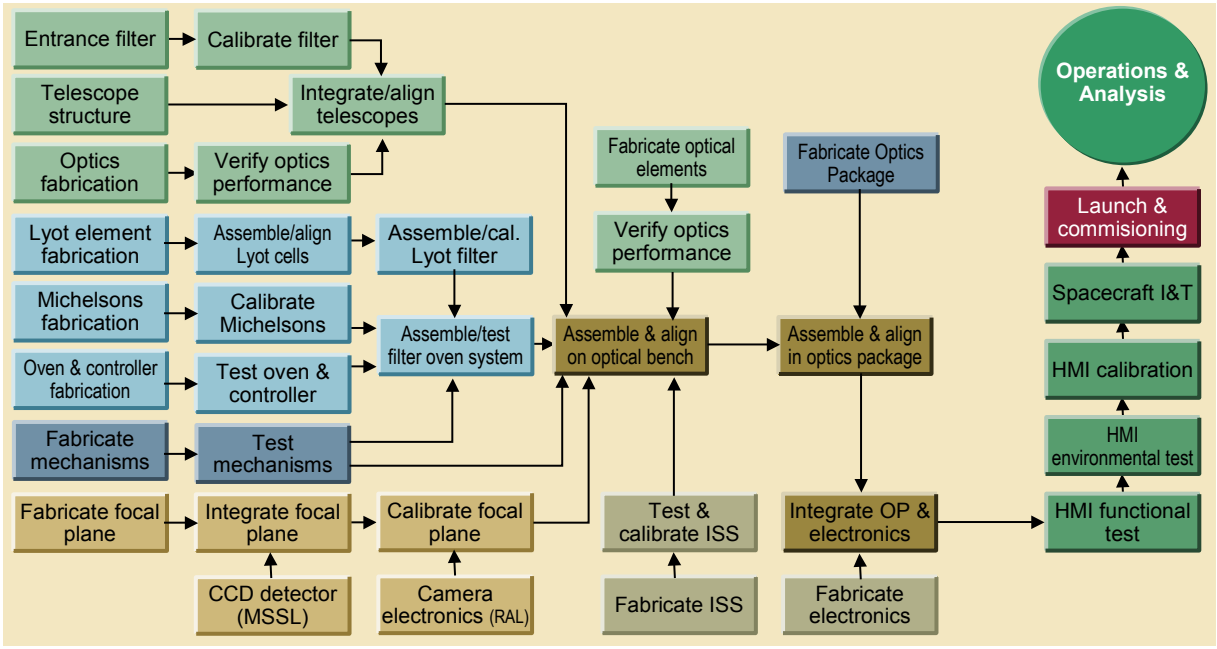

Figure C.17: HMI build, assembly and test flow

C.2.2.13 Build, Assembly, and Test flow

The assembly and testing of optical subsystems will be performed with a series of test and alignment fixtures. The goal is to have the flight optics and filter systems assembled as early as possible in order to undergo calibration and sunlight performance testing. The flight optics will be assembled in test fixtures on an optical table to verify their specifications and performance. The Lyot filter and Michelson interferometers will be characterized in the LMSAL filter lab using both tunable lasers and sunlight. Additional tests of the Michelsons will be performed in vacuum to measure their uniformity and verify their response to thermal transients.

The characterized optics and filters are assembled on an alignment fixture in a clean room. The combined optics and filter system performance will be carefully measured before transferring the subsystems to the flight optics structure. Final tests will be performed with sunlight, both in and out of vacuum. A brassboard camera can be used for much of the characterization testing.

The HMI fabrication, assembly, and test flow shown in **Figure C.17,** allows parallel development of the subsystems and efficient integration of the instrument. LMSAL will develop the electronics, internal mechanisms, optics and filters, and structures. RAL and MSSL will develop the CCDs and camera electronics.

The telescope optics and entrance filter are assembled and calibrated as a subsystem prior to integration with the other optics. The Lyot filter and Michelson inteferometers are assembled and calibrated before installation in the filter oven along with the filter tuning mechanisms. The calibration/focus and polarization selector mechanisms, shutters, ISS and cameras are individually assembled and tested. All these subsystem are then integrated on an alignment fixture for calibration. All units are then transferred to the flight optics package for final testing and calibration.

The HMI electronics are developed and tested with interface simulators and brassboards prior to integration with the telescope to become the HMI instrument. The entire instrument undergoes functional and performance testing prior to the start of the formal acceptance program.

The HMI verification matrix is in **Table C.6.**

Table C.6

HMI Verification Matrix

	Long Form Functional (CPT)	Short Form Functional (LPT)	EMI/EMC/Magnetics	Thermal Balance	Thermal Vacuum	Mass, Center of Gravity	Structural Loads (Quasistatic)	Modal Survey	Sine & Random Vibration	Mechanical Shock	Life Testing (Mechanical)	Pressure Profile (Launch)
FM HMI	T	T	T	T	T							
FM Electronics Box	T	T				T	T	T	T	T		A
FM Optics Package						T	T	T	T	T		
Telescope		T										A
Mechanisms		T							T		T	
Filter Oven System		T		T	T							
Lyot Filter		T			T							
Michelsons		T			T							
CCD Cameras		T										
Structural Thermal Model				T		T	T	T	T	T		

FM = Flight Model T=Test; A = Analysis

C.2.2.14 Relationship with the AIA

If both this HMI proposal and the LMSAL proposal for the Atmospheric Imaging Assembly (AIA) are selected, savings will be achieved in mass, power, and developmental costs. HMI and AIA use the same CCD and CCD header designs, identical (except for the number of data channels) camera electronic designs, similar mechanisms, and the same digital and power electronic systems. The two instruments share very similar flight software and image stabilization systems. Combining HMI and AIA eliminates an electronics box and saves 12.4 kg and 21 W.

C.3 Mission Operations

The goal of the HMI mission operations is to produce a uniform and continuous data set of solar Dopplergrams and magnetograms. Clean multi-day image time series are necessary for time-distance helioseismology analysis, and multi-year time series are essential for solar cycle studies. Our experience with MDI has demonstrated that even subtle changes in the observing program can influence the helioseismology analysis. Except for calibration support, we plan to operate a single observing sequence for the life of the HMI instrument in order to achieve the cleanest possible data set and a minimum level of operator support.

C.3.1 HMI Operations Support

The HMI operations are divided into three phases: launch and initial checkout, nominal operations, and coordinated spacecraft activities. During the first month after launch, the HMI instrument will be run through a preplanned sequence of commissioning and calibration activities. The goal is to verify the correct operation of all the HMI subsystems and to tune any instrument parameters necessary to achieve optimal performance. An extensive set of calibrations will be performed to crosscheck the on-orbit HMI characteristics against the ground calibration and to optimize the long-term on-orbit calibration sequences. A series of observing sequences will be tested to determine the most efficient observing program, both in terms of the resulting science data products and instrument resources. We expect that the coordinated spacecraft activities will be rehearsed. During launch and checkout, HMI personnel will be located at the SDO Mission Operations Center (MOC) with support from the HMI Science Operations Capability (SOC) at Stanford University.

Nominal operations begin at the completion of the commissioning activities, with a single observing program similar to that described in section C.2.1. All observations require the spacecraft to maintain nominal Sun center pointing as specified by the AO with the spacecraft roll adjusted to keep the projection of the solar rotation axis aligned to the HMI coordinate frame (similar to the SOHO spacecraft roll steering law). A complete observable cycle will have a 90 second period, and both cameras will generate a full image every 4.1 seconds. These images will be compressed to 6.1 bits/pixels using lossless compression algorithms resulting in a 50 Mbps downlink. This sequence is only interrupted for occasional calibration and spacecraft activities, and will continue to run through the periodic SDO eclipses. The on-orbit calibration support will be very similar to that implemented with the MDI instrument. A daily sequence of images will be taken in HMI "calibration mode" to monitor instrument transmission and CCD performance. This sequence will run for one to two minutes, and will be scheduled as part of the nominal observing sequence. Approximately every four weeks, a longer performance monitoring sequence will be run to measure the instrument focus, filter and polarization characteristics. This sequence will run for one to two hours, and will likely be initiated through ground command.

The coordinated spacecraft activities envisioned are station keeping and momentum management (SK/MM) activities, and spacecraft off-point and roll maneuvers. During SK/MM activities, the HMI ISS loop will be opened to minimize the large excursions of the active mirror. The HMI ISS commands could be included in the overall SK/MM script as was done for MDI during SOHO maneuvers. The spacecraft off-point and roll maneuvers are similar to those performed by the SOHO spacecraft. These are desired at six-month intervals, near the eclipse season in order to minimize interruptions during the non-eclipse periods. The off-point is used to determine the instrument flat-field, and requires 5 minute dwells at 15 to 20 off-point positions on the solar disk. It is expected that other SDO instruments will also require spacecraft off-

points. The roll maneuver is essential to determining the solar shape, and a similar activity has been performed with MDI to make solar oblateness measurements. The spacecraft rolls allow the instrumental and solar components of the observed shape to be separated, and requires a 360º roll with 15 minute dwells at 12 to 16 evenly spaced roll angles. Depending on spacecraft performance, the off-point activity is likely to take 2 to 3 hours, and the roll activity 6 to 8 hours. The HMI observing sequence for both activities would be similar to the nominal observing sequence and could be initiated as part of a spacecraft script.

C.3.1.1 Science Operations Capability

The HMI SOC will be located at Stanford University and will be responsible for science planning and operations, instrument health and safety monitoring, and data receipt and tracking. Training materials and operations scripts will be developed in coordination with the flight operations team. These activities will be similar to those performed by the Stanford group for the MDI operation and data recovery.

After commissioning is completed, HMI operations will primarily consist of instrument health monitoring and scheduling calibration and coordinated spacecraft activities. Instrument command timelines will be generated as required (a few times per week), and sent to the MOC for upload at the next scheduled command window. The HMI health monitoring will consist of automated processing of HMI housekeeping and summary science data with alerts generated when out of nominal conditions are identified. The summary health status will be reviewed daily, and long-term instrument trends will be monitored for anomalies. The MOC support described in the AO is sufficient to meet all HMI operational requirements.

C.3.2 Data Collection, Analysis, and Archiving

The HMI SOC will manage the essentially continuous stream of data from the instrument at the nominal rate of 50 Mbps for the duration of the mission. The data will be converted to standard formats, calibrated to physical observables, and key higher level scientific products will be produced. The SOC will capture the instrument data from the SDO MOC. It will support any mission operations as required, provide key forecast and planning information, manage the internal data flow necessary to support both pipeline analysis and research, provide high-quality and easily usable data to the scientific community, and provide a safe long-term archive for the key data products.

The observing and analysis procedures for HMI do not differ fundamentally from those we have previously developed for MDI. The principal differences are: the average data rate for HMI is 500 times higher; the processing of filtergrams to observables is performed on the ground rather than onboard, allowing improved but more complex calibration procedures; HMI provides a second channel of filtergrams describing the components of the vector magnetic field, filling factor, and thermodynamic state; and Level-2 and Level-3 science data processing modules will be in place in the processing pipeline from the beginning of the mission.

We believe that the data processing and management approach that has evolved to serve MDI is a good solution to meet the needs of HMI without fundamental redesign. This conclusion is based on conservative estimates for increases in processing power and data handling technology over the next few years.

HMI is committed to an open data policy. As with MDI, HMI data will be available to the science community in each level of reduction as soon as it is available at the HMI SOC. The current best calibration parameters and soft-

ware will also be freely available. HMI will coordinate with the other SDO investigations in Phase-A to determine appropriate formats for data exchange, catalog exchange, and archive locations. We will suggest that the HMI SOC be the NASA designated mission archive for HMI data for the duration of the mission. At the conclusion of the mission the raw, reduced, and calibrated data will be deposited in an appropriate NASA specified data archive.

A number of HMI data products will be of immediate value for space-weather analysis. These products will be computed from the best available data set in near real time for rapid delivery to users. The particular set will be determined in Phase-D but will certainly include full-disk magnetograms, continuum images, and farside activity images.

C.3.2.1 Observing the Archive and Processing Pipelines

A key concept in the SDO mission design is that the whole Sun will be observed all the time and events will be studied by "observing the archive". HMI supports this concept. Apart from calibration activities, HMI is designed to operate in a fixed observing mode throughout the mission, with no special instrument configurations or observing campaigns.

In addition to studies made from the archive data, many of the HMI science objectives require continuous streams of data at a higher level of processing. **Foldout.1.L** is a schematic flow diagram of this processing pipeline. The HMI SOC will provide the software and hardware infrastructure for the pipeline processing and Co-Investigators will provide software modules to generate the higher-level products.

Comparison of and combination of data from HMI and other instruments on SDO and elsewhere is vital to the goal of characterizing and understanding the solar and heliospheric complex. We expect the Virtual Solar Observatory (VSO) to provide the framework and tools for data mining and correlative analysis. We are taking an active role in the design and development of the VSO, and we will build the HMI archive to fully interoperate with VSO and related data archives at Stanford and LMSAL. If the LMSAL AIA is also selected, we plan to integrate the data archives and data processing and distribution functions. This will result in significant cost saving, and in seamless integration of the data access tools provided to the community via the VSO.

C.3.2.2 Science Data Processing

The basic data processing flow required for HMI is data-driven, so it can be summarized as a set of sequential steps. At the first level is data input from the MOC, including sorting and depacketizing with the ability to request data from the MOC to fill in gaps. The resulting ordered raw telemetry will be permanently archived within 30 days. We expect to maintain most recent 30 days of raw data online.

Raw data reconstruction involves decompression and reconstruction into the individual filtergrams, with tags for time and instrument configuration information. These constitute the Level 0 data and will be permanently archived. Since these data correspond simply to the raw data, but are easier to use by the next level of processing. We plan to keep them in an online cache for nominally 3 months.

The Level 0 data are calibrated from suitable combinations of filtergrams to line parameters: continuum intensity and equivalent line width, Doppler shifts and Stokes I, Q, U, and V components. These line parameters can in turn be interpreted by suitable inversions as physical observables such as the thermodynamic state variables, line-of-sight velocity, and magnetic field strength and orientation. Images of the line parameters and/or the derived physical observables constitute the Level 1 data.

Since there is a substantial difference in complexity between the production of line parameters and some physical calibrations, and a significant difference in the degree to which certain line parameters can be used as suitable proxies for the physical observables, the decision as to which observables are to be produced routinely and archived needs to be made on a case-by-case basis. Certainly the Doppler shift data will be fully archived, as they constitute the data for most helioseismic analysis. Magnetograph-method line-of-sight field and continuum intensity will be produced at full resolution but not all of these will necessarily be archived; lower-resolution Level 2 products may be archived instead, as appropriate for the demand. We expect that vector magnetic field data will be routinely produced at full cadence and resolution only around active regions, involving only a few percent of the available data. Line depth (equivalent width) will probably not be produced at all as a regular data product. All Level 1 observables will be available on demand during the mission by processing the Level 0 data.

A pipeline analysis of the Level 1 data will produce Level 2 and Level 3 analysis data products. Level 2 data products are the results of reorganization of the Level 1 data, such as sampling, filtering, map projections, transposition, and transforms. Examples of such products that will be regularly produced and archived include temporal averages (~10 min) of derotated line-of-sight magnetograms from the magnetograph method, and full-cadence spatial averages (~4 arc-sec resolution) of the Dopplergrams. If the Level-1 data are not archived, documentation of the algorithms, of the actual code, and of the calibration data used to produce them from the Level 0 data will accompany the higher-level data products as ancillary information. Level 3 data represent the results of scientific model analysis, such as helioseismic mode fits, mode inversions, magnetic and velocity field reconstruction, and feature identification. The exact set of analysis products is to be determined in Phase D. It will include results of global-mode helioseismic analysis of the Doppler data up to medium degree, and local-area helioseismic analysis performed over regular grids, including ring-diagram and time-distance analysis and acoustic holographic imaging. It will also include such derived Level 3 information as magnetic field configurations and feature identifications.

Table C.7 shows the various levels of data products with estimates of the volumes processed, cached, and permanently archived. Whether data at any level are stored compressed or uncompressed will depend on the relative costs of storage and processing. For purposes of estimating the requirements we assume only a minimal compression factor, achievable for example by disk cropping. The cache period for the Level 1 products represents an estimated average for selected products held online for the duration of the mission

Level	Description	Examples	Rate [GB/day]	Rate [TB/yr]	Cache [day]	Archived [%]
Raw	Telemetry	-	600	200	30	100
0	Filtergrams	-	1000	400	100	100
1	Observables	V_{LOS}, B_{LOS}, I_c, Vector Field Parameters	400	160	600	30
2	Reorganized data	Spatial/temporal Samples, Averages; Synoptic Maps	10	3	3000	100
3	Inferences	Global Modes, Analysis Maps, Farside Images, Coronal Fields	<1	<1	2000	100

Table C.7 – HMI Data Archive

and others for only a minimal period.

If the vector magnetic field is removed from the HMI "suite" the data volume of raw data will be reduced to half but the volume of higher-level products will be essentially unchanged.

C.3.2.3 System Architecture

Based on experience with MDI processing of similar data, the system hardware configuration is currently planned as a processing farm of 100 dual-CPU Intel servers with standard 72 GB disks and Linear Tape Open (LTO) and/or high density DVD technology for offline and near-line storage. The required combination of online and near-line cache storage is about 400 TB, and the required amount of permanent offline storage is around 450 TB per year of operation. The particular hardware architecture for the processors and data archive media will be determined two years before launch. The only constraint is the use of a Unix-family operating system to allow reuse of much of the MDI code.

The software architecture will be the basic architecture of the MDI system. Particular changes will be made to handle the HMI telemetry stream and required data product generation. A new simulation subsystem will be built to generate the telemetry formats and rates expected from HMI. There will be provisions for inserting known data so that data validation at each processing level can be performed.

The current MDI components of data validation, pipeline execution, standard data product generation, parallel virtual machine, data storage management, database server, data catalog, Oracle DBMS, media archive server, quality reporter, job management, SOAP data query URL, and extensive data export methods will be retained with modifications for the HMI demands. As a result, large-scale system prototyping can begin immediately following the initial system engineering studies. Changes do need to be made to data formats, and to remove hardware specific dependencies from some components.

C.3.2.4 Data Organization

The MDI data management approach was built around the concept of using a widely accepted standard data format (FITS) for most data products, and organizing the data archive by collections of such files. While this approach proved sound from the viewpoint of handling what was at the time a comparatively large data archive and providing useful data to the community rapidly with comparatively little user effort and required support, it imposed constraints that proved a serious inconvenience in the effort to provide the best calibrated data. These arose primarily from the necessity of binding the ancillary per record data to the image data, so that any change in a single calibration value, for example, required re-archiving an entire set (hour or day) of images.

An alternative approach is to archive the data in a private format suitable for quick access and manipulation, and to provide the necessary tools for users to be able to interpret the data and process them on the fly. We intend to follow a compromise path for HMI. We will produce higher level data products, but keep the data in very simple private formats, and provide basic tools to convert them to a standard format as required. An example is detachment of the header and data records of FITS files in the archive, to be combined at the point of access. This will allow us to maintain the powerful and efficient MDI data system for managing the bulk data via the database of image sets and a mixed-media archive, while also benefiting from the ability to use a complete online archive of ancillary data at the record level.

C.4. SCIENCE TEAM

There are two key aspects to the selection of a science team. First is to assure that the capabilities are present to complete the development of the flight program. No less important is the need to assure that those with the knowledge and capability to complete the science investigation are committed to the program. The HMI Science Team includes the Co-Investigators and other named individuals referred to as Associated Investigators (AI).

The Science Team as a whole is dedicated to ensuring that the best possible science investigation is accomplished within the SDO-HMI program. The HMI Science Team consists of leading experts in all of the science goals of the HMI investigation.

During Phase-A only the Stanford, LMSAL, HAO, MSSL, and RAL Co-Is have identified tasks. In Phase B-C the HAO definition role is complete. In Phase D a number of Co-Is will provide software for use in the level-1 through level-3 processing pipeline. This software will allow timely calibration of the data from the beginning of the flight phase and the production of higher level science data products required for later science analysis. These data products are those that require substantial volumes of data and processing that can not be expected to be available at Co-I and other science institutions. In the first two years of Phase-E (E-1) the Stanford, LMSAL, HAO, and international investigators will pursue their full science investigation as well as operations, data processing, calibration as appropriate. The US Co-Is who provided code in Phase-D will participate in the calibration to ensure the proper functioning of the code and algorithms and will pursue a reduced science investigation - sufficient to verify that the algorithms developed yield the science insights intended. In the final years, Phase E-2, the Stanford and LMSAL investigators will continue their operations and processing roles but will pursue only similarly limited science investigations. The support for the full exploitation of the HMI science opportunities by US investigators during this phase must come from sources other than the primary HMI program. This plan is consistent with the requirements specified in the AO Section 1.6 paragraph 2. The plan is outlined in Table C.4.1.

The Investigator team is listed in the table in Table C.4.2 on the next page. For each investigator the Phase A-D roles are identified.

Phase	A	B	C	D	E-1	E-2
Stanford	Full	Full	Full	Full	Ops, Data, Calib, Science	Ops, Data, Some Science
LMSAL	Full	Full	Full	Full	Ops, Calib, Science	Ops, Some Science
MSSL	Yes	Yes	Yes	Yes	Science	Science
RAL	Yes	Yes	Yes	Yes	Science	Science
HAO	Line Sel.	none	none	Code Develop	Calib, Science	none
Other US	none	none	none	Code Develop	Calib, Some Science	none
Other Intl					Science	Science

Table C.4.1 - Team Participation in Mission Phases

Name	Role	Institution	Phase B,C,D	Phase-E
Philip H. Scherrer	PI	Stanford University	HMI Investigation	Solar Science
John G. Beck	A-I	Stanford University	E/PO Science Liaison	Surface Flows
Richard S. Bogart	Co-I	Stanford University	Data Pipeline and Access	Near Surface Flows
Rock I. Bush	Co-I	Stanford University	Program Manager	Irradiance and Shape
Thomas L. Duvall, Jr.	Co-I	NASA Goddard Space Flight Center	Time-Distance Code	Helioseismology
Alexander G. Kosovichev	Co-I	Stanford University	Inversion Code	Helioseismology
Yang Liu	A-I	Stanford University	Vector Field Observable Code	Active Region Fields
Jesper Schou	Co-I	Stanford University	Instrument Scientist	Helioseismology
Xue Pu Zhao	Co-I	Stanford University	Coronal Code	Coronal Field Models
Alan M. Title	Co-I	LMSAL	HMI Instrument	Solar Science
Thomas Berger	A-I	LMSAL	* Vector Field Calibration	Active Region Science
Thomas R. Metcalf	Co-I	LMSAL	* Vector Field Calibration	Active Region Science
Carolus J. Schriiver	Co-I	LMSAL	AIA Liaison	Active Region Science
Theodore D. Tarbell	Co-I	LMSAL	HMI Calibration	Active Region Science
J. Leonard Culhane	Co-I	MSSL, University College London, UK	HMI CCD Cameras	Active Region Science
Richard A. Harrison	Co-I	Rutherford Appleton Laboratories, UK	HMI CCD Camera Electronics	Active Region Science
Bruce W. Lites	A-I	High Altitude Observatory	* Vector Field Inversions	Active Region Science
Steven Tomczyk	Co-I	High Altitude Observatory	* Vector Field Inversions	Active Region Science
Sarbani Basu	Co-I	Yale University	* Ring Analysis Code	Helioseismology
Douglas C. Braun	Co I	Colorado Research Associates	* Farside Imaging Code	Helioseismology
Philip R. Goode	Co-I	NJIT, Big Bear Solar Observatory	* Magnetic and Helioseismic Code	Fields and Helioseismology
Frank Hill	Co-I	National Solar Observatory	* Ring Analysis Code	Helioseismology
Rachel Howe	Co-I	National Solar Observatory	* Internal Rotation Inversion Code	Helioseismology
Jeffrey R. Kuhn	Co-I	University of Hawaii	* Limb and Irradiance Code	Irradiance and Shape
Charles A. Lindsey	Co-I	Solar Physics Research Corp.	* Farside Imaging Code	Helioseismology
Jon A. Linker	Co-I	Science Applications Intnl. Corp.	* Coronal MHD Model Code	Coronal Physics
N. Nicolas Mansour	Co-I	NASA Ames Research Center	* Convection Zone MHD Model Code	Convection Physics
Edward J. Rhodes, Jr.	Co-I	University of Southern California	* Helioseismic Analysis Code	Helioseismology
Juri Toomre	Co-I	JILA, Univ. of Colorado	* Sub-Surface-Weather Code	Helioseismology
Roger K. Ulrich	Co-I	University of California, Los Angeles	* Magnetic Field Calibration Code	Solar Cycle
Alan Wray	Co-I	NASA Ames Research Center	* Convection Zone MHD Model Code	Convection Physics
J. Christensen-Dalsgaard	Co-I	TAC, Aarhus University, DK	* Solar Model Code	Helioseismology
Bernhard Fleck	Co-I	European Space Agency	ILWS Coordination	Atmospheric Dynamics
Douglas O. Gough	Co-I	IoA, Cambridge University, UK	* Local HS Inversion Code	Helioseismology
Takashi Sekii	Co-I	National Astron. Obs. of Japan, JP		Helioseismology
Hiromoto Shibahashi	Co-I	University of Tokyo, JP		Helioseismology
Sami K. Solanki	Co-I	Max-Planck-Institut für Aeronomie, DE		AR Science
Michael J. Thompson	Co-I	Imperial College, UK		Helioseismology

Table C.4.2 - HMI Science Team *** Phase D only**

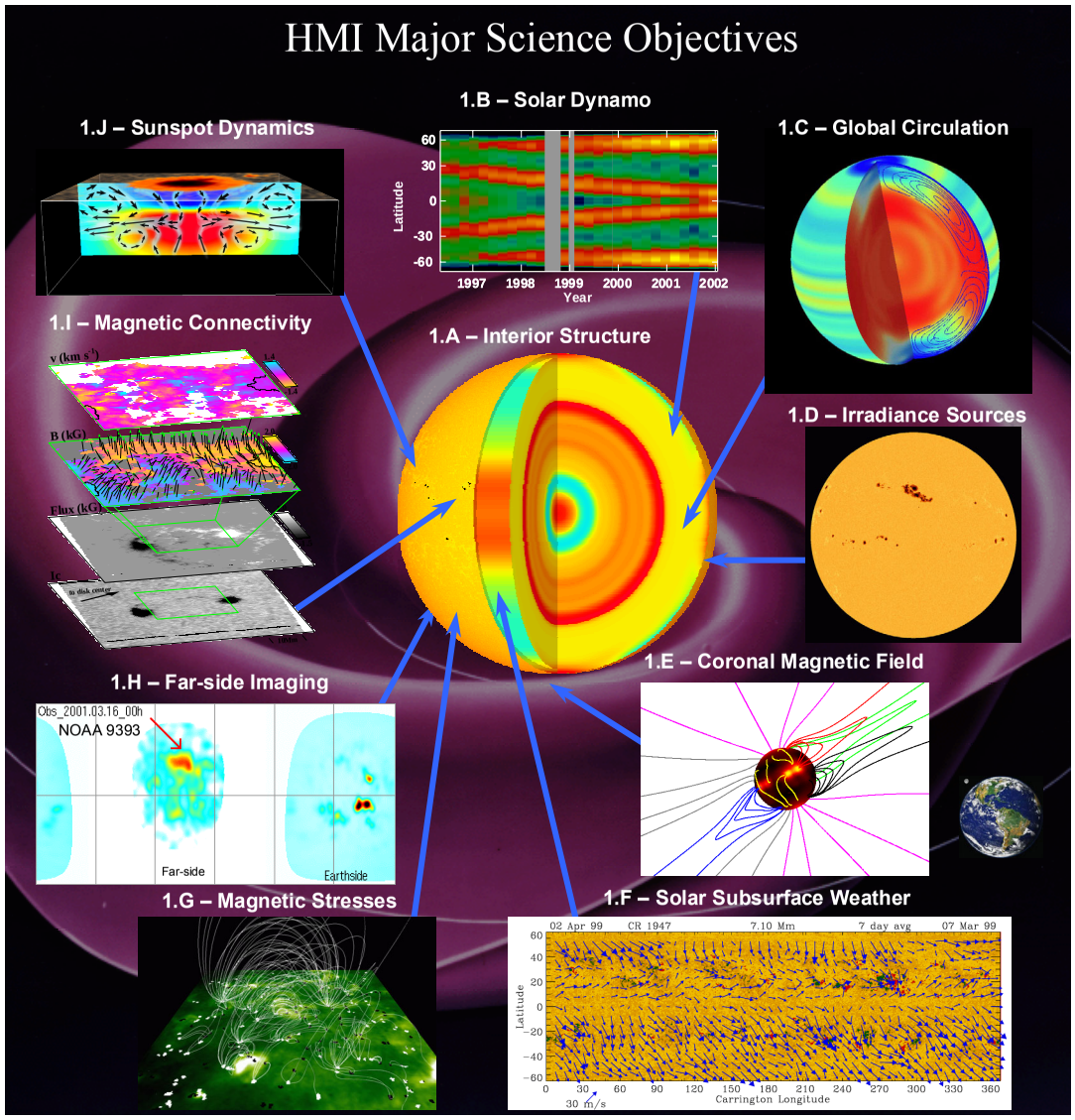

1.K - HMI Observables

Doppler Velocity	
Cadence	45 s
Precision	13 m/s
Zero point accuracy	0.05 m/s
Dynamic range	±6.5 km/s
Line-of-Sight Magnetic Flux	
Cadence	45 s
Precision	10 G
Zero point accuracy	0.05 G
Dynamic range	± 4 kG
Continuum Intensity	
Cadence	45 s
Precision	0.3%
Accuracy pixel to pixel	0.1%

Vector Magnetic Field	
Cadence	90 s
Precision:	
Polarization	0.22%
Sunspots (1kG<|B|<4kG) *	
|B|	18G
Azimuth	0.6°
Inclination	1.4°
Quiet Sun (0.1kG<|B|<2kG) *	
|B|	220 G
Total flux density	35 G
Azimuth	15°
Inclination	18°

* See Figure C.12 for details

1.L - HMI Data Products

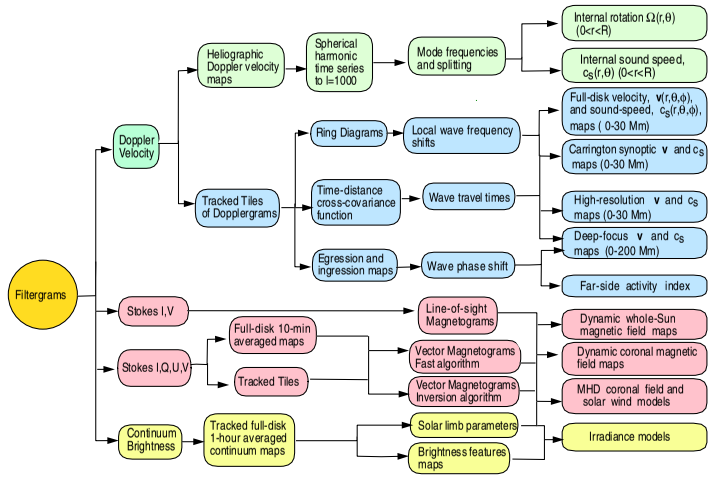

Figure Captions

1.A) Sound speed variations relative to a standard solar model.
1.B) Solar cycle variations in the sub-photospheric rotation rate.
1.C) Solar meridional circulation and differential rotation.
1.D) Sunspots and plage contribute to solar irradiance variation.
1.E) MHD model of the magnetic structure of the corona.
1.F) Synoptic map of the subsurface flows at a depth of 7 Mm.
1.G) EIT image and magnetic field lines computed from the photospheric field.
1.H) Active regions on the far side of the sun detected with helioseismology.
1.I) Vector field image showing the magnetic connectivity in sunspots.
1.J) Sound speed variations and flows in an emerging active region.

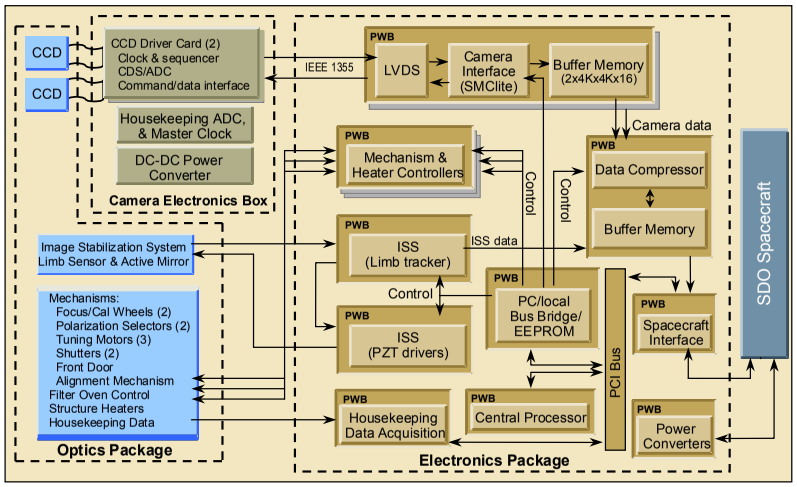

2.E - HMI Functional Block Diagram

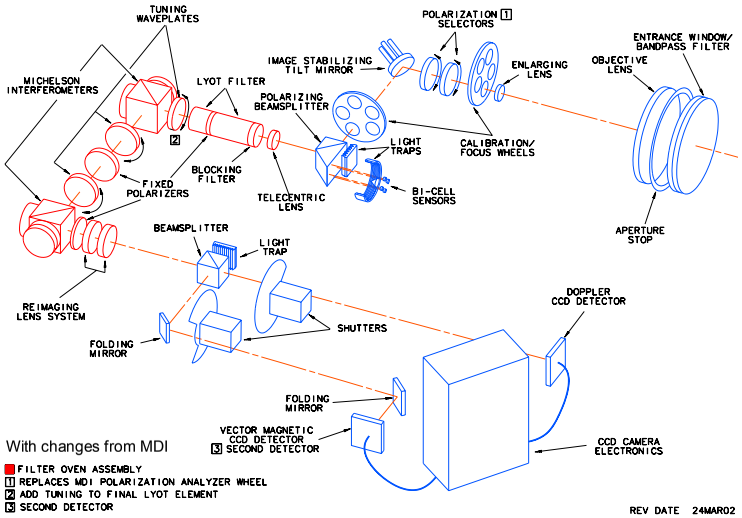

2.A - HMI Optical Schematic and Layout

2.D - MDI Flight Optics Package

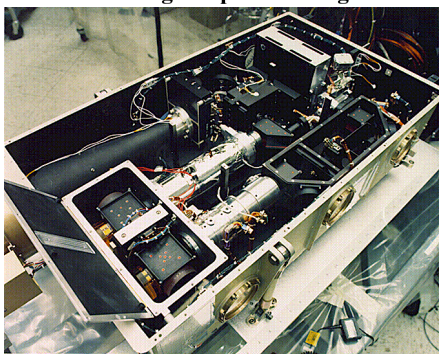

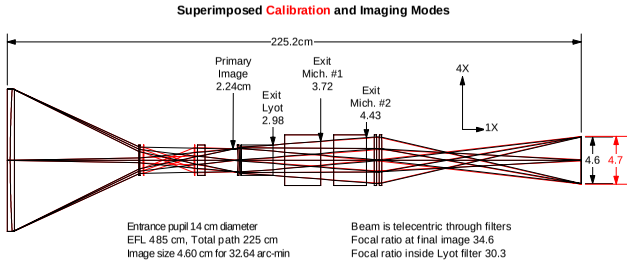

2.C - HMI Optical Design Raytrace

2.B - HMI Optics Package Structural Design

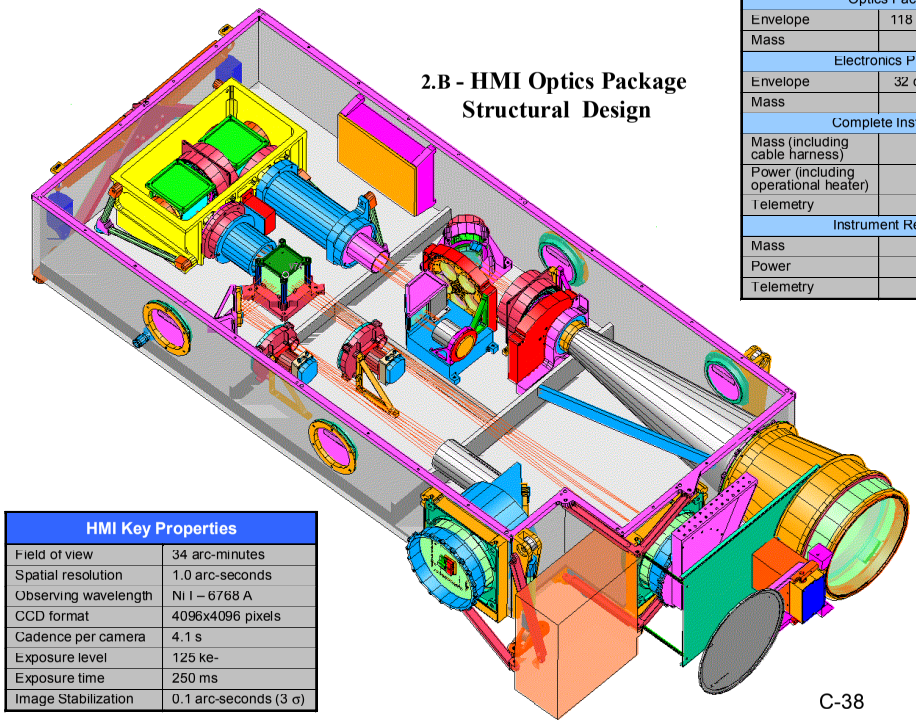

HMI Resources	
Optics Package	
Envelope	118 cm x 53 cm x 24 cm
Mass	28 kg
Electronics Package	
Envelope	32 cm x 28 cm x 21 cm
Mass	15 kg
Complete Instrument	
Mass (including cable harness)	46 kg
Power (including operational heater)	60 W
Telemetry	50 Mbit/s
Instrument Reserves	
Mass	9 kg
Power	12 W
Telemetry	5 Mbit/s

HMI Key Properties	
Field of view	34 arc-minutes
Spatial resolution	1.0 arc-seconds
Observing wavelength	Ni I – 6768 A
CCD format	4096x4096 pixels
Cadence per camera	4.1 s
Exposure level	125 ke-
Exposure time	250 ms
Image Stabilization	0.1 arc-seconds (3 σ)

D.1 EDUCATION AND PUBLIC OUTREACH PLAN

D.1.1 Overview and Objectives

"Our Sun is the only star proven to grow vegetables." This comment from the HMI PI underscores the importance of the Sun to human society. SDO's study of our star and its effects on Earth provides a singular opportunity to engage the public in scientific exploration and to work with educators to improve the teaching of science, math, and technology. Using public interest in SDO as a "hook," we intend to improve science literacy and public understanding of the Sun's role in the Earth's environment. Our key E/PO goal is to produce and disseminate solar science related information, materials, and activities to aid educators and the general public in understanding the star we live with. Multiple partnerships and student involvement provide leverage to expand the scope and effectiveness of our products. Our ultimate mission is to improve science literacy by inspiring and engaging people's imagination

In Phase A we will work with other SDO instrument teams and with the LWS E/PO program to develop a coordinated program.

D.1.2 Activities

Drawing upon the resources of our existing partnerships, forging new collaborations and jump-starting a program based on proven activities, our multi-faceted, highly leveraged E/PO program will have national impact. With undergraduates trained in the presentation of science materials, we will extend our reach into schools to field-test and assess developed activities. Similar programs have been piloted at Co-I institutes with great success.

The PI and Co-I institutes already have dynamic E/PO programs. These feature the award-winning Yohkoh Public Outreach Project (YPOP), SOLAR Center and TRACE websites[1]; the SOLAR B exhibition at the Chabot Space and Science Center[2]; teacher training workshops and media; science museum partnerships; and a wide range of popular curricula and educational resources that highlight the superb imagery and findings of previous missions. Co-Is routinely visit local schools to present videos, give talks and observing sessions, and distribute materials. Many participate in the Astronomical Society of the Pacific Project ASTRO, a national astronomy education NSF funded program. We have produced and distributed thousands of posters related to the Sun.

We propose to expand this successful work by partnering with Stanford's Haas Center for Public Service[3] and collaborating with science and education institutes. This will produce a dynamic, coordinated, and leveraged program that addresses our broader goals through three specific means:

- **Student Involvement/Service Learning:**

We will integrate university undergraduate students into our E/PO program. The students will work with scientists to develop, field-test, and assess educational materials. Students will also assist the team in developing information and resources for the press and general public. Some students will be involved with data analysis.

- **K-14 Activities and Involvement:**

With educators, we will develop, test, and assess a unified collection of science educational material. The goal is to quickly begin enhancing science literacy to make an immediate impact on classrooms even before mission data become available. Once students and the public are primed on the Sun, they will be more excited by SDO and eager to learn about its findings. Students and scientists will disseminate the material through teacher workshops, master teacher programs, the NSTA, and partnering institutes. Re-

sources supporting the activities will be submitted to NASA CORE for distribution.

- **Public Outreach and Access:**

After launch, we will focus on communicating the research results of the mission to the press and general public. To share the excitement of discovery, we will provide a direct link to the latest data and key scientists. Using our successful SOLAR Center website as a model, we will feature live solar image feeds, daily "solar weather" reports, weekly solar "nuggets", alerts of solar activity, a panel of solar astronomers to field questions on-line, and chat rooms for the public and educators. Existing relationships with the press and science magazines will be nurtured, as new relationships are established, so that the E/PO team will be an appropriate first source of information about solar activity. With the support of our students, we will prepare background materials to support NASA press releases and provide a reference to the general public. We will collaborate with science museums to distribute these materials.

D.1.3 Partnerships

We have existing or newly arranged partnerships with a variety of science and education institutes. These include Chabot Space and Science Center, Oakland, CA; The Tech Museum of Innovation, San Jose, CA; Morrison Planetarium (California Academy of Sciences), San Francisco, CA; Lawrence Hall of Science, Berkeley, CA: the Institute for Imagination and Innovation in Science Education (IIISE – a community college group), Milpitas, CA; the Haas Center, Stanford, CA. (Participation is summarized in table D-1.)

D.1.4 Collaboration with the AIA Team

Our most precious resource is collaboration with enthusiastic individuals who can supply singular and critical expertise to the program. If the LMSAL AIA is selected we will develop a merged program to include AIA components along with the LMSAL HMI role. Participants in the AIA team who are partnered with LMSAL have significant expertise in developing highly successful E/PO programs and materials. Drawing upon AIA's partnerships with students, science museums, and educational institutes we can pool resources to develop programs and materials; broaden our ability to distribute materials; share coordination and management roles; leverage off existing programs; coordinate student programs; and test our educational products in more diverse environments.

D.1.5 Implementation

We will train our involved students through a series of seminars and weeklong summer sessions. The Haas Center and partner institutes will pair the students with elementary, middle, and high schools in the local area to field-test science related materials, assess their value, and adjust the activities accordingly.

LMSAL, Stanford, Montana State University (MSU), and SAO have programs that involve science and technology students with educational and public service institutes. We propose to directly partner with Stanford's Haas Center to leverage our E/PO programs. The Haas Center supports over 40 programs that connect students with outside educational and public service institutions. Haas is nationally recognized as first[4] amongst this type of organization. Working with its partnering institutes, Haas is able to provide selection, training, support, and management of students to work with the science team. Haas will assist development of corporate donations for our competitively selected undergraduate "Science Fellows" stipends. We will work directly with the Haas Center Director, Nadinne Cruz, to develop this model student program that will be exportable to other institutions.

Haas also has a unique program to integrate service learning into the classroom. Haas works with faculty to generate assignments that benefit community institutes or adapt courses to a particular goal such as "Commu-

nicating Science." UC Berkeley has a similar program about which students remark the course "changed their life." Some have gone on to focus on careers in education as a result of participating in the program.[5]

The Haas Center has success with social science service learning and is eager to extend this program to science and technology. Possible service-learning opportunities include a public-oriented online LWS magazine, multimedia presentations of mission results, and generation of educational materials to support press releases. We expect to work with 20-30 students a year in this service-learning model. We will work with Haas and local faculty to develop an effective model program, exportable to a variety of institutes.

D.1.6 Yearly Focus Model

We will focus on developing one major, coordinated educational curriculum or program each year, for the development phase (B-D) of the mission. Educational materials will support the focus; Science Fellows will test the activities in classrooms; teacher workshops through partnering science museums will train in use of materials; webcasts and videos will present the focus activities; and DVDs will allow for use of the material in distance learning. Example projects include:

- Creating a solar-based interactive planetarium program appropriate for use with the Starlab portable planetariums.[6] The need for sun-related programs for Starlab has been recognized as a gap by SECEF.
- Developing a Great Expectations in Math and Science (GEMS) guide on a topic associated with living with an active star.[7]
- Developing a collection of teacher kits and grade-appropriate curricula to accompany our existing low-cost spectroscope.[8]
- Creating activity sets in tracking and understanding the Sun, suitable for a wide age range, school, and family participation.[9]
- Collaborating on coverage of a celestial event such as the transit of Venus or a solar eclipse.

The material and activities will be hands-on, inquiry based, and appropriately aligned to the National Science Education Standards.[10] We will coordinate our program with the interests of the OSS and LWS programs.[11] The basic concept to teach is that the Sun is an active, variable star that has significant impacts upon the Earth. We will draw upon existing resources and materials, presenting them in new and interesting ways and focusing on gaps as identified by the SECEF.

D.1.7 Webcasts

The solar science team at Stanford has already developed a unique webcast series which addresses solar science through a dialog between scientists and students in elementary through high school. Not only do the students learn scientific principles, they get to know the scientists as people and can participate in the show. Supplemental materials, including lesson plans and suggested activities, are available in advance. Viewers can perform the activities, record their results and submit video, data, or student teams for inclusion in the show. Students participate in the discussion through chat rooms. Thus students contribute substantially to the show. For the past two years, with our partner NASA Quest, this team has also hosted Sun-Earth Day webcasts which have been televised on NASA TV.

D.1.8 Evaluation/Assessment

Assessment provides important feedback to both instructors and students. There is an excellent research base in what constitutes effective educational assessment and evaluation[12]. We will rely heavily on this base to guide the development of assessment aspects for our programs. For the educational materials, and model programs, specific goals will be identified and "best practices"-based assessment techniques applied to evaluate the

extent to which goals are being achieved. Stanford's Haas Center has extensive expertise in evaluation and metrics. We will work collaboratively to prepare professional quality evaluation materials and to assess activities, curricula, and model programs.

D.1.9 Involvement

The PI and Co-Is will be closely involved in all aspects of the E/PO program. Scientists will work with educators to develop materials, train Science Fellows, and collaborate on dissemination of the material through teacher workshops and partnering institutes. Each Co-I not directly on the E/PO team will provide 1-4 days of E/PO each year. These will likely be seminars for Science Fellows, teacher workshops, or work on press releases. Scientists will also present the materials at NSTA, AGU, AAS, and similar conferences to reach a larger audience and to share experiences with other scientists.

D.1.10 Underrepresented Groups

Our partnering institutes and we have experience and interest in involving women and minorities in education and research. The San Francisco Bay Area is one of the most ethnically and culturally diverse communities in the nation. The Haas Center has outreach contacts and active programs with minority-based schools. LMSAL supports programs to encourage women to enter scientific professions. Our partner museums have teacher training and master teacher programs that particularly target minority populations. We will actively recruit minorities and women as Science Fellows, where they can serve as excellent role models in our K-14 classrooms. We will particularly focus on liaisons with educational institutes involving minorities and women. We will work with educators to assure our curricula and activities are culturally appropriate to the diversity in our areas.

D.1.11 Organization and Management

Deborah Scherrer, the developer of the Stanford SOLAR Center, will serve as the E/PO Coordinator. We will establish an Oversight Board to direct E/PO planning and development. The Board will be responsible for overall decision-making, choosing the yearly focus, evaluating various possibilities for activities and materials, and for key creative decisions. Most importantly, to encourage frequent contact with and input from scientists, the Board will maintain a steady stream of communication about the E/PO efforts within the science teams and with NASA.

Table D.1 Partnerships

Institution	*Student Involvement*	*K-14 Curr. Devel.*	*Teacher Workshops*	*Assessment Support*	*Multimedia Devel.*	*Distance Learning Support*	*Distribution of Materials*	*Access to Undeserved*	*Public/ infomal ed.*
Stanford	X	X	X	X	X	X	X	X	X
LMSAL	X	X			X		X	X	X
Stanford-Haas	X			X	X			X	X
MSU*	X	X	X	X	X	X	X	X	X
SAO*	X	X	X	X	X	X	X	X	X
The Tech Museum	X		X				X	X	X
Chabot SSC	X		X				X	X	X
Morrison Planetarium /CA Academy of Sciences	X		X				X		X
Lawrence Hall of Science		X	X	X			X	X	
IIISE		X					X		
NASA-CORE							X		

* If AIA is selected.

HMI E/PO BUDGET NOTES

Our proposal and partnerships with Haas, AIA, and the various science museums and educational groups have potential for generating a dynamic and exciting program. However, our proposal for E/PO activities exceeds NASA's guideline for funding. For all of SDO, the 1-2% guideline would be between $3.5 million and $7 million. HMI's 2% would be about $1.4 million, spread over 11 years. The program outlined above is $4.3 million, plus an additional $1.4 million that is cost-shared by Stanford and Haas. We are therefore requesting additional funding, beyond the normal E/PO scope.

According to the answers to official questions about SDO, such funding might come from additional sources rather than being charged against the proposed instrument. If additional funding is not available we will revert to our Descope Plan, below.

Staffing

A program of this scope requires the following staff:

a. 0.75 FTE E/PO Coordinator, Stanford, will be Deborah Scherrer, who will coordinate both HMI and AIA programs and will coordinate with the overarching LWS E/PO programs.
b. 0.2 FTE mission scientist, Stanford, to work directly with the E/PO program, particularly the webcasts. This will be Dr. John Beck.
c. 1 FTE to provide Hass Center student program development and management (first 4 years only)
d. 0.2 FTE for scientific visualization, programming, and web support
e. 1 FTE student support for distributing materials (not needed should NASA or LWS create a distribution program)

The staff is phased in during the initial year. Because we want to begin the E/PO efforts during Phase A, we have arranged for cost-sharing which immediately takes effect. Of the total $5.7 million program, Stanford is willing to cost-share about $1.4 million. They will:

a) Provide .75 FTE to support a Haas assessment and metrics expert (for first 4 years starting immediately after selection).
b) Provide .25 FTE clerical staff support through the Undergraduate Studies division, to assist with the student programs (for first 4 years, starting immediately after selection).
c) Provide support of 1 FTE for Haas student program management, for the initial 6 months of the program. This will allow us to get a student Science Fellow program in place for the first year.
d) Waive overhead on the HMI supported Haas staff person (4 years).
e) Haas will seek funding for the Science Fellow stipends through various charitable trusts (for the full 10 years of the mission). $5K per year per student (uninflated), with 6-8 students the first year and 10-12 each year afterwards.

In addition, scientist Co-Is who are not directly involved in E/PO will donate 1 to 4 days per year of effort. This is to be subsumed into their salaries and not reflected here.

Other Costs

Other E/PO activities and costs include:

a) A contract with Clockworks to produce our webcasts, 12 broadcasts per year for 9

years. (Funding is not included for NASA-TV broadcasts.)
b) NASA Quest production costs for the webcasts. Again, 12 broadcasts per year for 9 years.
c) Subcontracts with LMSAL scientists to directly participate in curricula design and development ($30K for 5 years, $15K for the remainder);
d) Subcontracts with LMSAL to support multimedia production work ($20K for each of 5 years);
e) $11K to purchase a small-sized StarLab for development phase of solar-based planetarium program and use in classrooms; $21K for full-sized StarLab for use in science museum presentations.
f) $10K per year (uninflated) for slides to support the planetarium show, posters, DVDs, training videos, and production of other materials and activities.
g) $50K to support the development of a PASS or GEMS guide.
h) Travel for scientists and E/PO coordinator to present staff-led workshops at major science conferences or conventions.
i) Travel for 3 Science Fellows per year to Montana to train with MSU team. (Not necessary if AIA team not chosen.)
j) Our Science Fellows will also participate in workshops and HMI team meetings. And scientists from the mission will present seminars and training sessions at the meetings. However, these meetings are held locally so no travel is required.
k) Travel funds to coordinate with the LWS E/PO program.

Strategies

Our strategies include:

a) Developing the classroom modules, drawn primarily from the numerous activities now part of OSS curricula or other programs, and when necessary, creating new materials.
b) Piloting and assessing the modules in local grade K-14 classrooms, working primarily with teachers arranged through Haas' networks.
c) Arranging for the publication of all printed and multimedia materials.
d) Disseminating these materials regionally through existing museum partners, educational group partnerships, NSTA and similar conferences, and regular NASA channels.
e) Collaborating with NASA Forum partners to integrate SDO-related themes into the Forum workshops and educational outreach.

Partnership Model

Our model for teacher and master teacher workshops is that the mission will provide one scientist and one Science Fellow, plus all materials, to present the workshop. The partnering museum/institute will provide the space, arrangements, and the teachers. We expect to develop one new workshop each year, for the first 5 years. These can be given through multiple museums (perhaps slightly adapted to their particular focus), with both old and new workshops available during each successive year. Our goal is to provide a minimum of 1 teacher workshop through each partnership per year.

Time-phased Activities

Overall the plan will start quickly in order to prepare materials and train student fellows and teachers early in the mission so they are in place before the flight phase.

Phase A and Bridge Phase

During Phase A we will work out details of coordinating with LWS and jump-starting our E/PO program to have it effectively running

by phase B. A detailed E/PO plan and budget will be prepared, including timelines, staffing, and implementation details. The yearly foci for the first 2 years will be determined.

Phase B

We will implement the first of the yearly foci. After testing by the Science Fellows, we will organize teacher and master teacher workshops through partnering science museums. We will also develop videos and DVDs for use in training and distance learning. Preliminary work on the public website will be started.

Phase C/D

During Phase C/D we will develop and implement the next four coordinated educational curricula, one for each year. Dissemination packages will be developed, for use at professional conferences such as the National Science Teachers Association or the AGU educational sessions. During this phase, we will also further develop our website.

Phase E

During Phase E, we will focus on communicating the research results of the mission to the press and general public. On our website we will feature live solar image feeds, daily "solar weather" reports, weekly solar "nuggets", predictions of solar activity, and so on. We will also provide background materials to support NASA press releases.

Descope Plan:

Should funds beyond 2% of HMI not be available to support our preferred program, we will scale back activities accordingly. At 2% of the HMI budget, we would have available less than $1.4 million, or $125K per year, including indirect, to cover activities for 11 years. This would be a lower level of funding than the present MDI E/PO program. This would decimate the Haas and most of the museum partnerships as well as our ability to hire a nearly full-time E/PO coordinator. The webcasts would be eliminated. We would continue the maintenance of the existing Solar Center website, and perhaps 1 training video per year. The Stanford Haas cost-sharing would be reduced or eliminated. If this option becomes our only choice, we will develop specific plans in the Phase A study.

The E/PO plan is unchanged with or without the vector magnetic field capability.

D.2 Technology Plan

The proposed HMI instrument contains little new technology. All of the techniques being used have been successfully applied in space previously or are modest extensions of such technologies.

The 4096×4096 pixel CCDs are certainly state-of-the-art for space use, but our vendor, Marconi Applied Technology, has already produced 2048×4096 devices for the Solar-B/FPP instrument, the larger devices are a straight forward next step. Other than a factor of two increase in one dimension, other relevant characteristics (such as noise, cosmetics, uniformity, radiation hardness, etc.) are not new.

Similarly, the data processing system software is an enhancement of that developed for the SOHO/MDI program and can not be considered new technology at this point.

As a result of having very little, if any, new technology, HMI is a low risk program from a technical/performance point of view.

D.3 Small Disadvantaged Business Plan

Stanford University will work to ensure the highest level of small business and small disadvantaged business support for the HMI program.

In Phase-A and the Bridge Phase there is little opportunity since there is little subcontracting other than the primary contract to LMSAL. The Phase-B through Phase-E plan will be developed during Phase-A.

Stanford will include the appropriate requirements in the LMSAL subcontract. (Actually the contract is to LMATC the parent organization to LMSAL.)

LMATC will work to ensure the highest level of small business and small disadvantaged business support to the HMI program. LMATC is a part of Lockheed Martin Space Systems Company- Missiles & Space Operations (LMSSC) which has an award-winning SBP (Small Business Program) that vigorously seeks small, minority, and woman-owned businesses and historically minority colleges and universities that have demonstrated ability to supply or develop products and expertise suitable for LMSSC programs. Lockheed Martin's government approved *Master Subcontracting Plan for Small Business Concerns* is available upon request.

LMSSC will submit a small business/small disadvantaged business subcontracting plan for Phase-A upon contract award. The subcontracting plan for Phases-B through E of the HMI program will be submitted at the end of Phase-A. LMSAL already has many established relationships with SB/SMB as a result of the current and previous program experience on MDI, TRACE, SXI, SXT, and Solar-B. During Phase-A they will aggressively work with LMATC's Small Business Office to identify small and small disadvantaged businesses that can support HMI. During the proposal phase they have identified the following small businesses that are under consideration for becoming part of our supplier team on the HMI program:

- Palo Alto Village Travel (woman-owned)
- Acton Research Corporation (SB)
- Luxel Corporation (SB)
- H Magnetics (SB)

E MANAGEMENT AND SCHEDULE

The HMI team is led by the Solar Physics group of the Stanford University Hansen Experimental Physics Laboratory (HEPL), in collaboration with the Lockheed Martin Solar and Astrophysics Laboratory (LMSAL), the Mullard Space Science Laboratory (MSSL), the Rutherford Appleton Laboratory (RAL), the High Altitude Observatory (HAO), and an exceptional group of science Co-Investigators.

This HMI team is committed to achieving the following objectives:

- Conduct the scientific investigation described in Section C of this proposal.
- Design, develop, fabricate, test, calibrate, integrate and operate the HMI instrument to acquire the necessary observational data.
- Manage the personnel, resources, and interfaces to accomplish the program on schedule, within budget, and in a manner that minimizes risk and maximizes the science return on expenditures.
- Accomplish the goals of the NASA/OSS education and public outreach strategy, as well as those for developing new technologies and involving small disadvantaged businesses.
- Perform the mission operations and data analysis activities after launch.

To accomplish these objectives, an extremely strong and experienced team has been assembled under the leadership of Prof. P. Scherrer as Principal Investigator (PI). The HMI flight instrumentation will be developed at LMSAL under the direction of Dr. A. Title with ongoing involvement of Stanford University personnel. The Stanford University and LMSAL groups have worked together for many years on successful NASA, ESA, and ISAS scientific space programs, including the MDI and TRACE investigations, which form the foundation for the HMI program.

In addition to the instrumentation developed at LMSAL, the CCD camera systems will be provided by RAL and MSSL in the UK, coordinated by Prof. J. L. Culhane of MSSL. MSSL is responsible for program management and CCD detector procurement and RAL is responsible for the CCD camera design. Expertise in vector magnetic field measurement techniques will be provided by HAO under the coordination of Dr. S. Tomczyk.

A focused group of Co-Investigators rounds out the capabilities of the HMI team. Meaningful educational opportunities for graduate students are available both at Stanford University and through our university partners. We anticipate that our Co-Investigators will provide a continuing base of knowledgeable personnel through extended operations of the HMI mission. Their responsibilities, as well as all of the items touched upon in this introduction, are described more fully in the following sections.

The HMI management approach builds on a process that has evolved in a successful series of programs. Many of the scientists and engineers who developed MDI will be involved in HMI effort. Years of experience in flight hardware, software, and ground data systems, combined with a thorough understanding of the GSFC approach to space missions, enables us to accomplish this major investigation at modest cost and with minimal risk. Further efficiencies will be realized if NASA selects the LMSAL proposal for AIA, since that instrument will be developed by LMSAL sharing many of the same hardware, software, and management elements as HMI. We cannot envisage a combination of personnel and institutional capabilities better suited to providing the HMI aspects of the SDO mission and LWS program.

E.1 Organizational Structure and Responsibilities

The HMI Program is under the direction of Prof. Philip Scherrer who as Principal Investigator is the formal interface to NASA and to Stanford University. He is responsible for

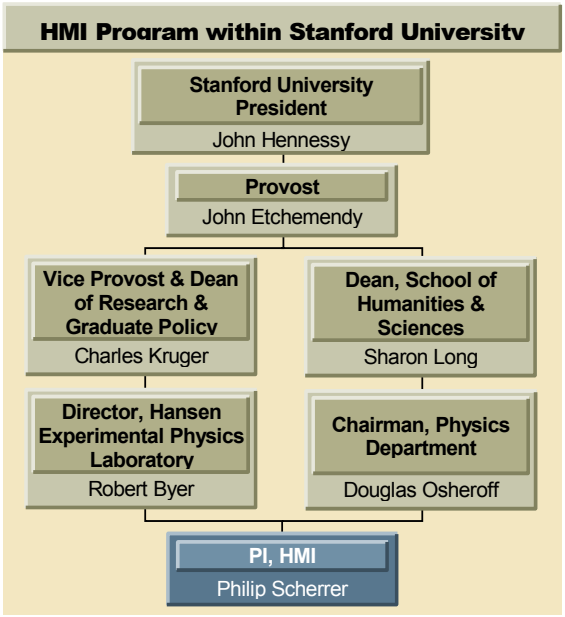

Figure E.1: Research functions are coordinated through the HEPL director in consultation with the Dean of Research. Academic matters are handled through the physics department chairman in coordination with the Dean of Humanities and Science.

scientific leadership, management, instrument development, ground and flight operations, E/PO, and data distribution, archiving, and analysis. Prof. Scherrer is extremely well qualified for this position. He is the PI for the MDI instrument; and has played a prominent role in developing and advancing the SDO concept. The organization chart in **Figure E-1** shows how the HMI program fits within Stanford University. Prof. Scherrer is ultimately responsible to the Stanford University president J. Hennessy.

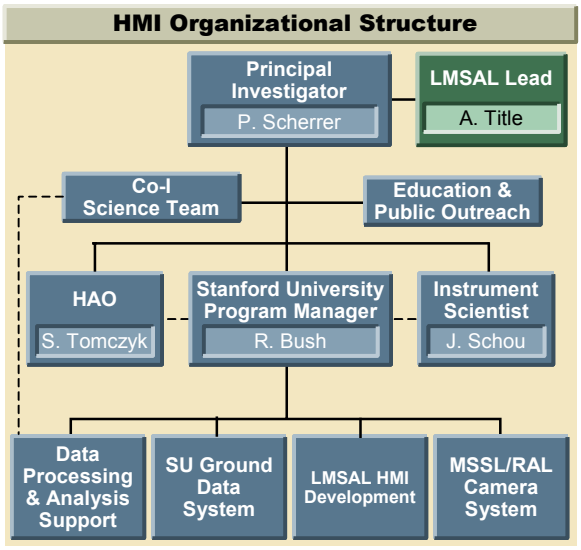

Figure E.2: The HMI organizational structure is similar to that used for the MDI program.

The HMI instrument development organizational structure is shown **Figure E-2.** The ultimate responsibility for the HMI program resides with the PI. The Stanford program management, ground data systems and mission operations is under the direction of Dr. R. Bush with the assistance of the HMI Instrument Scientist, Dr. J. Schou. The HMI program at LMSAL is under the direction of Dr. A. Title at LMSAL with the assistance of the HMI project manager, Mr. L. Springer.

The Stanford program manager, Dr. Bush, handled the MDI project management for Stanford and is currently in charge of MDI operations. He is responsible for the prime contract from NASA and for the interface with LMSAL and the other Co-Investigators. Dr. Schou, in conjunction with the HMI Science team, will establish the performance requirements for the HMI instrument. He will have oversight for the development, testing and calibration of the flight HMI instrument. Dr. Schou has been involved in similar activities during the MDI program.

E.1.1 Lockheed Martin Solar and Astrophysics Laboratory

The HMI functional organization within Lockheed Martin is totally contained within the Solar and Astrophysics Laboratory. **Figure E-3** shows the HMI organizational structure at LMSAL. Dr. A. Title is the lead for the HMI instrument development at LMSAL, and the contact to Lockheed-Martin management. He is a Senior Fellow at the ATC, a member of ATC Vice President A. Mika's staff, and is the PI for the TRACE and Solar-B/FPP programs.

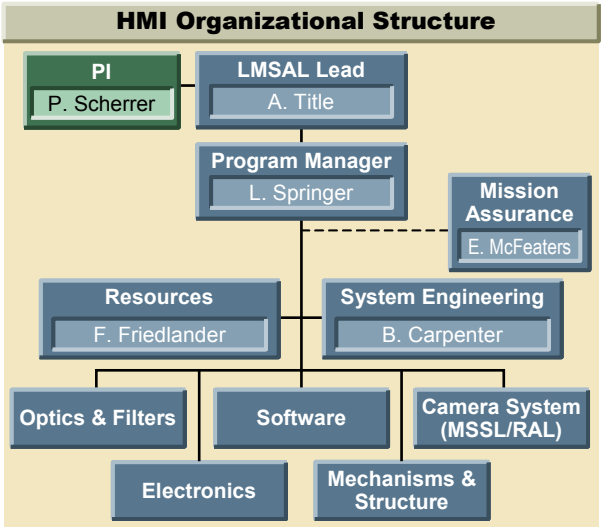

Figure E.3: The majority of the LMSAL team has worked together on prior solar physics space missions.

Mr. L. Springer, as the LMSAL Program Manager (PM), is responsible for day-to-day implementation of the program. He was the SXI PM during its early years and is presently PM for the LMSAL portion of SECCHI. The systems engineering, mission assurance, and resource management leads will support Mr. Springer, and have worked together with him on several similar programs. In particular, Mr. B. Carpenter was the Chief Systems Engineer on the SXI program during its design phase and is now the CSE on SECCHI. He and Mr. Springer will transition from SECCHI to HMI as SECCHI goes from design to fabrication.

E.1.2 UK Participants

In the UK, Prof. J. L. Culhane of MSSL will coordinate a scientific team for participation in the HMI investigation. He has been involved in many NASA missions, being the PI or UK PI on SMM/XRP, Spacelab-2/CHASE, Yohkoh/BCS, and Solar-B/EIS. Prof. R. Harrison of RAL will join Prof. Culhane in executing the UK hardware responsibilities He is the PI on SOHO/CDS and the UK PI on STEREO/HI.

MSSL has been active in space sciences for more than forty years and has provided instruments for more than thirty orbiting and interplanetary space missions, including Yohkoh, SOHO and Solar-B. Instrument development work is undertaken either in house by teams of professional engineers or on contract to industry. There is a strong management capability, with Prof. A. Smith in overall charge. He will be responsible for procurement and testing of the Marconi CCDs. Similar activities have been undertaken jointly with LMSAL in the SXI and FPP programs.

RAL has been active in experimental space science missions including HIRDLS, Yohkoh and SOHO. RAL is currently involved in Solar-B and in the provision of CCD cameras for the SECCHI investigation. This latter work, undertaken by Dr. N. Waltham, is of considerable relevance for HMI because the HMI CCD camera will be developed from the SECCHI cameras.

E.1.3 High Altitude Observatory

Requirements for the vector magnetic field capability of HMI will be supported at HAO under the leadership of Dr. S. Tomczyk and Dr. B. Lites. The HAO team has extensive experience in instrumentation for the observation of solar oscillations and magnetic fields (e.g. the LOWL oscillations experiment, the Advanced Stokes Polarimeter and the Solar-B/FPP spectropolarimeter), as well as in the inversion and interpretation of vector polarimetric data. In addition, they will development algorithms for the analysis of the vector magnetogram data from HMI.

E.1.4 Science Co-Investigators

The roles and responsibilities of all HMI Co-Investigators and their institutional affiliations are summarized in Table C.4.2. Those Co-Is whose roles have not already been described fall into two groups and are shown in the lower two sections of the table. The first group is U.S. Co-Is whose role is to produce analysis code that will be incorporated into the higher-level data pipeline processing shown in **Fold-out 1.L**. The second is non-U.S. investigators

who will be primarily providing science data analysis. All members of the U.S. Co-I team already have versions of analysis codes which are the prototypes for the needed HMI codes. Only those who have particular expertise to develop and verify the particular analysis techniques needed to produce HMI data products are included. Their role will be constrained by funds to implementing a version of their then-best code into the pipeline and, after launch, doing sufficient analysis to verify the processing.

Prof. S. Basu and Dr F. Hill will provide helioseismic ring analysis code to probe local velocity and structure. Prof. J. Toomre's group, which leads in the analysis and inversions using ring data, will provide code to convert the ring measurements into SSW flow maps. Dr. R. Howe and Prof. E. Rhodes will provide code for global helioseismology mode and frequency determination and inversions for interior motions and structure. Dr. C. Lindsey and Dr. D. Braun will provide the code to compute the farside active region maps. Prof. J. Kuhn will provide the code for limb shape fitting and continuum analysis of convection efficiency. Dr. N. Mansour and Dr. A. Wray will provide convection zone modeling code to allow testing of inferences from local methods. Prof R. Ulrich and Prof P. Goode will provide code to enable cross-comparisons of magnetic field observations to other line-of-sight long duration magnetic series and to ground-based IR magnetic observations. Dr. J. Linker will provide MHD models for solar wind prediction to be used in near-real-time space weather forecasts.

In addition to the instrument fabrication and calibration roles, Co-Is from Stanford and LMSAL will also have code provision roles. These include Dr. R. Bogart and Dr. J. Beck who will provide large scale flow analysis code from ring and time-distance methods; Dr. J. Schou who will provide p-mode frequency determination code; Dr. X. Zhao who will provide coronal field estimating code used in several higher level pipes; Dr. Y. Liu who will assist in vector field calibrations and coronal field models; Dr. A. Kosovichev who will provide time-distance inversion code; and Dr. T. Duvall (GSFC) who will continue to be in residence at Stanford and will provide time-distance time-delay measurement and inversion code. From LMSAL, Dr. T. Metcalf and Dr. T. Berger will provide vector field analysis code.

E.2 Management Implementation

The management approach for HMI is one that has evolved over several decades of developing instruments as an integral part of conducting scientific investigations. Foundations of the approach are:

- Clearly stated and documented requirements that flow down from the measurements necessary to achieve the scientific goals.
- A program structure consistent with requirements, and resources allocated to the elements of that structure.
- Continual evaluation of the matching of the resources to the requirements and the adjustment of requirements to minimize risks and maximize scientific return for resources expended.

This is done in an environment where scientists, engineers, technicians, and support personnel from not only Stanford University and LMSAL but from all of the involved institutions interact in an open and continuous process. A chain of very successful programs that have functioned in this manner validates our approach.

E.2.1 Requirements Management

The science objectives described in Section C of the proposal are the primary drivers for the HMI instrument design. The flow from science objectives to top-level instrument requirements that has begun with this proposal will be captured in an Instrument Performance Specification (IPS) document developed by the HMI team under the leadership of the PI

during Phase A of the program. We have demonstrated on the MDI and TRACE programs that a living IPS document provides the necessary bridge from the science requirements to the instrument specifications, and is crucial to assuring that optimal tradeoff decisions are made throughout the instrument development.

In the IPS, the system and subsystem requirements are traced back to an underlying mission, instrument, or derived requirement. The IPS will receive modifications as the program evolves. A set of Engineering Design Notes contains the details of individual hardware and software items, including the motivation for the approach being implemented to achieve the required performance. At these lower levels, the specifications are expanded to address the performance, the allocated resources and the interfaces to other subsystems.

During Phase B, the engineering staff under the direction of the Chief Systems Engineer will flow these requirements down to assemblies and subassemblies. With the oversight of the Mission Assurance organization, we will develop verification plans for various levels of assembly, flowing up from the responsible engineers to the Lead Engineers and the Instrument Scientists for review. The requirements traceability matrix will evolve to include the verification criteria for all requirements. An overall Verification Plan covering all levels of hardware and software will result from this process. As the requirements and designs for subsystems and assemblies solidify, the methods for verifying performance are established and documented by the responsible engineers.

Elements of HMI being developed by our UK partners are treated in a manner similar to those being developed at LMSAL. The ground data system requirements will also be documented in a manner analogous to the instrumental requirements. Our experiences on prior programs have demonstrated the effectiveness of this approach wherein all members of the team work with documentation that clearly shows the paths being taken.

E.2.2 Communications and Meetings

Continuous and open communications are inherent in our management approach. Although decisions are made in a structured manner, ideas are shared openly. The decisions are documented in meeting summary minutes and technical memos and then incorporated into the appropriate documents such as the IPS. The Stanford University and LMSAL groups are within a ten-minute drive, and the scientists, engineers, technicians and support personnel interact on an informal basis. In addition, everyone is tightly linked via e-mail and Web sites.

A one-hour, all hands, weekly meeting is an important aspect of our internal communications. At this meeting, each engineer reports on status, plans, and concerns. Focused meetings are then scheduled to resolve concerns or review designs in depth. The results of both the focused meetings and the weekly meeting are posted on the Web. Routine telecons are held with all major subcontractors and vendors to recognize and solve problems early and (especially) to include them as an integral part of the HMI team. Periodic visits are made to the subcontractor and vendor locations for the same reasons.

We anticipate having weekly telecons with the GSFC project management team, and will participate in routine telecons with all SDO projects. We will support appropriate engineering peer reviews, and the normal series of formal reviews (Conceptual, Preliminary Design, Critical Design, Pre-Environmental, Pre-Ship, Launch Readiness, etc.). Co-Investigator and community-wide science meetings held at six to twelve month intervals complete the review process. Often some of the most critical and helpful comments come from our scientific peers at these meetings.

A narrative monthly progress report will be provided to NASA and all team members. Besides providing program status, these reports discuss problem/risk areas, proposed solutions, and specific activities planned for the next month. The reports include information from our partners in a manner equivalent to that from the subsystem leads. Like almost all documentation, the reports are posted on the Web for archival use.

E.2.3 Cost and Schedule Control

The keys to controlling cost and schedule include (1) having a clearly defined set of requirements/tasks, (2) making accurate original cost estimates, (3) continual review of all requirements and interfaces, (4) making early and firm decisions based on these reviews, (5) replanning as the program evolves, and (6) using management tools that provide clear visibility into the status of the program. These features have been fine tuned on prior successful programs of this nature with the constant realization that the available resources only allow a task to be completed "well enough".

Event	Date
Phase A	1 Sep 2002 to 31 May 2003
Initial Confirmation Review	15 May 2003
Bridge Phase	1 Jun 2003 to 31 Aug 2003
Phase B (includes Bridge)	1 Jun 2003 to 31 Dec 2003
Preliminary Design Review	15 Oct 2003
Confirmation Review	15 Dec 2003
Phase C/D	1 Jan 2004 to 31 Aug 2007
HMI Delivery	1 Jun 2006
Integration	1 Jun 2006 to 31 Jul 2007
Launch	1 Aug 2007
HMI Commissioning	1 Aug 2007 to 31 Aug 2007
Phase E	1 Sep 2007 to 31 Aug 2013

Table E.1 - HMI Critical Dates

During the preparation of this proposal, the program was defined by the scientists and engineers in a coordinated manner and documented in a detailed WBS, schedule, and cost estimates. These will be refined during Phase A of the program, resulting in a formal proposal to NASA, and kept current thereafter. Monthly and quarterly financial reports will be provided to NASA in the standard 533M and 533Q formats, and the schedule will be

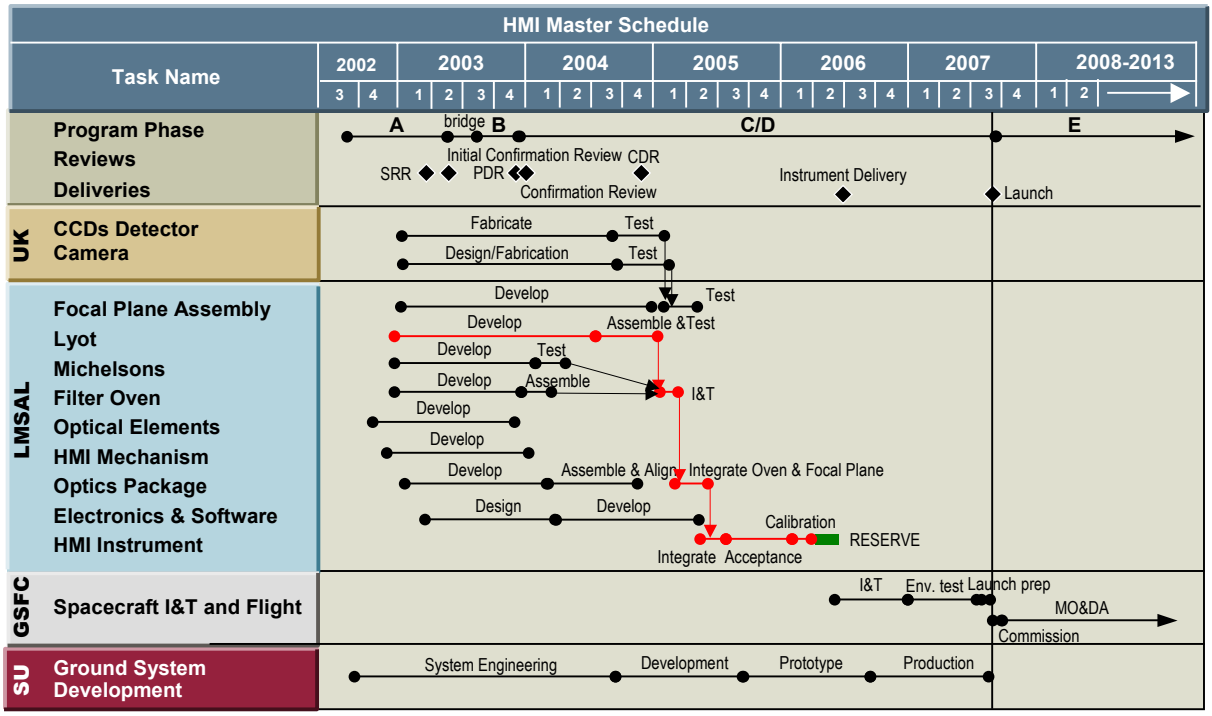

Figure E.4: The top-level HMI schedule shows key links, milestones, and the location of the activities. The EPO activities begin in Phase A and continue throughout the program. Funded reserves are shown in green; the critical path shows in red.

provided monthly using Microsoft Project.

E2.4 Schedule

Table E.1 shows our interpretation of the AO dates, and **Figure E.4** shows the top-level program schedule with major reviews. The total time span is consistent with our experiences on prior programs. The expenditure of about 6% of the contract funds during Phase A of the program will enable us to ramp up immediately after contract award in order to position ourselves for meeting the remainder of the schedule. The LMSAL experience on the TRACE program provides confidence that because the spacecraft will be built in-house at GSFC, detailed spacecraft interfaces and resource allocations can be established rapidly, a necessary feature to minimizing schedule and cost risk. We have already made a much more detailed schedule than that shown in **Figure E.4**. It will be revised during Phase A of the program with each responsible engineer creating a subsystem schedule, iterating it with the PM, "signing up to it", and reviewing it with the PM and Resource Manager at least monthly.

The E/PO program described in section D.1 will begin as quickly as possibly to have materials and training complete well before the flight phase of the mission.

E.2.5 Risk Management Plan

The HMI risk management approach has developed from the LMSAL involvement in a series major space programs, most recently the Solar-B and STEREO programs. By conceiving an instrument with extensive heritage and little new technology, we begin the program with minimal intrinsic risk. This will be further aided by beginning work early on elements that are likely to consume the most time. All members of the HMI team will be made fully aware that early identification of possible risks is an important component of their responsibilities.

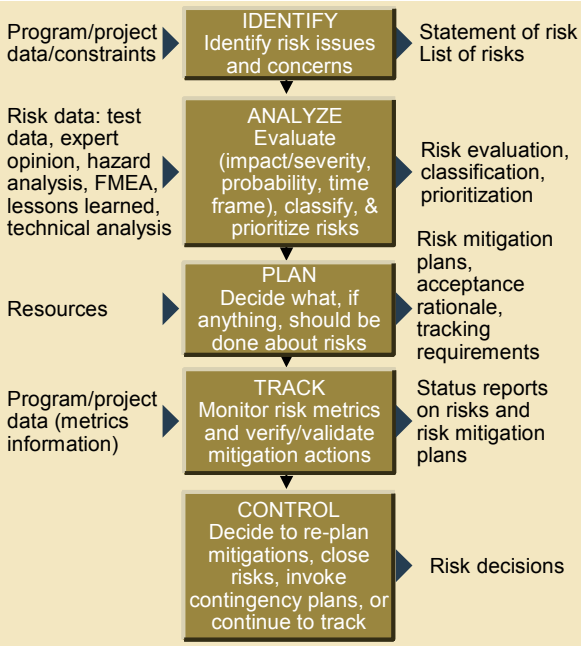

Figure E.5: Risk mitigation is a continuous process throughout the product lifecycle with the results integrated into the HMI development plan.

The Chief Systems Engineer, working with the relevant team members, is responsible for categorizing the risks following a procedure that assigns a probability of occurrence (high, medium, or low) and impact (high or low). All significant risks are thus documented. Those with medium impact and high probability are tracked weekly and any risk with high impact and high probability receives a formal abatement plan in addition to the tracking. The abatement plan includes closure criteria, optional paths, and anticipated cost, schedule and performance hits. Reserves will be allocated as warranted to accomplish the abatement, with NASA immediately involved should the available reserves and closure criteria be incompatible with the existing contract. **Figure E.5** demonstrates the process.

A Risk Management Plan that complies with §4.2 of NPG 7120.5A, as well as with the intent of LMMS Practices P3.1.2, will be formulated during Phase A of the program, as will the initial risk matrix. The risk matrix, which includes planned mitigation measures, will be part of every monthly progress report, enabling

the evolution of the risks to be easily tracked. It will also be presented at all major reviews.

E.2.6 Descope Plan

The HMI instrument is a suite as defined by the SDO AO. The "HVMI" component consists of the vector magnetic capability and is the only aspect of the HMI program that could be removed without completely incapacitating the investigation. As foreseen in the AO the vector magnetic capability is a simple enhancement of the HMI instrument. There are two aspects to this possible descope; the first is the CCD camera that is dedicated to the vector field measurements; the second is the capture, processing and distribution of the images generated by the second camera.

Removal of the second camera is estimated to reduce the instrument mass by 3.2 kg and the power by 7 W. It includes the second camera head and electronics, interface electronics, the final beamsplitter, two small flat mirrors, and a shutter. There will be additional mass savings by shrinking the Optics Package width as a result of removing the second light path. The estimated NASA cost savings, however, is only about $480K because the CCD and camera electronics are contributed by the UK. Removing the proposed polarization calibration would save an additional $200K.

The cost savings associated with reducing the ground data processing and science algorithm is harder to quantify. The basic data system is essentially unchanged except for the size of the 30-day data buffer and corresponding calibration processing. The vector field processing, however, is small compared to that required for the helioseismology processing. Reducing the ground data system hardware by 20% will save approximately $300K.

Similarly a 25% reduction in the pre-launch science operations and data analysis software development would save about $600K. Both of these savings would take place after the instrument is completed. A smaller savings would result after launch, because only the archive media costs and science analysis costs could be saved. Only two years of vector field science analysis has been provided in the proposed budget at about $600K.

The HMI instrument design and development plan as outlined in this proposal is based on the MDI instrument heritage and a simple, non-redundant design. The helioseismic and line-of-sight field component of the suite is the rest of the program and cannot be removed if any part of this proposal is selected.

E.2.7 Combined Development with the LMSAL AIA Program

LMSAL is proposing an investigation to accomplish the goals of the AIA portions of the SDO mission, with Dr. A. Title as the PI. The LMSAL AIA flight instrument, if selected, will be developed at LMSAL in collaboration with SAO. Dr. Title and others from LMSAL are Co-Investigators on HMI, and Prof. Scherrer and others from Stanford are Co-Investigators on AIA with the Stanford-Lockheed Institute for Space Research as a common element for both activities. This is the identical approach that was used on the successful MDI and TRACE programs.

If both HMI and AIA are selected, the two programs will be coordinated to eliminate duplication of effort. In addition, some hardware items will be identical, with several mechanisms being prime candidates. A common computer and software system will service both instruments and duplicate EGSE systems (hardware and software) will be used to test the instruments. The cost estimates provided in the next section of this proposal demonstrate the estimated savings that can be achieved by this synergy.

E.2.8 Mission Assurance

The HMI program will utilize the LMSAL Mission Assurance capability for flight hardware and software. The HMI mission assurance function is comprised of quality assurance

(hardware and software), systems safety, reliability, EEE parts control, materials and processes, and contamination control. These combined functions work in concert to ensure that the delivered products meet all requirements with the highest practical reliability. The HMI mission assurance manager, who has a separate reporting chain in the LMSAL management structure, thereby ensuring independent oversight of these critical program aspects, manages these functions. An HMI mission assurance plan, called the PAIP (Product Assurance Implementation Plan) will be written during Phase A in accordance with the SDO specific Instrument Mission Assurance Requirements (IMAR) document.

The LMSAL mission assurance approach ensures that reliability and performance requirements are met throughout the program. A structured system of checks and balances coupled with key inspection points provides the required control. The LMSAL mission assurance personnel are key members of the HMI design team and the design process. A separate LM mission success organization is employed to review the program at critical points. The HMI mission assurance program contains the following elements, each of which will be detailed in the PAIP.

LMSAL has a quality system that is certified to the ISO-9001-1994 standard by the British Standards Institute and is moving towards the newest ISO-9001-2000 standard. Hardware and software quality engineering plays an integral role in all program aspects including the review of all engineering drawings, code design and analysis, shop paper, procurement orders, test procedures and documentation.

A quality inspection function that is staffed with trained and certified inspection personnel who have significant space flight hardware experience. The inspection aspect of the program not only consists of those detailed inspections called out by the shop paper or receiving inspection, but also comprises area surveillance.

A systems safety engineer is involved with all aspects of the design, handling equipment, and GSE reviewing them for safety issues/concerns. In the event that hazards are identified, they are put into a formal hazards analysis format and presented at all major reviews.

A reliability engineer is involved in the program at the outset to ensure that the developed designs comply with of all HMI reliability requirements. This allows reliability driven impacts to be accommodated with minimal cost and schedule impact to the program.

An EEE parts engineer works with the design engineering team, including the reliability engineer, to ensure that all EEE parts requirements are met. The parts engineer manages all aspects of EEE parts program including the generation of the EEE parts list, conducting PCB (Parts Control Board) meetings, issuing PCB minutes, performing GIDEP and internal alert searches, directing the screening of parts, and performing failure analysis on any failed parts.

An M&P (Materials and Process) engineer ensures that those materials and processes selected are qualified and meet the HMI requirements. A materials and process list developed during the design phase of the project identifies the material used, the quantity, and the assembly/drawing number.

A contamination control engineer ensures that all HMI and SDO contamination control and cleanliness requirements are identified and met by working closely with the design engineering team, including the M&P engineer. An HMI Contamination Control Plan will be written during Phase A of the program.

E.2.9 Work Breakdown Structure

A preliminary WBS is shown in **Table E.2**. It reflects the efforts to be performed and is the basis for managing cost and schedule. As a living document, it will change modestly as the program evolves.

HMI WBS
1.0 Stanford University Investigation Development
1.1 Program Management
1.2 Science Development
1.3 Instrument Development Support
1.4 Integration and Test Support
1.5 Ground Data System Development
1.6 SU Pre-launch Science Ops & DA Development
1.7 Co-I Pre-launch Science Ops & DA Development
2.0 LMSAL Instrument Development
2.1 Program Management
2.2 Systems Engineering
2.3 Mission Assurance
2.4 Instrument Subsystems
2.4.1 HMI Optics Package
2.4.1.1 Feed Telescope
2.4.1.2 Image Stabilization System
2.4.1.3 Mechanisms
2.4.1.4 Filters
2.4.1.5 Optical Elements
2.4.1.6 Filter Oven
2.4.1.7 Structure
2.4.1.8 Internal Harness
2.4.2 Camera Subsystem (UK)
2.4.2.1 CCDs (MSSL/Marconi)
2.4.2.2 Camera (RAL/MSSL)
2.4.3 Focal Plane Subsystem
2.4.4 HMI Electronics Box
2.4.5 HMI Intra-Instrument Harness
2.5 Software (flight and GSE)
2.6 Ground support equipment
2.7 Instrument I&T and Calibration
2.8 Spacecraft I&T Support
2.9 Launch Support
2.10 Pre-launch Science Ops & DA Development
2.11 Special Launch Service Costs – N/A
2.12 Special Ground Data Systems Costs – N/A
2.13 Reserves
3.0 Science Operations & Data Analysis
3.1 SU Post launch Science Operations
3.2 SU Post launch Data analysis
3.2 Co-I Post launch Data analysis
3.2 LMSAL Post launch Science Operations s
3.2 LMSAL Post launch Data analysis
4.0 Education and Public Outreach
4.1 Pre-launch E/PO
4.2 Post launch E/PO

Table E-2. Phase B/C/D/E WBS

F COST ESTIMATING METHODOLOGY AND COSTS

The estimated total NASA cost of HMI as proposed here is $69M. We recognize that this is a sizeable fraction of the available costs identified in the AO and we have worked hard to identify achievable cost reductions in the program consistent with the science goals described in the AO. There is significant similarity in several elements of the investigation with the successful SOHO/MDI investigation.

The flight instrument in particular shares significant heritage with MDI. The estimate of effort for HMI is about 50% that expended to build MDI. We believe that the HMI estimate is well founded and reasonably reliable, so we have included only 15% reserve on the LMSAL technical effort. With inflation since MDI, the total cost of the flight instrument is about the same in real year dollars.

If some of the reserves allocated for the flight instrument development are unexpended we would expect them to be available in Phase-D to better prepare the science team to be ready to deal with the data.

The estimated costs for the HMI program were obtained using the same approach that we and our partner LMSAL have used on a long series of prior similar programs. The adjective "similar" is important, in that like HMI they were PI-led science investigations that involved producing an instrument to make the required measurements, and all of the key personnel involved in HMI were involved in one or more of these programs. The approach is to do a modified bottoms-up costing of each task by the person who will be responsible for carrying out the task. These are reviewed by the management team (PI and PM) to eliminate duplication of effort, rationalize the task plans, and uncover areas that were overlooked, and then revised accordingly. The agreement between proposed and actual costs of programs such as TRACE, MDI, SXT, and SXI provide confidence in our approach.

The approach is described as "modified bottoms-up" because heavy reliance has also been placed on the actual costs of analogous tasks on similar programs. This is especially relevant since HMI is an evolution of MDI, a program that completed on time and at expected costs. A cost model was not directly used, nor have we used one on prior programs. However, a sanity check using an LMATC model of costs as a function of program type, heritage, and complexity supports the estimate. The cost estimates will be iterated and refined during Phase-A resulting in a formal cost proposal for Phases B-E. Firm-fixed prices are provided for Phase-A and the Bridge Phase option. The remainder of this section describes the fundamental assumptions that went into the costing, elaborates on the basis for estimating the efforts, and describes the cost reductions associated with possible descopes as well as those that can be achieved by combining the HMI and LMSAL AIA programs.

F.1 TOP-LEVEL ASSUMPTIONS

We have had to make some top-level assumptions in estimating the costs of the HMI program and have done so with the knowledge that SDO is a cost constrained program. These assumptions include, but are not limited to:

- GSFC, as the spacecraft provider, will create and maintain the HMI-S/C ICD, using our inputs and reviews as appropriate.
- The spacecraft will have an appropriate contamination control program. The requirements for HMI are probably less than those for any selected EUV or coronagraph instruments.
- A class-2 EEE parts program will be implemented, as was clarified in the FAQ portion of the AO on the Web.
- A formal EVM system will not be required of PI-led investigations, including those that produce instrumentation.
- The schedule in the AO will be held to, with a funding profile that enables this.
- The STM that is delivered to the S/C will not contain functioning optics, electronics,

or mechanisms. It will be delivered in January 2005; the AO did not specify a date.
- A specific SDO IMAR, as contrasted to the draft LWS MAR that applies to all elements of LWS including spacecrafts, will be provided during Phase-A.

The discussion that follows details first the Stanford and Co-I component of the program, then the LMSAL component. The order of discussion generally follows the WBS.

F.2 Basis of Cost estimates - Stanford Component

The following narrative briefly describes the basis for estimating the proposed program costs. Stanford effort levels are estimated in Full-Time-Equivalent (FTE) in salaried person-years if not otherwise indicated.

F.2.1 Program Management

The HMI program will be implemented in the same manner as the successful MDI program. Based on a science collaboration, LMSAL will provide the flight instrument. Stanford will provide calibration, operations, data processing, and science. We have estimated 8.5 FTE through Phase-D.

F.2.2 Science Development

This task includes overview of the HMI investigation to insure that it continues to meet the needs of the LWS science goals. Team meetings are included in this element. We estimate 3.5 FTE for this task.

F.2.3 Instrument Development Support

This task consists of overview of the instrument development including verification that the IPS is met. Needed updates to the IPS are included here. Calibration procedures are also included here. This is a scientist-intensive task and will require about 7 FTE.

F.2.4 Integration and Test Support

This task includes assistance of the LMSAL team to perform ground calibrations. This is estimated to be 2 FTE.

F.2.5 Ground Data System Development

The ground data processing system proposed also has significant heritage from MDI. As a result the development hours proposed are less than half those actually used in the MDI data processing and pipeline analysis development. There are improvements needed in order to handle 500 times more data than MDI, and without a planned mission science center, additional support of non-local investigators is also required. The net effect with inflation but with the continuation of "Moore's law" yields a net program cost less than MDI. We have included no reserve for the ground system following the methods used for MDI development. The data capture, calibration, and archiving are components which must be ready by launch and their reserve is contained in the science analysis component. We estimate 11.5 FTE for these tasks. We estimated the computing hardware and media costs based on current prices for a minimum system with a conservative deflation model. We include a total of $1,600K for processors, disks, and near-line storage systems.

F.2.6 HMI Pre-launch Ops and DA development

This task includes the development of software for instrument monitoring, Level-1 calibration, and the Level-2 and Level-3 components of the pipeline that are Stanford Co-I tasks. The development of science analysis tools will be done on a best-effort basis, so no reserve is included. We estimate 5.8 FTE.

F.2.7 Co-I Pre-launch Science Support

While the HMI program does include a number of Co-Investigators it should be noted that most of the Co-Is will not be involved in the development of the flight hardware. Their contributions will be very important in the processing of the HMI data into forms suitable for scientific analysis. Most U.S. Co-Is are only needed to produce software to be included in the pipeline processing for the pro-

duction of Level-2 or Level-3 data products. These high-level products will enable the separately funded science investigations of the Co-Is as well as those of a number of other Guest Investigators not yet identified (some of whom are not yet in high school). Costs are included for the code development needed to insert their then-current best models into the HMI processing and just enough science analysis to ensure that the code is properly functioning.

We are counting on the Co-I efforts of three NASA employees and have indicated their costs as TBD in the cost table as civil servant costs since we were not able to obtain accurate estimates under full cost accounting from either GSFC or ARC.

We are counting on contributions from Thomas Duvall of GSFC throughout the mission with most effort after launch, approaching a full time commitment.

We are also relying on a 25% commitment from both Nagi Mansour and Alan Wray of NASA Ames Research Center in FY06-FY09 or earlier if possible. Along with the ARC labor we need some ARC supercomputer time.

Since we have been unable to determine accurate costs for these components they are listed as TBD. None of these costs are needed in Phase-A or the first 3-months of Phase-B and they can presumably be determined during Phase-A.

F.2.8 Post-launch Ops/Data Analysis Costs

The HMI program is a full science investigation for some of the science goals described in section C. We can not afford, and do not desire, to fund the full scope of science possible with HMI. However it would not be appropriate for us to propose a mission plan without sufficient resources to enable key science goals of SDO and LWS. We have included costs for the key science goals of the Stanford, LMSAL, and HAO Co-Is in the first two years. We have included costs for the part of the science goals of other Co-Is to ensure that the code they provide is functioning properly and returning scientifically useful analyses. After the first two years the Stanford and LMSAL science efforts will be significantly reduced. The other U.S. funded Co-Is will receive no funding from the HMI program in the third and later years of Phase-E. Non-U.S. Co-Is have no such constraints and they will make significant contributions toward the HMI science goals.

Throughout all of Phase-E we must maintain sufficient staffing to operate the instrument, monitor its health, capture the data, perform calibration and processing in the established pipeline to the Level-3 products in place at the end of year 2.

We estimate 25.2 FTE for these Phase-E activities.

F.2.9 Education and Public Outreach

The E/PO program described in section D exceeds 2% of the estimated HMI total cost. It is about 6% of HMI. In case no more than 2% is allowed for this important aspect of the HMI program, we provide a descope plan in the section D cost narrative. This descope would reduce the E/PO cost by about $2.5M to a level below 2% of HMI.

The full E/PO program we propose is only about 1% of the SDO mission cost. We believe our full plan would make a significant contribution to the E/PO goals for the mission and for LWS as a whole.

If the LMSAL AIA is also selected we will do a merged E/PO program, most of the components of which are already included in our full plan.

F.3 BASIS OF COST ESTIMATES - LMSAL COMPONENT

The following narrative briefly describes the basis for estimating the proposed program costs. LMSAL effort levels are indicated in Equivalent Persons (EP) units where one EP is 1812 hours.

F.3.1 Program Management

Program management involves overseeing the entire program on a day-to-day basis including managing cost and schedule resources as well as risks. It also includes configuration management activities and all travel costs. Our estimate for these efforts is based on the actual costs for similar prior programs and roughly equates to an average EP level during Phases A, B-D, and E of 1.4, 10.5, and 0.0 respectively.

F.3.2 Systems Engineering

Systems engineering includes defining interfaces (internal and external), analysis activities (mechanical and thermal math models, error budgets, etc.), reviews (internal, peer, Project), requirements specifications and verification, and other general systems engineering activities. Our estimate for these efforts is based on the actual costs for similar prior programs and roughly equates to an average EP level during Phases A and B-D of 1.5 and 10.3 respectively.

F.3.3 Mission Assurance

Mission Assurance includes the normal disciplines of safety, reliability, and quality plus parts engineering, materials and processes activities, and contamination control. It also includes software and product assurance activities and presenting the program at LM mission success reviews. Due to the increased emphasis on MA by NASA we have based this estimate on our SXI experience rather than on TRACE and MDI. This amounts to about 11.4 EP, which is 19.6% of the technical hours.

F.3.4 Instrumentation

Instrumentation is the largest cost element at this level of the WBS. This element includes 4.75 EP in Phase-A, 33.3 EP for Phase B-D. The instrumentation is subdivided into five pieces, each of which is briefly discussed below.

The **HMI optics package** contains the instrument structure, telescope, polarization selector, focus and calibration, ISS, limb sensor, filter system, and reimaging system.

Camera subsystems are provided by the United Kingdom under a no exchange of funds arrangement. They include characterized CCDs as well as the camera electronics. The estimated value of this contribution is shown in Cost Table B-2. Our UK colleagues made this estimate based on their experiences on prior programs, especially STEREO and Solar-B.

Focal plane subsystems include the CCD cooling and shielding systems, beamsplitter, shutters, and the effort of integrating these items with the UK-provided camera subsystems. The overall mechanical/thermal approach is an evolution of that being used on Solar-B and estimated accordingly; only modest NRE is required. Similarly, the shutters, tuning, and calibration/focus wheels have extensive heritage at LMSAL. They are simply scaled versions of evolutionary preferred designs, so their costs are well understood. Life testing for each type of mechanism that is used extensively is included.

The **electronics subsystem** contains all of the HMI electronics except the camera electronics. The heart of the system is a RAD 750 computer purchased from BAE. We received a quote from BAE for this proposal. The remaining electronics are all very similar to electronics LMSAL has developed previously. In fact, the mechanism controller boards that are being used on Solar-B and SECCHI will be used on HMI to minimize costs in these areas. From recent and similar programs equations have developed for estimating electronics development costs based on the number of boards, their complexity, and the number of FPGA designs that are required. Several of the FPGA designs are slight modifications of designs being used on Solar-B, and this has been taken into account.

Intra-instrument harness costs were estimated based on our experiences in prior pro-

grams. It is assumed that GSFC will provide the harness from the S/C to the electronics box and that LMSAL will supply the harness between the electronics box and the optics box.

F.3.5 Software

Software will be quite simple on HMI due to the conveniences (and constraints) of the very high data rate, full disk imaging, and unchanging observing sequence. There will be no onboard image processing. Data compression is done in hardware "on the fly". Thus, the software only controls the observing program, labels the images, controls the down link, controls the thermal systems, and provides typical housekeeping information with a modest ability to react to out-of-nominal conditions. Our experience with similar software systems on prior programs yields good estimates for both of these efforts. GSE software is included in this WBS element.

F.3.6 Ground Support Equipment

Ground support equipment contains optical, mechanical, and electrical elements as well as a software development system. The optical GSE includes a Stimulus Telescope for illuminating the flight telescope. All of the items are basically identical to those developed for MDI, so their costs are well understood.

F.3.7-9 Integration & Test Activities

Integration and test activities at LMSAL, GSFC, and the launch site assume a level of effort that is based on prior program experiences. TRACE is a prime example since it was a GSFC in-house spacecraft like SDO. Test facility costs are well known from other programs where the baseline is to perform acoustics at the LM Sunnyvale facility, thermal balance/vacuum in our LMSAL building, and EMI and vibration at the facilities of outside vendors. This is the most cost-effective approach based on our past experience, and the costs are well understood.

F.3.10 HMI Pre-launch Science Support

As dictated by the AO, the scope of pre-launch science activities is limited to tasks that directly relate to producing the instrumentation and to being prepared to handle the large data stream when it begins to flow. These efforts are primarily Stanford tasks. At LMSAL the effort is approximately 2 EP to assist development of calibration and vector field analysis code. With this limited, and non-traditional, approach the LMSAL Co-Is must apply for and obtain funding from sources such as the LWS Targeted Research & Technology (TR&T) program in order to properly prepare for and conduct the SDO mission.

F.3.11-12 Special Launch Services/ Special Ground Data Systems

We have identified no costs for special launch services or for special ground data systems.

F.3.13 Financial Reserves

After estimating the entire program costs both Stanford and LMSAL revisited the tasks to determine what level of financial reserves would be appropriate for the instrument development portion of the program, Phases B-D. The extensive heritage of the instrumentation resulted in rather modest reserves to cover the surprises that seem to always occur no matter how well things are understood. The result is a reserve of $4,350K or 15% of LMSAL's Phase B-D costs.

F.3.15. Post-launch Ops/Data Analysis

The LMSAL role after launch is to assist Stanford with HMI operations, calibration, and some analysis of science data. Again some of the science support, and, after the first two years of operation, all of the science support for LMSAL Co-Is must come from other sources of funding.

F.3.16 Education and Public Outreach

LMSAL will support the Stanford led E/PO program with multimedia programming support and scientist creation of materials as described in section D.

G4 STATEMENT OF WORK

This Appendix contains a draft Statement of Work (SOW) for Phases A-E of the HMI Program. This program is a collaboration between Stanford University and the Lockheed Martin Solar and Astrophysical Laboratory (LMSAL). This SOW is divided into three sections describing Phase A, Phases B/C/D, and Phase E.

PHASE A – CONCEPT DEFINITION

Scope

Stanford University will develop the HMI concept to the level where detailed mission, science, and instrument development are defined, and spacecraft interfaces and allocations determined. This will permit the establishment of firm costs for all subsequent phases. In addition to LMSAL, Stanford will work in collaboration with the Mullard Space Sciences Laboratory (MSSL) and the Rutherford Appleton Laboratory (RAL) in their definition of the CCD's and cameras, respectively for this mission. Phase A will culminate with a study report of the effort and a cost proposal for all subsequent phases. The E/PO program will be initiated in Phase-A.

Deliverables

- Monthly Progress Reports
- Final Report (Concept Study)
  - Executive Summary
  - Science Investigation Description
  - Instrument Performance Specification
  - Implementation Plan
    - Organization
    - Responsibilities
    - Key Personnel
    - Subcontracting Approach
    - Schedules
    - Risk Management
    - Reporting and Reviews
    - Instrument Design
    - Instrument Fabrication
    - Instrument Testing/Calibration
    - PAIP
    - Interface Definitions
    - Technical Readiness Level Status
    - E/PO
- Preparation for and support of
  - Systems Requirements Review
  - Initial Confirmation Review
- Statements of Work for Phases B-E.
- Cost Proposal for Phases B-E

Government Responsibilities

- Establish a Letter of Agreement between the UK and USA
  - MSSL
  - RAL

PHASE B/C/D – DESIGN & IMPLEMENTATION

Scope

LMSAL, with direction from Stanford will perform a preliminary design, detailed design, and fabricate, test and commission the HMI instrument.

The preliminary design activities will include, but not be limited to, defining both internal and external interfaces, conducting the systems engineering and performance analysis, develop preliminary test plans, define the GSE, and establish the operational concept. Updated and refined schedules for the implementation phase will be established.

The detailed design activities will bring the design to the point where fabrication and procurement activities can start. An instrument integration plan will be developed and the GSE design will be completed. The flight and GSE software architecture will be completed and code implementation initiated.

The implementation phase will commence with the fabrication and procurement of all hardware elements. All of the subsystems will be integrated. This includes the telescopes provided by SAO, the camera from RAL, and the CCD's from MSSL. Test procedures will be developed from the test plans and all flight hardware will be fully tested to the specified

requirements established in the instrument performance specification. Instrument calibrations will be performed. The instrument team will support the launch and the subsequent 30 days of on-orbit commissioning, culminating in the completion of this mission phase.

Stanford will design, implement, and test the ground data processing system.

Stanford and the science team will work with NASA to continue implementation of a comprehensive E/PO program.

Deliverables

- Preparation for and support of:
  - Preliminary Design Review
  - Confirmation review/Non-Advocate Review
  - Critical Design Review
  - Pre-Environmental Review
  - Pre-Ship Review
  - Mission Readiness Review
  - Flight Readiness Review
  - Launch Readiness Review
  - Flight Operations Review
  - Mission Operations Review
- Monthly Reports
  - Progress Report
  - Financial Report
  - Schedules
- Other Reports
  - Education and Public Outreach Report
  - Parts and Materials List
  - Contamination Control Plan
  - Software Development plan
  - Complete Set of Drawings
  - Verification Plan
  - Test Plan
  - Test Procedures
  - Instrument Specification
  - Mission Operations Plan
  - Data Analysis Plan
  - Science Preparation Summary
- Other Items
  - STM
  - Flight Instrument
  - Flight and GSE Software
  - GSE
- Government Responsibilities
  - Augment the Letter of Agreement between the UK and USA to include
    - Imperial College
    - Cambridge University

PHASE E – MISSION OPERATIONS

Scope

The HMI team will support mission operations, data reduction, and data analysis activities for the five year period starting 30 days after launch, and data analysis for a sixth year. The data will be processed and archived. The health and safety of the HMI instrument will be monitored, and on-orbit performance affecting scientific analysis will be characterized.

Deliverables

- Publications in Scientific Journals
- Preparation of Data for Public Use
- Calibrated Data Sets for NASA Archiving
- Education and Public Outreach Report
- Monthly Reports
  - Progress Report
  - Financial Report

Government Responsibilities

Operate SDO and the SDO MOC.

APPENDIX G.5: REFERENCES

References for Section C.1

1. Hale, G.E., et al., 1919. *The Magnetic Polarity of Sun-Spots.* Astrophysical Journal, **49**: p. 153.
2. Schrijver, C.J., et al., 1997. *Sustaining the Quiet Photospheric Network: The Balance of Flux Emergence, Fragmentation, Merging, and Cancellation.* Astrophysical Journal, **487**: p. 424.
3. Title, A.M. and C.J. Schrijver. *The Sun's Magnetic Carpet*. in *ASP Conf. Ser. 154: Cool Stars, Stellar Systems, and the Sun*. 1998.
4. Kosovichev, A.G., 1996. *Helioseismic Constraints on the Gradient of Angular Velocity at the Base of the Solar Convection Zone.* Astrophysical Journal, **469**: p. L61.
5. Basu, S., 1997. *Seismology of the base of the solar convection zone.* Monthly Notices of the Royal Astronomical Society, **288**: p. 572-584.
6. Charbonneau, P., et al., 1999. *Helioseismic Constraints on the Structure of the Solar Tachocline.* Astrophysical Journal, **527**: p. 445-460.
7. Spiegel, E.A. and J.-P. Zahn, 1992. *The solar tachocline.* Astronomy and Astrophysics, **265**: p. 106-114.
8. Canuto, V.M. and J. Christensen-Dalsgaard, 1998. *Turbulence in Astrophysics: Stars.* Annual Review of Fluid Mechanics, **30**: p. 167-198.
9. Durney, B.R., 2000. *Meridional Motions and the Angular Momentum Balance in the Solar Convection Zone.* Astrophysical Journal, **528**: p. 486-492.
10. MacGregor, K.B. and P. Charbonneau, 1997. *Solar Interface Dynamos. I. Linear, Kinematic Models in Cartesian Geometry.* Astrophysical Journal, **486**: p. 484.
11. Gilman, P.A. and P.A. Fox, 1999. *Joint Instability of Latitudinal Differential Rotation and Toroidal Magnetic Fields below the Solar Convection Zone. III. Unstable Disturbance Phenomenology and the Solar Cycle.* Astrophysical Journal, **522**: p. 1167-1189.
12. Gough, D.O., et al., 1996. *The Seismic Structure of the Sun.* Science, **272**: p. 1296.
13. Thompson, M.J., et al., 1996. *Differential Rotation and Dynamics of the Solar Interior.* Science, **272**: p. 1300-1305.
14. Kosovichev, A.G., 1996. *Tomographic Imaging of the Sun's Interior.* Astrophysical Journal, **461**: p. L55.
15. Kosovichev, A.G. and T.L. Duvall, Jr. *Acoustic tomography of solar convective flows and structures*. in *ASSL Vol. 225: SCORe'96 : Solar Convection and Oscillations and their Relationship*. 1997.
16. Giles, P.M., T.L. Duvall, Jr. , and A.G. Kosovichev. *Solar rotation and large-scale flows determined by time-distance helioseismology MDI*. in *IAU Symp. 185: New Eyes to See Inside the Sun and Stars*. 1998.
17. Haber, D.A., et al. *Solar Shear Flows Deduced From Helioseismic Dense-Pack Samplings of Ring Diagrams*. in *SOHO-9 Workshop on Helioseismic*

Diagnostics of Solar Convection and Activity. 1999.

18. Haber, D., et al., 2000. *Solar Shear Flows Deduced from Helioseismic Dense-Pack Samplings of Ring Diagrams.* Solar Physics, **192**: p. 335-350.

19. Gizon, L., T.L. Duvall, Jr. , and R.M. Larsen, 2000. *Seismic Tomography of the Near Solar Surface.* Journal of Astrophysics and Astronomy, **21**: p. 339.

20. Basu, S. and H.M. Antia, 2000. *Temporal Variation of Large Scale Flows in the Solar Interior.* Journal of Astrophysics and Astronomy, **21**: p. 353.

21. Haber, D.A., et al., 2001. *Daily variations of large-scale subsurface flows and global synoptic flow maps from dense-pack ring-diagram analyses.* Proceedings of the SOHO 10/GONG 2000 Workshop: Helio- and asteroseismology at the dawn of the millennium, 2-6 October 2000, Santa Cruz de Tenerife, Tenerife, Spain. Edited by A. Wilson, Scientific coordination by P. L. Pallé. ESA SP-464, Noordwijk: ESA Publications Division, ISBN 92-9092-697-X, 2001, p. 209 - 212, **464**: p. 209.

22. Haber, D.A., et al. *Subsurface Flows with Advancing Solar Cycle Using Dense-Pack Ring-Diagram Analyses*. in *IAU Symposium*. 2001.

23. Gizon, L., T.L. Duvall, Jr. , and R.M. Larsen. *Probing Surface Flows and Magnetic Activity with Time-Distance Helioseismology*. in *IAU Symposium*. 2001.

24. Kosovichev, A.G. and J. Schou, 1997. *Detection of Zonal Shear Flows beneath the Sun's Surface from f-Mode Frequency Splitting.* Astrophysical Journal, **482**: p. L207.

25. Schou, J., 1999. *Migration of Zonal Flows Detected Using Michelson Doppler Imager F-Mode Frequency Splittings.* Astrophysical Journal, **523**: p. L181-L184.

26. Schou, J., et al., 1998. *Helioseismic Studies of Differential Rotation in the Solar Envelope by the Solar Oscillations Investigation Using the Michelson Doppler Imager.* Astrophysical Journal, **505**: p. 390-417.

27. Howe, R., et al., 2000. *Deeply Penetrating Banded Zonal Flows in the Solar Convection Zone.* Astrophysical Journal Letters, **533**(2000 April 20): p. L163-L166.

28. Giles, P.M., T.L. Duvall, Jr. , and P.H. Scherrer. *Time-distance Measurements of Meridional Circulation Deep in the Convection Zone*. in *SOHO-9 Workshop on Helioseismic Diagnostics of Solar Convection and Activity*. 1999.

29. Giles, P.M., et al., 1997. *A Flow of Material from the Suns Equator to its Poles.* Nature, **390**: p. 52.

30. Haber, D.A., et al., 2001. *Development of multiple cells in meridional flows and evolution of mean zonal flows from ring-diagram analyses.* Proceedings of the SOHO 10/GONG 2000 Workshop: Helio- and asteroseismology at the dawn of the millennium, 2-6 October 2000, Santa Cruz de Tenerife, Tenerife, Spain. Edited by A. Wilson, Scientific coordination by P. L. Pallé. ESA SP-464, Noordwijk: ESA Publications Division, ISBN 92-9092-697-X, 2001, p. 213 - 218, **464**: p. 213.

31. Braun, D.C. and Y. Fan, 1998. *Helioseismic Measurements of the Subsurface Meridional Flow.* Astrophysical Journal, **508**: p. L105.

32. Hindman, B., et al., 2000. *Local Fractional Frequency Shifts Used as Tracers of Magnetic Activity.* Solar Physics, **192**: p. 363-372.

33. Dziembowski, W.A., et al., 2000. *Signatures of the Rise of Cycle 23.* Astrophysical Journal, **537**: p. 1026-1038.

34. Haber, D.A., et al., 2002. *Evolving Submerged Meridional Circulation Cells Within the Upper Convection Zone Revealed by Ring-Diagram Analysis.* Astrophysical Journal, **570**: p. 855-864.

35. Labonte, B.J. and R. Howard, 1982. *Torsional waves on the sun and the activity cycle.* Solar Physics, **75**: p. 161-178.

36. Benevolenskaya, E.E., et al., 1999. *The Interaction of New and Old Magnetic Fluxes at the Beginning of Solar Cycle 23.* Astrophysical Journal Letters, **517**: p. L163.

37. Howe, R., et al., 2000. *Deeply Penetrating Banded Zonal Flows in the Solar Convection Zone.* Astrophysical Journal, **533**: p. L163-L166.

38. Covas, E., R. Tavakol, and D. Moss, 2001. *Dynamical variations of the differential rotation in the solar convection zone.* Astronomy and Astrophysics, **371**: p. 718-730.

39. Parker, E.N., 1987. *The dynamo dilemma.* Solar Physics, **110**: p. 11-21.

40. Dikpati, M. and P.A. Gilman, 2001. *Flux-Transport Dynamos with α-Effect from Global Instability of Tachocline Differential Rotation: A Solution for Magnetic Parity Selection in the Sun.* Astrophysical Journal, **559**: p. 428-442.

41. Giles, P.M., *Time-Distance Measurements of Large-Scale Flows in the Solar Convection Zone*, in *Department of Applied Physics*. 1999, Stanford University: Stanford. p. 144.

42. Chou, D.-Y. and D.-C. Dai, 2001. *Solar Cycle Variations of Subsurface Meridional Flows in the Sun.* Astrophysical Journal, **559**: p. L175-L178.

43. Libbrecht, K.G. and M.F. Woodard, 1990. *Solar-cycle effects on solar oscillation frequencies.* Nature, **345**: p. 779-782.

44. Libbrecht, K.G. and M.F. Woodard. *Observations of Solar Cycle Variations in Solar p_Mode Frequencies and Splittings*. in *LNP Vol. 367: Progress of Seismology of the Sun and Stars*. 1990.

45. Bumba, V. and R. Howard, 1965. *Large-Scale Distribution of Solar Magnetic Fields.* Astrophysical Journal, **141**: p. 1502.

46. Ambroz, P., et al. *Opposite Polarities in the Development of Some Regularities in the Distribution of Large-Scale Magnetic Fields*. in *IAU Symp. 43: Solar Magnetic Fields*. 1971.

47. Gaizauskas, V., et al., 1983. *Large-scale patterns formed by solar active regions during the ascending phase of cycle 21.* Astrophysical Journal, **265**: p. 1056-1065.

48. Zwaan, C., 1996. *A Dynamo Scenario|Observational Constraints on*

Dynamo Theory. Solar Physics, **169**: p. 265-276.

49. de Toma, G., O.R. White, and K.L. Harvey, 2000. *A Picture of Solar Minimum and the Onset of Solar Cycle 23. I. Global Magnetic Field Evolution.* Astrophysical Journal, **529**: p. 1101-1114.

50. Leighton, R.B., 1964. *Transport of Magnetic Fields on the Sun.* Astrophysical Journal, **140**: p. 1547.

51. Sheeley, N.R., Jr. , C.R. Devore, and J.P. Boris, 1985. *Simulations of the mean solar magnetic field during sunspot cycle 21.* Solar Physics, **98**: p. 219-239.

52. Wang, Y.-M., N.R. Sheeley, Jr. , and A.G. Nash, 1991. *A new solar cycle model including meridional circulation.* Astrophysical Journal, **383**: p. 431-442.

53. Wang, Y.-M. and N.R. Sheeley, Jr., 1994. *The rotation of photospheric magnetic fields: A random walk transport model.* Astrophysical Journal, **430**: p. 399-412.

54. Ribes, J.C. and E. Nesme-Ribes, 1993. *The solar sunspot cycle in the Maunder minimum AD1645 to AD1715.* Astronomy and Astrophysics, **276**: p. 549.

55. Castenmiller, M.J.M., C. Zwaan, and E.B.J. van der Zalm, 1986. *Sunspot nests - Manifestations of sequences in magnetic activity.* Solar Physics, **105**: p. 237-255.

56. Sheeley, N.R., Jr. *The Flux-Transport Model and Its Implications*. in *ASP Conf. Ser. 27: The Solar Cycle*. 1992.

57. Antalova, A. and M.N. Gnevyshev, 1983. *Latitudinal distribution of sunspot areas during the period 1874-1976.* Contributions of the Astronomical Observatory Skalnate Pleso, **11**: p. 63-93.

58. Harvey, K.L. *The Cyclic Behavior of Solar Activity*. in *ASP Conf. Ser. 27: The Solar Cycle*. 1992.

59. Benevolenskaya, E.E., et al., 2002. *Large-scale Solar Coronal Structures in Soft X-rays and Their Relationship to the Magnetic Flux.* Astrophysical Journal, **570**.

60. Zhao, J., A.G. Kosovichev, and T.L. Duvall. *Time-distance Helioseismology Study Over a Rotating Sunspot*. in *American Geophysical Union, Fall Meeting 2001, abstract #SH11B-0708 (http://soi.stanford.edu/press/agu12-01)*. 2001.

61. Parker, E.N., 1979. *Sunspots and the physics of magnetic flux tubes. I - The general nature of the sunspot. II - Aerodynamic drag.* Astrophysical Journal, **230**: p. 905-923.

62. Fan, Y., G.H. Fisher, and A.N. McClymont, 1994. *Dynamics of emerging active region flux loops.* Astrophysical Journal, **436**: p. 907-928.

63. Hurlburt, N.E. and A.M. Rucklidge, 2000. *Development of structure in pores and sunspots: flows around axisymmetric magnetic flux tubes.* Monthly Notices of the Royal Astronomical Society, **314**: p. 793-806.

64. Foukal, P. *Solar Luminosity Variation*. in *ASP Conf. Ser. 27: The Solar Cycle*. 1992.

65. Leka, K.D., et al., 1996. *Evidence for Current-carrying Emerging Flux.* Astrophysical Journal, **462**: p. 547.

66. Pevtsov, A.A., R.C. Canfield, and A.N. McClymont, 1997. *On the Sub-photospheric Origin of Coronal Electric Currents.* Astrophysical Journal, **481**: p. 973.

67. Sakurai, T. and E. Hiei, 1996. *New observational facts about solar flares from ground-based observations.* Advances in Space Research, **17**: p. 91-.

68. Brown, J.C., et al., 1994. *Energy release in solar flares.* Solar Physics, **153**: p. 19-31.

69. Sammis, I., F. Tang, and H. Zirin, 2000. *The Dependence of Large Flare Occurrence on the Magnetic Structure of Sunspots.* Astrophysical Journal, **540**: p. 583-587.

70. Fan, Y., 2001. *The Emergence of a Twisted Ω-Tube into the Solar Atmosphere.* Astrophysical Journal, **554**: p. L111-L114.

71. Linton, M.G., et al., 2001. *Multi-mode kink instability as a mechanism for δ-spot formation.* Advances in Space Research, **26**: p. 1781-1784.

72. Magara, T. and D.W. Longcope, 2001. *Sigmoid Structure of an Emerging Flux Tube.* Astrophysical Journal, **559**: p. L55-L59.

73. Canfield, R.C., et al., 1993. *The morphology of flare phenomena, magnetic fields, and electric currents in active regions. I - Introduction and methods.* Astrophysical Journal, **411**: p. 362-369.

74. Kosovichev, A.G. and V.V. Zharkova, 2001. *Magnetic Energy Release and Transients in the Solar Flare of 2000 July 14.* Astrophysical Journal, **550**: p. L105-L108.

75. Harvey, J.W. *Search for Photospheric Magnetic Field Changes with Flares and CMEs*. in *American Geophysical Union, Spring Meeting 2001, abstract #SH22A-01*. 2001.

76. Kosovichev, A.G., T.L. Duvall, Jr., and P.H. Scherrer, 2000. *Time-Distance Inversion Methods and Results.* Solar Physics, **192**: p. 159-176.

77. Feynman, J. and S.F. Martin, 1995. *The initiation of coronal mass ejections by newly emerging magnetic flux.* Journal Geophysical Research, **100**: p. 3355-3367.

78. Subramanian, P. and K.P. Dere, 2001. *Source Regions of Coronal Mass Ejections.* Astrophysical Journal, **561**: p. 372-395.

79. Chen, P.F. and K. Shibata, 2000. *An Emerging Flux Trigger Mechanism for Coronal Mass Ejections.* Astrophysical Journal, **545**: p. 524-531.

80. Wang, Y.-M. and N.R. Sheeley, Jr., 1999. *Filament Eruptions near Emerging Bipoles.* Astrophysical Journal, **510**: p. L157-L160.

81. Priest, E.R. and T.G. Forbes, 2002. *The magnetic nature of solar flares.* Astronomy and Astrophysics Review, **10**: p. 313-377.

82. Handy, B.N. and C.J. Schrijver, 2001. *On the Evolution of the Solar Photospheric and Coronal Magnetic Field.* Astrophysical Journal, **547**: p. 1100-1108.

83. Takeuchi, A. and K. Shibata, 2001. *Magnetic Reconnection Induced by Convective Intensification of Solar Photospheric Magnetic Fields.* Astrophysical Journal, **546**: p. L73-L76.

84. Moore, R.L., et al., 1999. *On Heating the Sun's Corona by Magnetic Explosions: Feasibility in Active Regions and Prospects for Quiet Regions and Coronal Holes.* Astrophysical Journal, **526**: p. 505-522.

85. Longcope, D.W. and C.C. Kankelborg, 1999. *Coronal Heating by Collision and Cancellation of Magnetic Elements.* Astrophysical Journal, **524**: p. 483-495.

86. Luhmann, J.G., et al., 1998. *The Relationship Between Large-Scale Solar Magnetic Field Evolution and Coronal Mass Ejection.* Journal of Geophysical Research, **103**: p. 6585.

87. Mikic, Z. and A.N. McClymont. *Deducing Coronal Magnetic Fields from Vector Magnetograms*. in *ASP Conf. Ser. 68: Solar Active Region Evolution: Comparing Models with Observations*. 1994.

88. Amari, T., T.Z. Boulmezaoud, and Z. Mikic, 1999. *An iterative method for the reconstructionbreak of the solar coronal magnetic field. I. Method for regular solutions.* Astronomy and Astrophysics, **350**: p. 1051-1059.

89. Falconer, D.A., et al., 2000. *An Assessment of Magnetic Conditions for Strong Coronal Heating in Solar Active Regions by Comparing Observed Loops with Computed Potential Field Lines.* Astrophysical Journal, **528**: p. 1004-1014.

90. Lee, J., et al., 1999. *A Test for Coronal Magnetic Field Extrapolations.* Astrophysical Journal, **510**: p. 413-421.

91. Priest, E.R. and C.J. Schrijver, 1999. *Aspects of Three-Dimensional Magnetic Reconnection - (Invited Review).* Solar Physics, **190**: p. 1-24.

92. Antiochos, S.K., C.R. Devore, and J.A. Klimchuk, 1999. *A Model for Solar Coronal Mass Ejections.* Astrophysical Journal, **510**: p. 485-493.

93. Démoulin, P., et al., 2002. *What is the source of the magnetic helicity shed by CMEs? The long-term helicity budget of AR 7978.* Astronomy and Astrophysics, **382**: p. 650-665.

94. Pevtsov, A.A., R.C. Canfield, and T.R. Metcalf, 1994. *Patterns of helicity in solar active regions.* Astrophysical Journal, **425**: p. L117-L119.

95. Rust, D.M. and A. Kumar, 1994. *Helical magnetic fields in filaments.* Solar Physics, **155**: p. 69-97.

96. Rust, D.M. *Magnetic Helicity, MHD Kink Instabilities and Reconnection in the Corona*. in *ASP Conf. Ser. 111: Magnetic Reconnection in the Solar Atmosphere*. 1997.

97. Rust, D. *Magnetic Helicity, Coronal Mass Ejections and the Solar Cycle*. in *SOLSPA 2001 Euroconference: Solar Cycle and Space Weather*. 2001.

98. Berger, M.A. and G.B. Field, 1984. *The Topological Properties of Magnetic Helicity.* Journal of Fluid Mechanics, **147**: p. 133-148.

99. Kusano, K., et al. *Numerical Studies on Magnetic Helicity in Solar Corona*. in *Multi-Wavelength Observations of*

Coronal Structure and Dynamics -- Yohkoh 10th Anniversary Meeting. 2001.

100. Linker, J.A., et al., 1999. *Magnetohydrodynamic modeling of the solar corona during Whole Sun Month.* Journal Geophysical Research, **104**: p. 9809-9830.

101. Li, Y., et al., 2001. *Earthward Directed CMEs Seen in Large-Scale Coronal Magnetic Field Changes, SOHO/LASCO Coronagraph and Solar Wind.* Journal of Geophysical Research, **106**(A11): p. 25,103-25,120.

102. Zhao, X. and D.F. Webb, *Large-scale closed field regions and hole coronal mass ejections*, in *American Geophysical Union 2000 Fall Meeting, Abstract #SH72B-03*. 2000.

103. Riley, P., J.A. Linker, and Z. Mikic, 2001. *An empirically-driven global MHD model of the solar corona and inner heliosphere.* Journal Geophysical Research, **106**: p. 15889-15902.

104. Zhao, X.P. and J.T. Hoeksema, 1995. *Predicting the Heliospheric Magnetic Field Using the Current Sheet - Source Surface Model.* Advances in Space Research, **16**: p. (9)181-184.

105. Jiao, L., A.N. McClymont, and Z. Mikic, 1997. *Reconstruction of the Three-Dimensional Coronal Magnetic Field.* Solar Physics, **174**: p. 311-327.

106. Balogh, A., et al., 1999. *The Solar Origin of Corotating Interaction Regions and Their Formation in the Inner Heliosphere.* Space Science Reviews, **89**: p. 141-178.

107. Arge, C.N. and V.J. Pizzo, 2000. *Improvement in the prediction of solar wind conditions using near-real time solar magnetic field updates.* Journal Geophysical Research, **105**: p. 10465-10480.

108. Lindsey, C. and D.C. Braun, 2000. *Seismic Images of the Far Side of the Sun.* Science, **287**: p. 1799-1801.

109. http://soi.stanford.edu/data/farside/.

110. Braun, D.C. and C. Lindsey, 2001. *Seismic Imaging of the Far Hemisphere of the Sun.* Astrophysical Journal, **560**: p. L189-L192.

111. Webb, D.F., et al., 2000. *Relationship of halo coronal mass ejections, magnetic clouds, and magnetic storms.* Journal Geophysical Research, **105**: p. 7491-7508.

112. Zhao, X.P. and J.T. Hoeksema, 1998. *Central axial field direction in magnetic clouds and its relation to southward interplanetary magnetic field events and dependence on disappearing solar filaments.* Journal Geophysical Research, **103**: p. 2077.

113. Graham, J.D., et al., 2002. *Inference of Solar Magnetic Field Parameters from Data with Limited Wavelength Sampling.* Solar Physics: p. in press.

REFERENCES FOR SECTION C.2

1. Scherrer, P.H., et al., 1995. *The Solar Oscillations Investigation - Michelson Doppler Imager.* Solar Physics, **162**: p. 129.
2. Corliss, C. and J. Sugar, 1981. *Energy Levels of Nickel, Ni I through Ni XXVIII.* J. Phys. Chem. Ref. Data, **10**(1): p. 197.
3. Rees, D. in *Numerical Radiative Transfer*. 1987.
4. Jefferies, J., B. Lites, and A. Skumanich, 1989. *Transfer of Line Radiation in a Magnetic Field.* Astrophysical Journal, **343**: p. 920.
5. Landi Degl'Innocenti, E., *Magnetic Field Measurements*, in *Solar Observations: Techniques and Interpretation*, F. Sánchez, M. Collados, and M. Vázquez, Editors. 1992. p. 71.
6. Hagyard, M.J. and J.I. Kineke, 1995. *Improved Method for Calibrating Filter Vector Magnetographs.* Solar Physics, **158**: p. 11.
7. Sakurai, T., et al., 1995. *Solar Flare Telescope at Mitaka.* PASJ, **47**: p. 81.
8. Graham, J.D., et al., 2002. *Inference of Solar Magnetic Field Parameters from Data with Limited Wavelength Sampling.* Solar Physics: p. in press.
9. López Ariste, A. and M. Semel, 1999. *DIAGONAL: A numerical solution of the Stokes transfer equation.* A & AS, **139**: p. 417.
10. Akin, D., R. Horber, and J. Wolfson. *Three High Duty Cycle, Space-Qualified Mechanisms*. in *27th Aerospace Mechanisms Symposium*. 1993. Moffett Field, CA: NASA.
11. Kuhn, J.R., H. Lin, and D. Loranz, 1991. *Gain Calibrating Nonuniform Image-array Data Using Only the Image Data.* Astronomical Society of the Pacific Publications, **103**: p. 1097.

REFERENCES FOR SECTION D

1. YPOP: http://solar.physics.montana.edu/YPOP

   Stanford SOLAR Center: http://solar-center.stanford.edu

   TRACE: http://vestige.lmsal.com/TRACE/Public/eduprodu.htm

2. Solar B Exhibition at CSSC: http://www.chabotspace.org/vsc/exhibits/Solarb

3. Stanford University's Haas Center for Public Service: http://haas-fmp.stanford.edu

4. "Publication Ranks Stanford First in Community Service," Stanford Report, January 11, 2002; http://news-sevice.stanford.edu/january16/workstudy-116.htm

5. Lynn Barakos, personal correspondence.

6. Planetarium Activities for Student Success (PASS) guides: Developed by the Lawrence Hall of Science, UC Berkeley. http://www.lhs.berkeley.edu/pass/

7. Great Explorations in Math and Science (GEMS) Guides: Developed by the Lawrence Hall of Science, UC Berkeley; http://www.lhs.berkeley.edu/GEMS/gemspubs.html

8. http://solar-center.stanford.edu/cots

9. Modeled after the Astronomical Society of the Pacific's "Night Sky Adventure: Fun for the Whole Family from Project Astro": http://www.astrosociety.org/education/family/about/about.html

10. "National Science Education Standards," National Academy Press, Washington DC, 1995.

11. OSS: http://spacescience.nasa.gov/education/resources/strategy

    LWS: http://lws-edu.gsfc.nasa.gov

12. See The Educational Resources Information Center Clearing House on Assessment and Evaluation (http://ericae.net/); Field-tested Learning Assessment Guide (http://www.wcer.wisc.edu/nise/cl1/flag/); and articles such as "The Role of Assessment in the Development of the College Introductory Astronomy Course," Gina Brissenden, Timothy Slater, Robert Mathieu, in "Astronomy Education Review," (http://aer.noao.edu/AERArticle.php?issue=1&section=1&article=1)

ACRONYM LIST

AAS	American Astronomical Society
ACE	Advanced Composition Explorer
ADP	Ammonium Dihydrogen Phosphate
AGU	American Geophysical Union
AI	Associated Investigator
AIA	Atmospheric Imaging Assembly
AO	Announcement of Opportunity
AR	Active Region
ARC	Ames Research Center
ASIC	Application-Specific Integrated Circuit
ASP	Astronomical Society of the Pacific
ASP	Advanced Stokes Polarimeter
ASSL	Astrophysics and Space Science Library
ATC	Advanced Technology Center
AXAF	Advanced X-ray Astrophysics Facility
BAE/BAe	British Aerospace
BBSO	Big Bear Solar Observatory
BCS	Bragg Crystal Spectrometer
CCD	Charge Coupled Device
CCSDS	Consultive Committee for Space Data Systems
CDS	Coronal Density Spectrometer
CHASE	Coronal Helium Abundance Spacelab Experiment
CME	Coronal Mass Ejection
CORE	Central Operation of Resources for Educators
CPU	Central Processing Unit
CSE	Chief Systems Engineer
Co-I	Co-Investigator
DA	Data Analysis
DBMS	Database Management System
DC	Direct Current
DVD	Digital Video Disk
EEE	Electrical, Electronic and Electromagnetic
EEPROM	Electrically Erasable Programmable Read-Only Memory
EIS	Extreme Ultra-Violet Imaging Spectrometer
EMC	ElectroMagnetic Compatibility
EMI	ElectroMagnetic Interference
EP	Equivalent Person
E/PO	Education and Public Outreach
ESA	European Space Agency
EUV	Extreme Ultraviolet
EVM	Engineering Verification Model
EW	Equivalent Width
FAQ	Frequently-Qsked Questions
FITS	Flexible Image Transport System
FMEA	Failure Mode and Effects Analysis
FOV	Field Of View
FPGA	Field Programmable Gate Array
FPP	Focal Plane Package
FTE	Full-Time Equivalent
FWHM	Full-Width Half-Maximum
GCU	Ground Calibration Unit
GEMS	Great Expectations in Math and Science
GEVS	General Environmental Verification Specification
GI	Guest Investigator
GIDEP	Government-Industry Data Exchange Program
GONG(+)	Global Oscillations Network Group
GSE	Ground Support Equipment
GSFC	Goddard Space Flight Center
HAO	High Altitude Observatory
HEPL	W. W. Hansen Experimental Physics Laboratory
HI	Heliospheric Imager
HIRDLS	High Resolution Dynamics Limb Sounder
HMI	Helioseismic and Magnetic Imager
HRC	High Resolution Camera
HS	HelioSeismology
HSC	Hierarchical Storage Controller
HVMI	Helioseismic and Vector Magnetic Imager
IAU	International Astronomical Union
ICD	Interface Control Document
IEEE	Institute of Electrical and Electronic Engineers
IIISE	Institute for Imagination and Innovation in Science Education
ILWS	International Living With a Star
IMAR	Instrument Mission Assurance Requirements
IPS	Instrument Performance Specification
ISAS	Institute of Space and Astronautical Science
ISS	Image Stabilization System
I&T	Integration and Testing
ITAR	International Traffic in Arms Regulations
IoA	Institute of Astronomy
KDP	Potassium(K) Dihydrogen Phosphate
LASCO	Large Angle and Spectrometric COronagraph
LCP	Left-hand Lircular Lolarization
LM	Lockheed-Martin
LMATC	Lockheed-Martin Advanced Technology Center
LMMS	Lockheed-Martin Missiles & Space

LMSAL	Lockheed-Martin Solar and Astrophysics Laboratory
LMSSC	Lockheed-Martin Space Systems Company
LNP	Lecture Notes in Physics
LOS	Line-Of-Sight
LOWL	Low-L
LPARL	Lockheed Palo Alto Research Laboratory
LTO	Linear Tape Open
LVDS	Low Voltage Differential Signal
LWS	Living With a Star
M&P	Materials and Process
MA	Mission Assurance
MAR	Mission Assurance Requirements
MDI	Michelson Doppler Imager
ME	Milne-Eddington
MHD	MagnetoHydroDynamic
MO&DA	Mission Operations and Data Analysis
MOC	Mission Operations Center
MOSFET	Metal Oxide Semiconductor Field Effect Transistor
MSSL	Mullard Space Science Laboratory
MSU	Montana State University
NASA	National Aeronautics and Space Administration
NPG	NASA Policies and Guidelines
NRA	NASA Research Announcement
NRE	Non-Recurring Engineering
NSF	National Science Foundation
NSTA	National Science Teachers Association
OSS	Office of Space Sciences
PAIP	Product Assurance Implementation Plan
PASS	Planetarium Activities for Student Success
PCB	Printed Circuit Board
PCB	Parts Control Board
PCI	Peripheral Component Interconnect
PI	Principal Investigator
PM	Program Manager
PPARC	Particle Physics and Astronomy Research Council
PSF	Point-Spread Function
PZT	PieZoelectric Transducer
RAL	Rutherford Appleton Laboratory
RCP	Right-hand Circular Polarization
RFI	Request For Information
ROM	Read-Only Memory
RY	Real Year
S/C	SpaceCraft
SAO	Smithsonian Astrophysical Observatory
SB	Small Business
SBP	Small Business Program
SCORe	Solar Convection and Oscillations and their Relationship
SDO	Solar Dynamics Observatory
SDRAM	Synchronous Dynamic Random Access Memory
SECCHI	Sun Earth Connection Coronal and Heliospheric Investigation
SECEF	Sun-Earth Connection Education Forum
SEU	Single-Event Upset
SIE	Spectrometer for Irradiance in the EUV
SK/MM	Station Keeping and Momentum Management
SM	Structural Model
SMB	Small Minority-owned Business
SMM	Solar Maximum Mission
SOAP	Simple Object Access Protocol
SOC	Science Operations Capability
SOHO	Solar and Heliospheric Observatory
SOLIS	Synoptic Optical Long-term Investigations of the Sun
SOLSPA	Solar Cycle and Space Weather Euroconferences
SOW	Statement Of Work
SSC	Space and Science Center
SSW	Solar Subsurface Weather
STEREO	Solar Terrestrial Relations Observatories
STM	Structural / Thermal Model
SU	Stanford University
SUROM	Start-Up Read-Only Memory
SXI(-N)	Solar X-ray Imager
SXT	Soft X-ray Telescope
TAC	Theoretical Astrophysics Center
TRACE	Transition Region And Coronal Explorer
TR&T	Targeted Research and Technology
UC	University of California
URL	Uniform Resource Locator
UV	UltraViolet
VSO	Virtual Solar Observatory
WBS	Work Breakdown Structure
WCI	White-light Coronagraphic Imager
XRP	X-Ray Polychromator
XRT	X-Ray Telescope
YPOP	Yohkoh Public Outreach Project